

UC Davis

UC Davis Electronic Theses and Dissertations

Title

Development of New Techniques to Study Metabolism in Giardia lamblia Highlights the Importance of Amino Acid Metabolism

Permalink

<https://escholarship.org/uc/item/3x89q9h0>

Author

Starcevich, Hannah Nichole

Publication Date

2022

Peer reviewed|Thesis/dissertation

Development of New Techniques to Study Metabolism in *Giardia lamblia* Highlights the
Importance of Amino Acid Metabolism

By

HANNAH NICHOLE STARCEVICH
DISSERTATION

Submitted in partial satisfaction of the requirements for the degree of

DOCTOR OF PHILOSOPHY

in

Microbiology

in the

OFFICE OF GRADUATE STUDIES

of the

UNIVERSITY OF CALIFORNIA

DAVIS

Approved:

Scott C. Dawson, Chair

Jeroen Saeij

Renee Tsois

Committee in Charge

2023

ABSTRACT

Giardia lamblia is a protozoan intestinal pathogen that infects a wide range of mammals, including humans. The global burden of giardiasis is especially detrimental to young children in developing countries. Evidence of drug-tolerant and drug-resistant strains have been reported. *Giardia* has a unique microaerophilic metabolism, with many potential druggable targets, but further research is needed. To study the effect of specific metabolites, I first designed a defined base medium and then added known concentrations of metabolites to that base medium. ATP generation was measured using a luminescence assay and the transcriptomic response to specific metabolites was measured using RNA-Seq analysis. Amino acids, not glucose, were found to have a significant effect on ATP generation and transcriptional response to nutrient availability. The arginine dihydrolase (ADH) pathway plays an important role in *Giardia* amino acid metabolism, generating one molecule of ATP from one molecule of arginine. The potential energy flux through the ADH pathway is approximately 7-8 fold higher than that from glucose and the energy produced through the ADH pathway is also thought to compensate for the reduction of ATP generation from glycolysis that occurs during encystation. Using CRISPR-Cas9 technology, the first complete metabolic knockout in *Giardia* was created, disrupting all four copies of the arginine deiminase (ADI) gene. When ADI is knocked out, there was a significant reduction in ATP generation through the ADH pathway and down regulation of genes associated with amino acid metabolism.

ACKNOWLEDGEMENTS

Although there is only my name on the cover page, this whole graduate school experience would not have been possible without the support of so many people. The Dawson Lab provided both interesting research projects and amazing people to work with. To everyone who has worked in the lab while I was there: thank you so much for the chats about science, conference fun, crossword puzzles, trivia nights, and staying out too late at Wunderbar. Kari Hagen deserves a special shout-out (and so much more). She is an amazing scientist, but, more importantly, an amazing person. This acknowledgement section could be dedicated only to her because I would never have gotten this far without her support. Outside of the Dawson lab, I also received scientific support and education from the T32 Clinical and Translational Research training grant, Charles Smith at the Center for Molecular and Genomic Imaging, and a life-changing summer at Woods Hole taking the Microbial Diversity course. Thank you to Dr. Jim Nestler, my PI for my Master's Degree, for letting me join his lab and providing support, freedom, and inspiration, both as a scientist and as a person. Thank you to everyone, from my closest friends to random acquaintances that I only met once, all of whom provided some form of welcome distraction from grad school. The cats can't read, but thank you to Sir Wobbles and Morris (and Carl, when he was my roommate) for being small, cuddly beasts that greeted me when I came home after a long day in the lab. Lastly, thank you to my family, for supporting me though what must seem like a series of confusing life decisions. I promise that I will get a real job, start a Roth IRA, and never be a student again. From childhood, you have supported me in all of my educational pursuits and showered me with books. That's **Dr.** "Girl Scientist" to you.

TABLE OF CONTENTS

ABSTRACT	ii
ACKNOWLEDGEMENTS	iii
TABLE OF CONTENTS	iv
Chapter 1: Introduction to <i>Giardia</i> Metabolism: Pathways of Energy Generation	1
<i>Giardia</i> trophozoite metabolism is a key factor in pathogenesis and the primary target of anti- <i>Giardia</i> drugs	1
The life cycle of <i>Giardia</i> : Trophozoites and cysts	2
Amitochondrial trophozoites are defined by a unique microaerophilic metabolism	3
Novel aspects of glycolysis in <i>Giardia</i>	4
Overview of pyruvate metabolism in <i>Giardia</i>	8
Metabolism during encystation in <i>Giardia</i>	10
Energy production by arginine metabolism in <i>Giardia</i>	11
Using new genetic tools to interrogate <i>Giardia</i> trophozoite metabolism <i>in vitro</i> and <i>in vivo</i>	13
FIGURES	15
REFERENCES	22
Chapter 2: Development of Defined Medium for <i>in vitro</i> Metabolic Assays: Amino Acids, Not Glucose, Have a Significant Effect on ATP Generation and Transcriptional Response to Nutrient Availability	29
INTRODUCTION	29
METHODS	33
RESULTS	36
Composition and rationale for GBM + additions	36
Addition of peptides or amino acids alone to <i>Giardia</i> Base Medium returns ATP production to levels of conventional TYI medium	36
Medium formulations that include amino acids have more similar transcriptomes	39
Four primary groupings of transcriptomes are associated with either supplementation of amino acids, arginine, or glucose	39
Each group has a set of unique genes that are always differentially expressed when compared to the other three groups	40
Transcriptional differences are seen between TYI and GDMM	42
DISCUSSION	43
ATP generation is stimulated by the presence of amino acids, but not glucose	43
Unique transcription profiles correspond with nutrient choice and availability	44
Transcriptional regulation in response to nutrient availability	47
Successful development of a defined metabolic medium but further work needs to be done to develop a defined growth medium	49
FIGURES & TABLES	51
SUPPLEMENTAL MATERIAL	64
REFERENCES	78
Chapter 3: Knockout of the Arginine Deiminase (ADI) Gene Causes Significant Reduction in ATP Generation Through the ADH Pathway and Down Regulates Genes Associated With Amino Acid Metabolism	81
INTRODUCTION	81
METHODS	84
RESULTS	86

ADH knockdown strains produce less ATP than wild type when glucose is present, but arginine alone has limited effect	86
Knockout of ADI affects arginine metabolism but has no effect on glucose metabolism	87
Arginine deiminase (ADI) is significantly downregulated in ADI4XKO compared to wild type	88
DISCUSSION	89
Knockout of the ADI gene has a significant effect on ATP production and transcription	89
FIGURES & TABLES	95
SUPPLEMENTAL MATERIAL	104
REFERENCES	113

Chapter 1: Introduction to *Giardia* Metabolism: Pathways of Energy Generation

***Giardia* trophozoite metabolism is a key factor in pathogenesis and the primary target of anti-*Giardia* drugs**

Giardia lamblia (also known as *Giardia intestinalis* or *Giardia duodenalis*) is a protozoan intestinal pathogen that infects a wide range of mammals. In developed countries, the prevalence of human giardiasis ranges from 3-7%, but in developing countries, prevalence commonly reaches 20-30%, with 100% prevalence being reported in some populations (Halliez and Buret 2013; Jensen et al. 2009; Roxstrom-Lindquist et al. 2006). However, this is probably an underestimate as infections can be asymptomatic (Osman et al. 2016). The Foodborne Disease Burden Epidemiology Reference Group estimated that there were 183 million cases of giardiasis and 171,000 disability adjusted life years attributed to *Giardia* infections in 2010 (Currie et al. 2017; Torgerson et al. 2015).

The most common symptoms are diarrhea, nausea, vomiting, and weight loss (Adam 2021). The effects of *Giardia* infection can be especially detrimental to young children and in countries where *Giardia* is endemic; repeated and persistent infection is common. Recurrent infection in young children is associated with growth stunting, failure to thrive, and cognitive impairment (Berkman et al. 2002; Donowitz et al. 2016; Rogawski et al. 2017). Giardiasis has also been associated with increased risk of chronic disorders such as irritable bowel syndrome and chronic fatigue syndrome (Hanevik et al. 2014; Svendsen, Bytzer, and Engsbro 2019). Disease severity is affected by various factors, such as parasite strain and health of the host (integrating factors including age, diet, and immune response (Certad et al. 2017)).

Giardia is non-invasive and attaches extracellularly to the small intestinal epithelium using the ventral disc, a *Giardia*-specific organelle (Guerrant, Walker, and Weller 2011; Martínez-Gordillo et al. 2014). Several mechanisms, both direct and indirect, have been proposed for symptomatic infections. Cellular

pathology associated with giardiasis include: apoptosis of enterocytes (Chin et al. 2002; Panaro et al. 2007), loss of epithelial-barrier function (Troeger et al. 2007), inhibition of brush-border enzymes (Farthing 1997), microvillus shortening (Scott, Yu, and Buret 2004), malabsorption of nutrients and electrolyte imbalance (Troeger et al. 2007), and interference with bile salt metabolism (Troeger et al. 2007). The composition of the intestinal microbiota can affect the infectivity of giardiasis (Singer and Nash 2000) and *Giardia* infection has been shown to alter the microbiome composition during infection (Barash 2017a).

A better understanding of trophozoite metabolism could thus have important relevance not only for understanding cellular pathology but also for the development of anti-*Giardia* drugs. Clinically, the most commonly antiparasitic prescribed for giardiasis is metronidazole, one of the formulations in the 5-nitroimidazoles class (Watkins and Eckmann 2014). Metronidazole is a pro-drug that must be activated after entering the cell. In *Giardia*, pyruvate:ferredoxin oxidoreductase (PFOR) and thioredoxin reductase (TRR) have been proposed to reduce the prodrug into its active form (Land and Johnson 1999). However, this frontline therapy fails in up to 20% of cases (Gardner and Hill 2001; Watkins and Eckmann 2014) and there is evidence of drug resistant or drug tolerant strains of *Giardia* (Emery et al. 2018; Lalle and Hanevik 2018). Based on the impact of giardiasis in developing countries and the rising evidence of evolving drug resistance, the World Health Organization has added *Giardia* to its 'Neglected Diseases Initiative' (Savioli, Smith, and Thompson 2006).

The life cycle of *Giardia*: Trophozoites and cysts

Giardia has a simple life cycle with two stages: the proliferating trophozoite form and the infectious cyst form. The cyst is defined by its thick glycosaminoglycan cell wall (Erlandsen et al. 1996) which allows the cyst to survive and persist outside of a host. The cyst is dormant and metabolic rate is only 10-20% of that seen in trophozoites (Paget et al. 1989). The cyst is stable in the environment and is usually

transmitted to a new host through ingestion of contaminated water. Ingestion of as few as 10 cysts can be sufficient for infection (Rendtorff 1954).

Upon ingestion, the cyst passes through the acidic environment of the stomach which triggers the cyst to begin the process of excystation (Bingham and Meyer 1979; Rice and Schaefer 1981). As the trophozoites emerge from the cyst, they attach to the epithelium of proximal small intestine. The trophozoite is the disease-causing form of the parasite. The trophozoites replicate and attach along the small intestine, forming localized foci of parasites with a high concentration in the proximal small intestine (Barash 2017b). The final stage of infection involves the differentiation of the trophozoite back into the cyst form for transmission to new hosts. Encystation is induced by numerous factors, including parasite density (Barash 2017b), high levels of primary bile salts (Gillin et al. 1987), low levels of cholesterol (H D Luján et al. 1996), and a basic pH (Boucher and Gillin 1990). The cysts are then passed with the feces and have the potential to survive in the environment until they can infect a new host.

Amitochondrial trophozoites are defined by a unique microaerophilic metabolism

Giardia is often described in the literature as an “anerobic” protist, but it would be more accurate to refer to *Giardia* as a microaerophilic organism, as it thrives in environments with low dissolved oxygen (dO_2) between the range of 5-80 μM . Yet trophozoites cannot survive under atmospheric dO_2 conditions (298 μM) (Krieg and Hoffman 1986; Lindmark 1980). This microaerophilic metabolic profile is likely shaped by exposure to the fluctuating oxygen levels in the small intestine, which can range from 0-80 μM , based on the metabolic activity of host enterocytes and the oxygen affinity of members of the small intestinal microbiome (Espey 2013).

Only a few catabolic metabolic pathways have been predicted in *Giardia* (Figure 1) and confirmed by *in vitro* experiments. The glycolysis pathway is present in *Giardia* but it does have a few variations from the canonical pathway exemplified by its preference for pyrophosphate as a phosphate source. In *Giardia*,

glycolysis can generate between 2-5 molecules of ATP from one molecule of glucose, depending on enzyme usage (Figure 1). However, *Giardia* lacks most of the enzymes that form the tricarboxylic acid cycle and those involved in oxidative phosphorylation (Han and Collins 2012) and is entirely dependent on substrate-level phosphorylation for energy generation.

Additional energy is generated through pyruvate metabolism. The pyruvate produced through glycolysis can be further metabolized by three different enzymes, whose activity is linked to oxygen concentration. Thus, depending on the particular pathway, one additional molecule of ATP can be produced (Figure 1). During encystation, energy generation from glycolysis and pyruvate metabolism is significantly reduced, as an early product of glycolysis is shunted to the N-acetyl-galactosamine pathway (which makes the carbohydrate portion of the cyst wall).

Giardia can also generate one ATP molecule from arginine metabolism as the parasite possesses all of the enzymes necessary for the arginine dihydrolase (ADH) pathway (Edwards et al. 1992; P.J. Schofield et al. 1990). Based on phylogenetic analyses, the ADH pathway was most likely acquired through lateral gene transfer from anaerobic bacteria (Morrison et al. 2007). This pathway is completely independent of glycolysis and it is hypothesized that ADH pathway compensates for the reduction of ATP from glycolysis and pyruvate metabolism during encystation (Figure 1).

Novel aspects of glycolysis in *Giardia*

All the major enzymes of glycolysis were found in *Giardia* (Figure 2). Interestingly, many of these enzymes showed greater similarity to bacterial orthologues than to eukaryotic orthologs. *Giardia* glycolytic enzymes that show greater similarities to bacteria orthologues include glucokinase (GK; GL50803_8826), phosphofruktokinase (PFK; GL50803_14993), fructose-bisphosphate aldolase (FBA; GL50803_11043), glyceraldehyde-3-phosphate dehydrogenase (GAPDH; GL50803_17043), and phosphoglycerate mutase (PGM; GL50803_8822) while *Giardia* glycolytic enzymes that show greater

similarity to eukaryotic orthologues include glucose-6-phosphate isomerase (GPI; GL50803_9115), triosephosphate isomerase (TPI; GL50803_93938), phosphoglycerate kinase (PGK; GL50803_90872), and enolase (ENO; GL50803_11118) (Han and Collins 2012).

In canonical glycolysis, the first step is the energy-consuming process of converting glucose to glucose-6-phosphate and is performed by hexokinase; however, there was no evidence of hexokinase in the *Giardia* genome. Instead, *Giardia* performs the first step of glycolysis using glucokinase, an isozyme of hexokinase. Glucokinase has a lower affinity for glucose than hexokinase and it is not clear as to why *Giardia* only has a copy of the lower affinity kinase. One reason may be that there is an abundance of glucose in the small intestine, so a high affinity glucose kinase may not be necessary. This reaction requires transferring a phosphate group from a molecule of ATP, thus ATP must be present for this step of glycolysis to begin (Han and Collins 2012; Henze et al. 2001). Glucose-6-phosphate can also be obtained from the isomerization of glucose-1-phosphate through the activity of phosphoglucomutase (PGM; GL50803_17254) (Han and Collins 2012; Mitra et al. 2010). This conversion does not require a molecular of ATP and could be used to bypass the ATP requirement when ATP levels are low.

In all domains of life, the conversion of fructose-6-phosphate to fructose-1,6-bisphosphate is most often catalyzed by an ATP-dependent phosphofructokinase. This is an irreversible reaction which commits the cell to the glycolysis pathway, and, as such, is tightly regulated. However, in *Giardia*, this step is catalyzed by a pyrophosphate-dependent phosphofructokinase and this enzyme activity is reversible and unregulated as far as we know. This flexibility could be advantageous when ATP levels are low, as the preparatory phase of canonical glycolysis requires the hydrolysis of two ATP molecules, whereas when the pyrophosphate-dependent phosphofructokinase is utilized, only one ATP molecule is needed to convert one molecule of glucose into two molecules of pyruvate (Z. J. Li and Phillips 1995; E. Mertens 1993; Emmanuel Mertens 1990; Phillips and Li 1995). This step is also catalyzed by a pyrophosphate-

dependent phosphofructokinase in other protist unicellular parasites, such as *Entamoeba histolytica* (Reeves et al. 1974) and *Trichomonas vaginalis* (Emmanuel Mertens, Van Schaftingen, and Müller 1989).

The *Giardia* fructose-1,6-bisphosphate aldolase (FBA) has been a target for rational drug design, with inhibitors being predicted, synthesized, and tested *in vitro* (Galkin et al. 2009; Z. Li et al. 2011; Méndez et al. 2019). The FBA enzyme comes in two different flavors: class I (which uses an active site lysine in Schiff base formation) and class II (which uses a Zn^{2+} cofactor). Mammals operate the class I FBA mechanism and do not have class II FBAs, so the *Giardia* FBA (a class II FBA) is a good potential drug target as it impacts an important energy-generating pathway in *Giardia* but has no effect on the mammalian host (Galkin et al. 2007; Henze et al. 1998).

The *Giardia* triosephosphate isomerase (TPI) gene (ORF) has also been an attractive drug target to researchers. TPI catalyzes the reversible isomerization between glyceraldehyde-3-phosphate (GAP) and dihydroxyacetone phosphate (DAP). Although Han & Collins found that the *Giardia* TPI gene was more similar to eukaryotic orthologues (Han and Collins 2012), the structure of the *Giardia* TPI is unique and thus targetable. Structurally, TPI is usually a homodimer, but in *Giardia*, TPI may exist during some parts of the trophozoite's lifecycle as a tetramer in which two homodimers are covalently linked by disulfide bonds (Banerjee, Balaram, and Balaram 2009; López-Velázquez et al. 2004; Mowatt et al. 1994).

Protein pump inhibitors have been found to have a species-specific effect on *Giardia* TPI by binding to the Cys222 residue, disrupting the disulfide bond and the quaternary structure of the protein. Although human TPI also has a cysteine residue in the equivalent position as the *Giardia* TPI, human TPI is affected 200-fold less than *Giardia* TPI when exposed to these inhibitors. This indicates that there are unique structural differences between the two TPis, perhaps preventing inhibitor interaction by steric interference in the human form of TPI (Enríquez-Flores et al. 2011). Both omeprazole (Reyes-Vivas et al. 2014) and rabeprazole (García-Torres et al. 2016) have been shown to have a significant inhibitory effect

on *Giardia* TPI. In the field of drug development, these are two promising leads as they have already been tested and approved for use in humans for other uses.

Giardia has two enzymes that catalyze the final step of glycolysis: the conversion of phosphoenopyruvate to pyruvate, with concomitant energy production. In the canonical glycolysis pathway, this reaction is catalyzed by pyruvate kinase (PK) and generates one molecule of ATP per reaction. This enzyme is present in two copies in *Giardia* (GL50803_3206; GL50803_17143) (Park, Schofield, and Edwards 1997), but unlike other eukaryotes, pyruvate orthophosphate dikinase (POD; GL50803_9909) is also present (Hrdy, Mertens, and Nohynkova 1993). POD also converts phosphoenopyruvate into pyruvate, but it has an energetic advantage over PK, as POD produces two molecules of ATP per reaction by using pyrophosphate (as well as phosphoenopyruvate) as phosphate donors (Bruderer, Wehrli, and Köhler 1996; Hiltbold, Thomas, and Kohler 1999; E. Mertens 1993).

The parasite *Entamoeba histolytica* and anaerobic bacterium *Clostridium symbiosum* also possess POD, but in those organisms it appears to take the place of PK. *Propionibacterium shermanii* has both PK and POD, but they are separated by compartmentalization, with PK functioning in glycolysis, while POD participates in gluconeogenesis. This is because, unlike PK, POD is reversible. (Park, Schofield, and Edwards 1997). *Giardia* is missing two key gluconeogenesis genes so it is unlikely that it can convert pyruvate entirely to glucose (Han and Collins 2012). It still remains unclear as to how glycolytic metabolism is regulated through both POD and PK in *Giardia* (Hiltbold, Thomas, and Kohler 1999).

The specific activity of the *Giardia* PK enzyme is four-fold higher than that of POD, suggesting that PK does play a significant role in glycolysis (Park, Schofield, and Edwards 1997). To force glycolysis to be an ATP-generating pathway, there must be a highly exergonic reaction, preventing the reverse anabolic route. PK, as an irreversible generator of ATP, may play this role in *Giardia*. Canonical glycolysis is also controlled by intracellular ATP levels and one level of regulation involves PK as it is inhibited by ATP.

POD is not regulated by ATP, so it cannot be used to sense intracellular ATP and adjust metabolism accordingly (Park, Schofield, and Edwards 1997).

On the other hand, Feng et al. used the hammerhead ribozyme method to decrease POD transcripts. With the ribozyme activity, POD transcript level was decreased to 20% of wild type. With POD expression inhibited, the effect of PK was investigated. This decrease in POD expression was correlated with a reduction in ATP levels to 3% of normal, indicating that PK plays a very small role in energy production (Feng et al. 2008).

To round out the picture of energy generation from glucose, adenylate kinase is also active in *Giardia* (GL50803_7009). Adenylate kinase can generate one molecule of ATP and one molecule of AMP from 2 molecules of ADP. This process may increase the efficiency of glycolysis as it can generate ATP from the ADP pool, including the ADP generated during the first step of glycolysis (Rozario and Müller 1995). *Giardia* also has all of the enzymes for glycogenesis, suggesting that *Giardia* may also be able to synthesize glycogen from glucose to create an energy reserve (Han and Collins 2012).

Overview of pyruvate metabolism in *Giardia*

Under anaerobic conditions, *Giardia* produces primarily ethanol, CO₂, and some acetate based on an analysis using ¹H-NMR to monitor end products made by *Giardia* when incubated with glucose. As oxygen concentration increases, these end products shift toward production of acetate and CO₂. At a dO₂ concentration of 46 μM O₂, acetate production was 25 times greater than under anoxic conditions. Under anoxic conditions, alanine and ethanol are produced in equimolar amounts, but when oxygen is increased to 46 μM O₂, alanine could not be detected (Paget et al. 1990). This suggested that there were multiple enzymes that could metabolize pyruvate and that their activity may be influenced by oxygen concentration (Figure 2).

Alanine is produced from the activity of alanine aminotransferase (AAT) and glutamate dehydrogenase (GDH). AAT can convert pyruvate, water, and glutamate into alanine and α -ketoglutarate. The WBC6 isolate of *Giardia lamblia* has two copies of the AAT gene (GL50803_12150, GL50803_16363). GDH (GL50803_21942) converts α -ketoglutarate into glutamate, which then can be used by AAT with a new molecule of pyruvate to generate more alanine. As glutamate is being produced, GDH also oxidizes the reduced NADPH back to NADP⁺ (Paget et al. 1993). This cofactor is not used in glycolysis, so it is unclear as to what role NADP⁺ plays in *Giardia* metabolism.

As little as 0.25 μM O₂ is enough to significantly inhibit alanine production and stimulate ethanol production (Figure 2). The process of ethanol formation in *Giardia* differs from that seen in eukaryotes that have mitochondria. First, pyruvate must be converted to acetyl-CoA. In *Giardia*, this is catalyzed by an iron-sulfur protein, pyruvate:ferredoxin oxidoreductase (PFOR; GL50803_17063, GL50803_114609) rather than by the pyruvate dehydrogenase complex. Ferredoxin (Fd) is the electron acceptor in this direction and thus becomes reduced. *Giardia* then uses a bifunctional fusion enzyme, aldehyde/alcohol dehydrogenase (biADH; GL50803_93358), to first convert acetyl-CoA into acetaldehyde and then to ethanol. Both of these steps also convert a molecule of NADH to NAD⁺, regenerating the pool of the oxidized cofactor that is required for the sixth step of glycolysis (Sánchez 1998).

As oxygen concentration increases (tested up to 46 μM O₂), the end products are shifted to primarily acetate, through the activity of acetyl-CoA synthetase (ACS; GL50803_13608). The generation of acetate is also energy-producing pathway as the free energy released from the breakage of the thioester bond of acetyl-CoA can be corralled into substrate level phosphorylation, converting a molecule of ADP into a molecule of ATP (Sánchez, Galperin, and Müller 2000). Thus, colonizing the microaerophilic small intestine (where oxygen concentration can range from 0-80 μM) may provide *Giardia* with an energetic advantage (Espey 2013), allowing them to outgrow obligate anaerobes.

Metabolism during encystation in *Giardia*

Encystation is an important step in the *Giardia* life cycle and is required for transmission to new hosts. The cyst wall is composed of 40% protein and 60% carbohydrate. The protein component is composed of three cyst wall proteins (CWPs): CWP1, CWP2, CWP3 (Lauwaet et al. 2011; Hugo D. Luján et al. 1995). The carbohydrate portion is comprised of a novel N-acetyl-galactosamine (GalNac) polysaccharide (Karr and Jarroll 2004).

This pathway is tightly regulated and is one of the few where there is any information about gene regulation mechanisms. A myb-like protein was the first to be identified as a encystation-specific transcription factor (Sun et al. 2002) and its binding activates the transcription of 37 genes, most of which are hypothetical proteins, but also include the three cyst wall proteins (Morf et al. 2010) and the enzymes involved in UDP-N-acetyl-galactosamine synthesis (Lopez et al. 2003; Timothy Macechko et al. 1992).

The first enzyme in this pathway, glucosamine-6-phosphate (GNPDA), is upregulated almost 200-fold when myb activates transcription (Figure 2). The other four enzymes in this pathway (Das and Gillin 1996; Karr and Jarroll 2004; Mok et al. 2005) are also upregulated but not to the extent seen with GNPDA (Lopez et al. 2003; Timothy Macechko et al. 1992). In the first step of this synthesis pathway, fructose-6-phosphate (from the glycolysis pathway) is converted to glucosamine-6-phosphate (Keulen et al. 1998; Steimle, Lindmark, and Jarroll 1997), which is further modified by the next four enzymes of the pathway, generating the final product of N-acetyl-galactosamine for incorporation into the cyst wall. Interestingly, glucose-6-phosphate isomerase (the second step of glycolysis that converts glucose-6-phosphate into fructose-6-phosphate) is also upregulated during this phase, perhaps to keep the fructose-6-phosphate pool high to have a large amount of substrate to be sent through the N-acetyl-galactosamine synthesis pathway (Morf et al. 2010).

This glycolytic shunt, where a product of glycolysis is diverted away for cyst formation, occurs early in glycolysis, before any of the ATP-generating steps occur, so it would be expected that flux through glycolysis (and thus its ATP producing potential) would be reduced as fructose-6-phosphate is fed to the encystation pathway (Figure 2). This reduction of ATP generation through glycolysis may be compensated for by the activity of the arginine dihydrolase pathway.

Energy production by arginine metabolism in *Giardia*

Using $^1\text{H-NMR}$ to screen medium for end products and changes in amino acid concentration over time, a dramatic disappearance of arginine was observed which corresponded with the appearance of an ornithine peak (Edwards et al. 1989). These results suggested that the arginine dihydrolase (ADH) pathway was present in *Giardia* (Figure 2) and this was confirmed by enzyme assays performed on the cell supernatant. Under those conditions, the activities of the enzymes of the ADH pathway were as follows: arginine deiminase (ADI; GL50803_112103): 203 ± 64 nmoles min^{-1} mg protein^{-1} ; ornithine carbamoyltransferase (OCT; GL50803_10311): 0.7 ± 0.2 nmoles min^{-1} mg protein^{-1} ; carbamate kinase (CK; GL50803_16453): 2350 ± 250 nmoles min^{-1} mg protein^{-1} . It is thus likely that OCT is the rate limiting step of the ADH pathway (P.J. Schofield et al. 1990). This was the second time that the ADH pathway had been identified in an eukaryotic organism, with the first being another parasitic protozoan, *Trichomonas vaginalis* (Linstead and Cranshaw 1982). Of note, the activity of the *Giardia* ADI was 200-fold higher than that reported for *T. vaginalis* (P.J. Schofield et al. 1990).

All prior metabolic studies of *Giardia* metabolism have been performed in TYI medium. This medium contains 3 mM arginine. When the initial arginine concentration was increased to 10 mM, there was a concurrent increase in ammonia production, suggesting that the arginine flux through the pathway in TYI is suboptimal and the ADH pathway has the capacity to provide large amounts of energy (P.J. Schofield et al. 1990).

When arginine was depleted by pretreatment with arginase, cell growth was reduced to only 30-50% of that seen under normal conditions. On the other hand, when an additional 5 mM or 10 mM arginine was added to TYI medium, the growth rate increased. After 48 hours, the cell number had doubled compared to that seen with conventional TYI medium. Further, either the presence or absence of 50 mM glucose had no effect, indicating that the effect of arginine was independent of glucose availability. The available arginine is depleted from the medium by 48 hours, but supplementation with additional arginine at the time promoted further cell growth. Thus arginine may be an important source of energy during the early stages of *Giardia* growth (Edwards et al. 1992).

Subsequently, this enzyme assay was optimized and the activities of the three enzymes were re-evaluated. The specific activities of ADI and CK remained in the range as previously reported, but OCT activity was much higher (in the direction of citrulline utilization: 170 ± 22 nmoles min^{-1} mg protein $^{-1}$, in the direction of ornithine utilization: 2100 ± 100 nmoles min^{-1} mg protein $^{-1}$). Although these values suggest that OCT (when alone) would tend to convert ornithine to citrulline, the addition of both the ADI and CK enzymes (both of which have extremely high specific activities) keeps the ADH pathway shifted in the direction of ATP generation (Philip J. Schofield et al. 1992).

The potential arginine flux was calculated to be much greater than the potential glucose flux. At 1 mM arginine, the arginine flux rate was 30 nmoles min^{-1} mg protein $^{-1}$, while when 1 mM glucose is present, the glucose flux is only 2 nmoles min^{-1} mg protein $^{-1}$. Metabolite flux through those pathways produces ATP (one molecule from arginine, two molecules from glucose), so the energy yield when arginine and glucose are present at equimolar concentrations is approximately 30 nmoles min^{-1} mg protein $^{-1}$ ATP from arginine and 4 nmoles min^{-1} mg protein $^{-1}$ ATP from glucose, indicating that the potential energy yield from arginine may be 7-8 times higher than that from glucose. Arginine concentration in duodenal juice is between 0.2-0.4 mM, so, using 0.3 mM arginine as the physiological arginine concentration, the arginine flux and ATP yield was approximately 21 nmoles min^{-1} mg protein $^{-1}$, 3-4 fold more than that

from physiological glucose concentrations (Philip J. Schofield et al. 1992). Part of the increased flux through the ADH pathway is due to the high specific activities of all three enzymes involved, but the fact that the ADH pathway generates ATP directly by substrate-level phosphorylation is also predicted to play a role, as the ADH pathway can operate independent of oxygen tension and the need to regenerate oxidized forms of enzyme cofactors.

Using new genetic tools to interrogate *Giardia* trophozoite metabolism *in vitro* and *in vivo*

Primary studies of *Giardia* metabolism discussed were performed almost 40 years ago – before the genome, genetic tools, or modern methods of metabolomics were available. Later studies have focused on structural biochemistry and omics data, but there remain many open questions regarding basic *Giardia* metabolism. The interplay between PK and POD in glycolysis remains to be elucidated, as does the role of the ADH pathway during encystation. With the genetic tools that have been developed, we can now begin to dissect the interplay of pathways in *Giardia* both *in vitro* and in the host.

I developed luciferase-tagged strains that allow the monitoring of both transcriptional and protein-level enzyme expression *in vivo* and *in vitro*. Specifically, I created transcriptional bioreporters of the following glycolytic, pyruvate, and arginine metabolic enzymes: pyruvate:orthokinase dikinase, malate dehydrogenase, pyruvate:ferredoxin oxidoreductase, arginine deiminase, ornithine transcarbamoylase, and carbamate kinase (as well as transcriptional bioreporters for enzymes involved in other cell processes) (Figure 3).

The transcriptional strains have utility both for *in vitro* metabolic studies (Figure 3) as well as tracking expression of these key enzymes *in vivo* using non-invasive bioluminescent imaging (Figure 4). GDH-FLuc is a constitutive transcriptional bioreporter that has been well-characterized and is a proxy for *Giardia* cell number (Barash 2017b) and two new transcriptional bioreporters are described here. POD-FLuc expression steadily increased as the infection progressed (Figure 4A). GDH-FLuc (and by proxy, cell

number) begins to start decreasing on Day 06 post-infection, but POD-FLuc continues to increase up to Day 07 pi (Figure 4C) regardless of whether the infection load was increasing or decreasing. This suggests that POD is highly transcribed during infection and increases as infection progresses. An interesting follow-up would be to develop a PK-FLuc bioreporter strain and then compare the transcription of POD and PK during the course of an infection.

Cathepsin B (CTB) is a cysteine protease that is released into the extracellular environment upon interaction with host cells and is considered to be involved in immune evasion and modulation (Cotton et al. 2014). CTB-FLuc expression (Figure 4B) rose and fell in parallel with shifts in parasite load (Figure 4C). Infection usually peaks on Day 06 or Day 07 post-infection, so CTB may only play an important role during the early growth and replication, helping the trophozoites bind to the small intestine epithelium and protecting them from the host's early immune response.

Nanoluc is a small luciferase tag used to monitor protein expression. I created two C-terminal Nanoluc (NLuc) fusions of key metabolic enzymes, which provide an additional measure of metabolic enzyme expression. The arginine deiminase (ADI) gene and the pyruvate:orthophosphate dikinase (POD) gene were both tagged with Nanoluc (see Chapter 2). Nanoluc is many times brighter than firefly luciferase and both forms of luciferase can be used for noninvasive bioluminescent imaging studies. Firefly luciferase and Nanoluc each use a different substrate for light generation, so it would be possible to design *Giardia* strains where two genes are tagged and measured *in vivo*.

The following chapters focus on my development of a defined medium to monitor energy and transcriptional changes with specific medium components including amino acids, glucose, and lipids. Further, I focus on the energy generation and transcriptional analysis of ADI4XKO – the first metabolic gene knockout in *Giardia*.

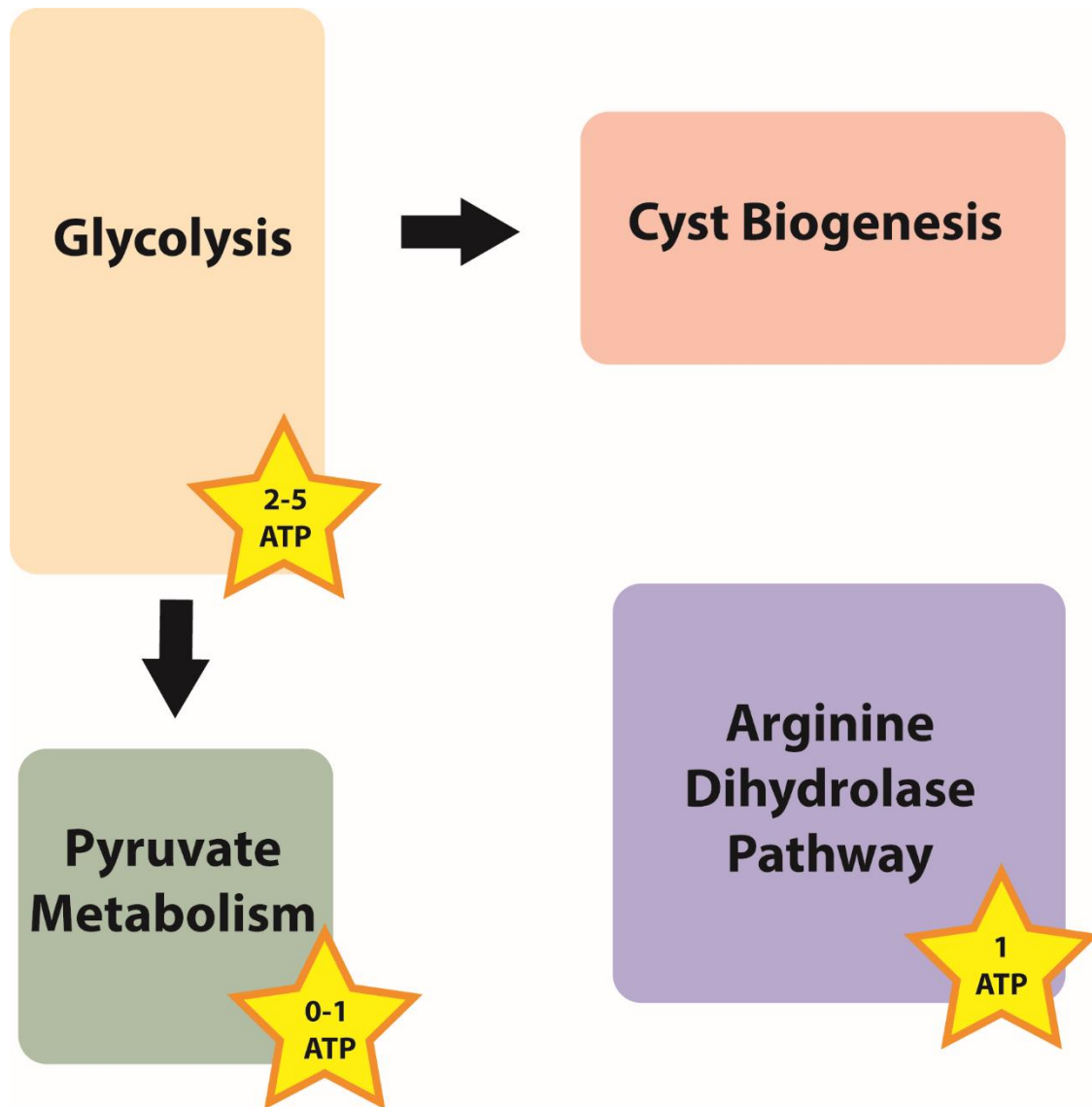


Figure 1. A simplified schematic of energy generation in *Giardia lamblia*. Depending on which enzymes are utilized, a single molecule of glucose can produce between 2-5 molecules of ATP. Pyruvate can be metabolized by three different pathways which are affected by oxygen concentration. Under microaerophilic conditions, *Giardia* can produce one molecule of ATP from one molecule of pyruvate. The arginine dihydrolase pathway is a prokaryotic pathway which produces one molecule of ATP from one molecule of arginine. Encystation is a *Giardia*-specific process that involves the production of protein and carbohydrate cyst wall components. When the N-acetyl-galactosamine cyst wall synthesis

pathway is active, a significant amount of a glycolytic intermediate, fructose-6-phosphate, is diverted from glycolysis.

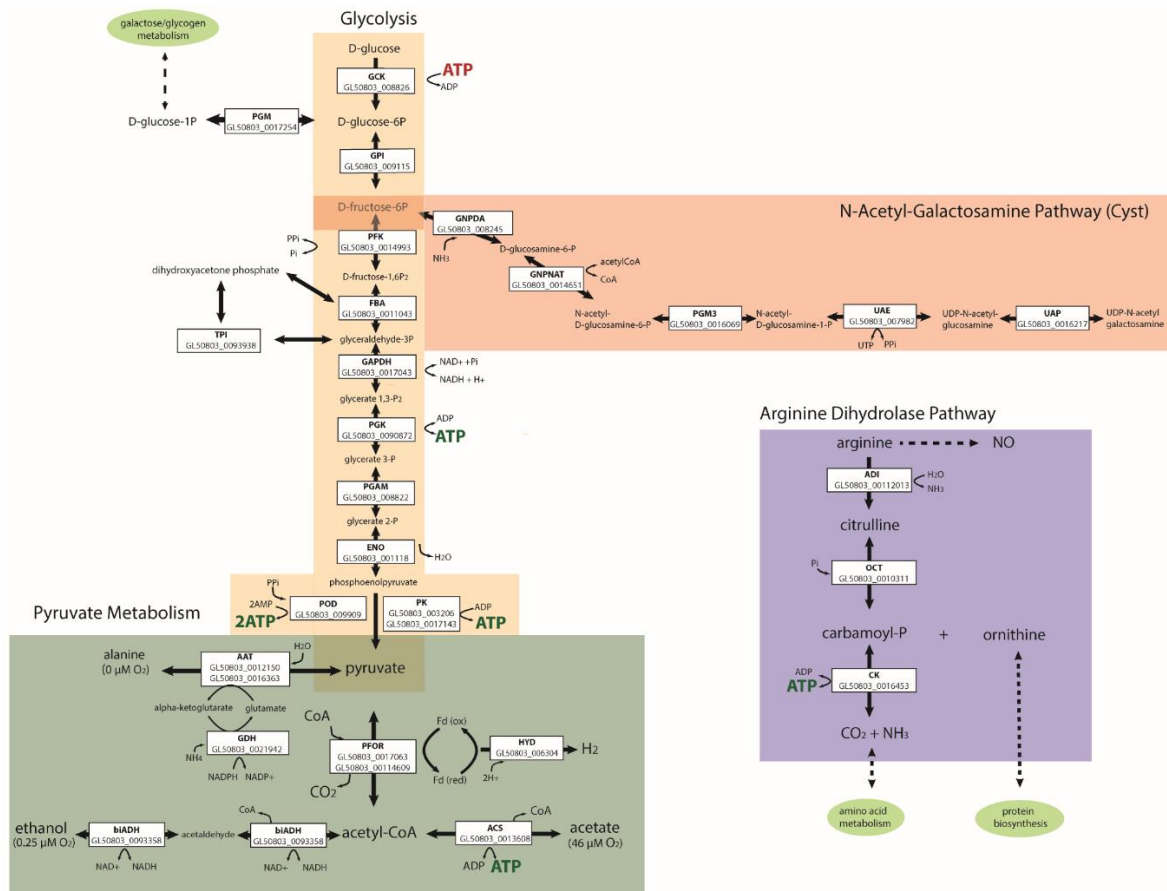


Figure 2. Detailed schematic of energy generation in *Giardia lamblia*, including ORF IDs for *Giardia*

Assemblage A, isolate WB6. Full enzyme names as follows. **Glycolysis:** GCK: Glucokinase, PGM:

Phosphoglucomutase, GPI: Glucose-6-phosphate isomerase, PFK: Phosphofruktokinase, FBA: Fructose-

bisphosphate aldolase, TPI: Triose phosphate isomerase, GAPDH: Glyceraldehyde-3-phosphate

dehydrogenase, PGK: Phosphoglycerate kinase, PGAM: Phosphoglycerate mutase, ENO: Enolase, POD:

Pyruvate:orthophosphate dikinase, PK: Pyruvate kinase. **Pyruvate metabolism:** AAT: Alanine

aminotransferase, GDH: NADP-specific glutamate dehydrogenase, PFOR: Pyruvate:ferredoxin

oxidoreductase, biADH: bifunctional alcohol/aldehyde dehydrogenase E, ACS: Acetyl-CoA synthetase.

Arginine dihydrase pathway: ADI: Arginine deiminase, OCT: Ornithine carbamoyltransferase, CK:

Carbamate kinase. **N-acetyl-galactosamine pathway:** GNPDA: Glucosamine-6-phosphate deaminase,

GNPNAT: Glucosamine-6-phosphate *N*-acetyltransferase, PGM3: Phosphoacetylglucosamine mutase,
UAP: UDP-*N*-acetylglucosamine diphosphorylase, UAE: UDP-*N*-acetylglucosamine 4-epimerase.

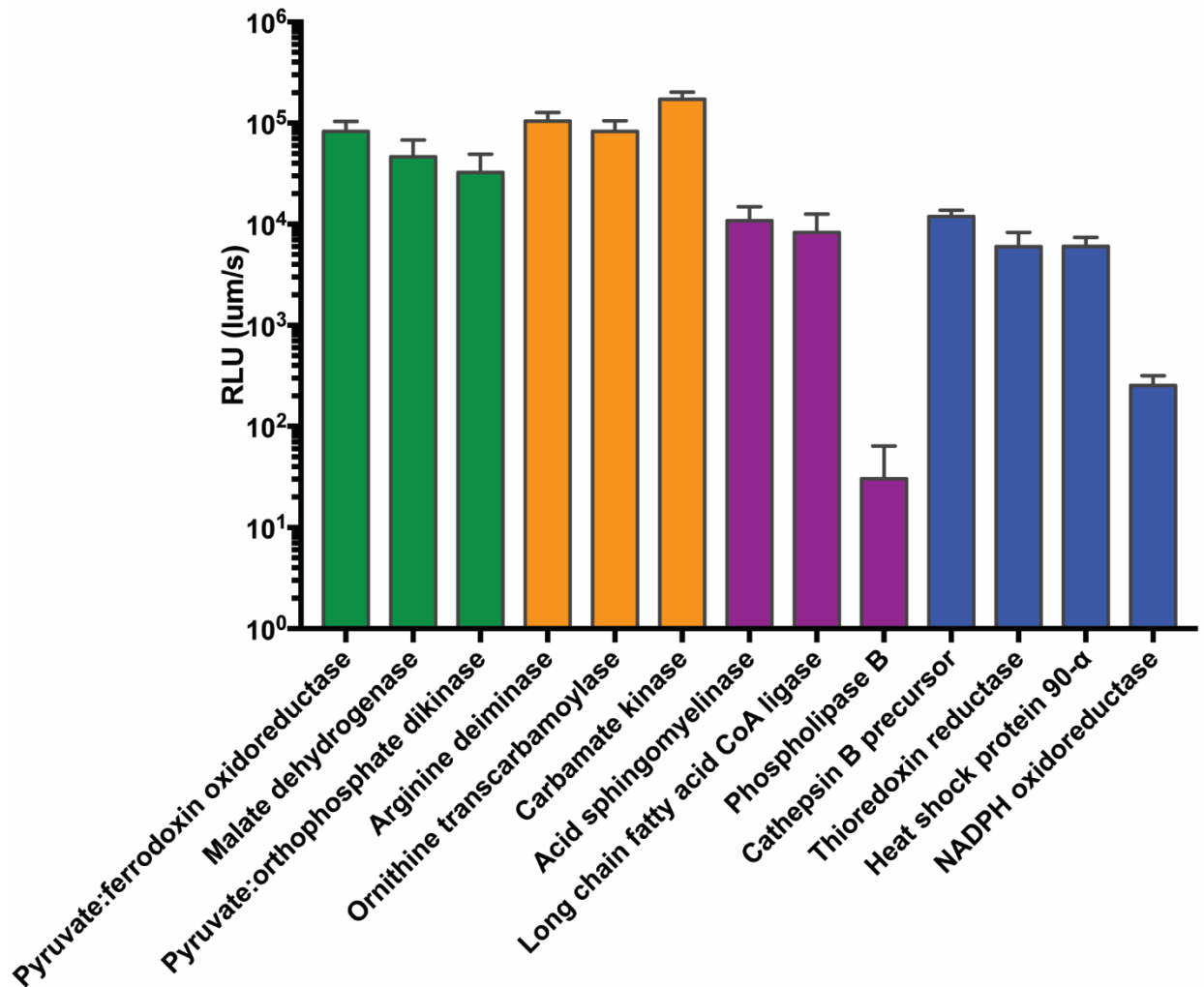
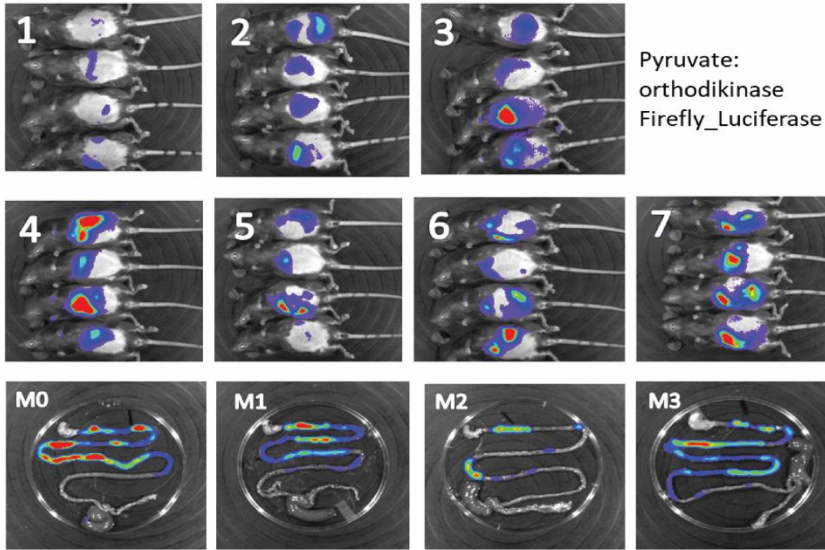
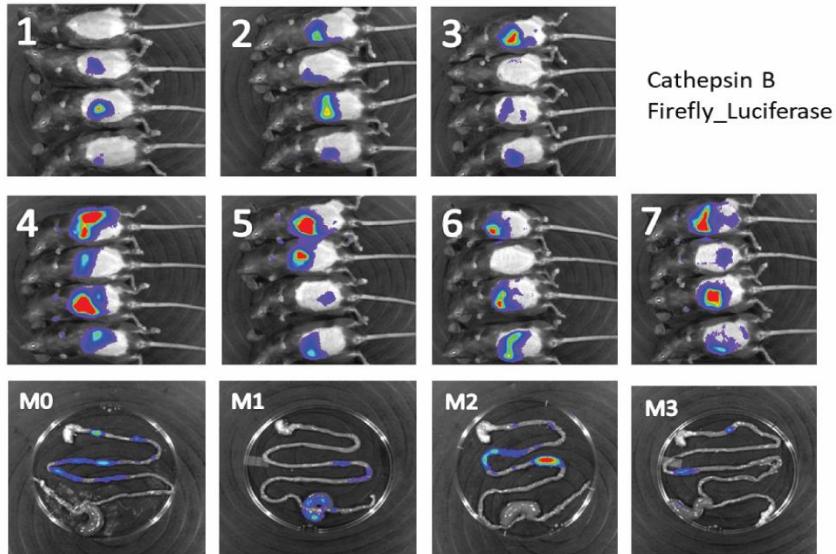


Figure 3. Transcriptional bioreporters were constructed by fusing the promoter region of the gene of interest (in *Giardia*, promoters are not yet well-defined, so the 200 bp region upstream of the start site is considered to be the 'promotor') to firefly luciferase (FLuc). Strains were incubated in TYI medium for 4 hours and then luciferase was measured using a plate reader (open filter, 3 second collections). Strains are color-coded by enzyme function: green (glycolysis, pyruvate metabolism), orange (arginine dihydrolase pathway), purple (lipid metabolism), and blue (oxidative stress response).

A



B



C

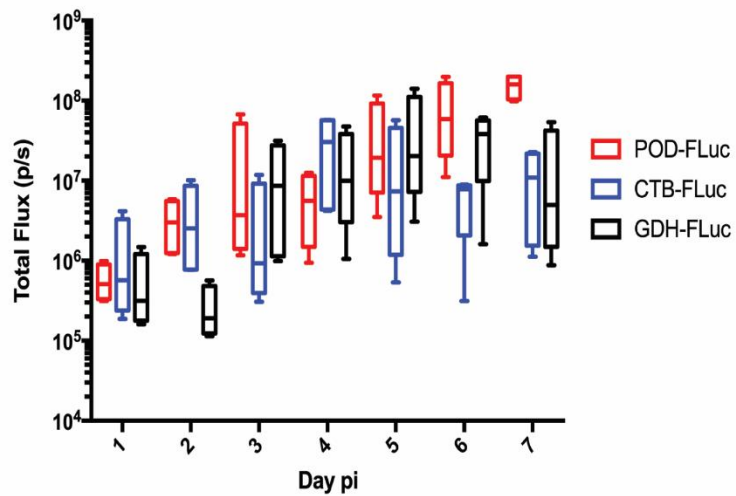


Figure 4. Transcriptional bioreporters were integrated into the *Giardia* genome to create strains that could be used to study gene expression over the course of infection *in vivo*. Mice were infected with the pyruvate:orthophosphate dikinase (POD-FLuc) strain (**A**) or the cathepsin B (CTB-FLuc) strain (**B**). Luciferase activity was measured for the first seven days of infection (using noninvasive bioluminescent imaging). The animals were sacrificed on Day 07 post-infection and the intestinal tract was imaged *ex vivo*. **C.** The GDH-FLuc strain (black) is the constitutive bioreporter that has been used in published papers and its activity over the course of an infection in a mouse has been well-described. POD-FLuc expression (red) increases over time, while CTB-FLuc (blue) peaks on day 04 post-infection and then begins to decrease.

References

- Adam, Rodney D. 2021. "Giardia Duodenalis: Biology and Pathogenesis." *Clinical Microbiology Reviews* 34(4): e00024-19.
- Banerjee, Mousumi, Hemalatha Balaram, and Padmanabhan Balaram. 2009. "Structural Effects of a Dimer Interface Mutation on Catalytic Activity of Triosephosphate Isomerase." *The FEBS Journal* 276(15): 4169–83.
- Barash, N. R. 2017a. "Giardia Alters Commensal Microbial Diversity throughout the Murine Gut." *Infect Immun* 85(6): e00948-16.
- . 2017b. "Giardia Colonizes and Encysts in High Density Foci in the Murine Small Intestine." *mSphere* 2(3): e00343-16.
- Berkman, Douglas S et al. 2002. "Effects of Stunting, Diarrhoeal Disease, and Parasitic Infection during Infancy on Cognition in Late Childhood: A Follow-up Study." *The Lancet* 359(9306): 564–71.
- Bingham, Alan K., and Ernest A. Meyer. 1979. "Giardia Excystation Can Be Induced in Vitro in Acidic Solutions." *Nature* 277(5694): 301–2.
- Boucher, S E, and F D Gillin. 1990. "Excystation of in Vitro-Derived Giardia Lamblia Cysts." *Infection and Immunity* 58(11): 3516–22.
- Bruderer, Thomas, Claudia Wehrli, and Peter Köhler. 1996. "Cloning and Characterization of the Gene Encoding Pyruvate Phosphate Dikinase from Giardia Duodenalis." *Molecular and Biochemical Parasitology* 77(2): 225–33.
- Certad, Gabriela, Eric Viscogliosi, Magali Chabé, and Simone M. Cacciò. 2017. "Pathogenic Mechanisms of Cryptosporidium and Giardia." *Trends in Parasitology* 33(7): 561–76.
- Chin, A. C. et al. 2002. "Strain-Dependent Induction of Enterocyte Apoptosis by Giardia Lamblia Disrupts Epithelial Barrier Function in a Caspase-3-Dependent Manner." *Infection and Immunity* 70(7): 3673–80.
- Cotton, J. A. et al. 2014. "Giardia Duodenalis Cathepsin B Proteases Degrade Intestinal Epithelial Interleukin-8 and Attenuate Interleukin-8-Induced Neutrophil Chemotaxis." *Infect Immun* 82(7): 2772–87.
- Currie, S. L. et al. 2017. "Under-Reporting Giardiasis: Time to Consider the Public Health Implications." *Epidemiology and Infection* 145(14): 3007–11.
- Das, Siddhartha, and Frances D. Gillin. 1996. "Giardia Lamblia: Increased UDP-N-Acetyl-d-Glucosamine And N-Acetyl-d-Galactosamine Transferase Activities during Encystation." *Experimental Parasitology* 83(1): 19–29.
- Donowitz, Jeffrey R. et al. 2016. "A Prospective Longitudinal Cohort to Investigate the Effects of Early Life Giardiasis on Growth and All Cause Diarrhea." *Clinical Infectious Diseases* 63(6): 792–97.

- Edwards, Michael R., Frances V. Gilroy, Barbara M. Jimenez, and William J. O'Sullivan. 1989. "Alanine Is a Major End Product of Metabolism by *Giardia Lamblia*: A Proton Nuclear Magnetic Resonance Study." *Molecular and Biochemical Parasitology* 37(1): 19–26.
- Edwards, Michael R., Philip J. Schofield, William J. O'Sullivan, and M. Costello. 1992. "Arginine Metabolism during Culture of *Giardia Intestinalis*." *Molecular and Biochemical Parasitology* 53(1): 97–103.
- Emery, Samantha J et al. 2018. "Differential Protein Expression and Post-Translational Modifications in Metronidazole-Resistant *Giardia Duodenalis*." *GigaScience* 7(4): giy024.
- Enríguez-Flores, Sergio et al. 2011. "Determining the Molecular Mechanism of Inactivation by Chemical Modification of Triosephosphate Isomerase from the Human Parasite *Giardia Lamblia*: A Study for Antiparasitic Drug Design." *Proteins: Structure, Function, and Bioinformatics* 79(9): 2711–24.
- Erlandsen, Stanley L., Paul T. Macechko, Harry Van Keulen, and Edward L. Jarroll. 1996. "Formation of the *Giardia* Cyst Wall: Studies on Extracellular Assembly Using Immunogold Labeling and High Resolution Field Emission SEM." *Journal of Eukaryotic Microbiology* 43(5): 416–30.
- Espey, Michael Graham. 2013. "Role of Oxygen Gradients in Shaping Redox Relationships between the Human Intestine and Its Microbiota." *Free Radical Biology & Medicine* 55: 130–40.
- Farthing, Michael J. G. 1997. "The Molecular Pathogenesis of Giardiasis." *Journal of Pediatric Gastroenterology and Nutrition* 24(1): 79–88.
- Feng, X. M. et al. 2008. "The Catalyzing Role of PPK in *Giardia Lamblia*." *Biochem Biophys Res Commun* 367(2): 394–98.
- Galkin, Andrey et al. 2007. "Characterization, Kinetics, and Crystal Structures of Fructose-1,6-Bisphosphate Aldolase from the Human Parasite, *Giardia Lamblia**." *Journal of Biological Chemistry* 282(7): 4859–67.
- . 2009. "Structural Insights into the Substrate Binding and Stereoselectivity of *Giardia* Fructose-1,6-Bisphosphate Aldolase,." *Biochemistry* 48(14): 3186–96.
- García-Torres, Itzhel et al. 2016. "Proton Pump Inhibitors Drastically Modify Triosephosphate Isomerase from *Giardia Lamblia* at Functional and Structural Levels, Providing Molecular Leads in the Design of New Antigiardiasic Drugs." *Biochimica et Biophysica Acta (BBA) - General Subjects* 1860(1, Part A): 97–107.
- Gardner, T. B., and D. R. Hill. 2001. "Treatment of Giardiasis." *Clinical Microbiology Reviews* 14(1): 114–28.
- Gillin, Frances D. et al. 1987. "Encystation and Expression of Cyst Antigens by *Giardia Lamblia* in Vitro." *Science* 235(4792): 1040–43.
- Guerrant, Richard L., David H. Walker, and Peter F. Weller. 2011. *Tropical Infectious Diseases: Principles, Pathogens and Practice E-Book*. Elsevier Health Sciences.

- Halliez, M. C., and A. G. Buret. 2013. "Extra-Intestinal and Long Term Consequences of Giardia Duodenalis Infections." *World J Gastroenterol* 19(47): 8974–85.
- Han, Jian, and Lesley J. Collins. 2012. "Reconstruction of Sugar Metabolic Pathways of Giardia Lamblia" ed. Vladimir Uversky. *International Journal of Proteomics* 2012: 980829.
- Hanevik, Kurt et al. 2014. "Irritable Bowel Syndrome and Chronic Fatigue 6 Years After Giardia Infection: A Controlled Prospective Cohort Study." *Clinical Infectious Diseases* 59(10): 1394–1400.
- Henze, Katrin et al. 2001. "Unique Phylogenetic Relationships of Glucokinase and Glucosephosphate Isomerase of the Amitochondriate Eukaryotes Giardia Intestinalis, Spiroplasma Birkbeckii and Trichomonas Vaginalis." *Gene* 281(1): 123–31.
- Henze, Katrin, Hilary G Morrison, Mitchell L Sogin, and Miklós Müller. 1998. "Sequence and Phylogenetic Position of a Class II Aldolase Gene in the Amitochondriate Protist, Giardia Lamblia1The Giardia Lamblia Fba-Sequence Has Been Submitted to GenBank under the Accession No. AF079109.1." *Gene* 222(2): 163–68.
- Hiltbold, A., R. M. Thomas, and P. Kohler. 1999. "Purification and Characterization of Recombinant Pyruvate Phosphate Dikinase from Giardia." *Molecular and Biochemical Parasitology* 104(2): 157–69.
- Hrdy, I., E. Mertens, and E. Nohynkova. 1993. "Giardia Intestinalis: Detection and Characterization of a Pyruvate Phosphate Dikinase." *Experimental Parasitology* 76(4): 438–41.
- Jensen, Lauritz A., Jerry W. Marlin, David D. Dyck, and Harold E. Laubach. 2009. "Prevalence of Multi-Gastrointestinal Infections with Helminth, Protozoan and Campylobacter Spp. in Guatemalan Children." *Journal of Infection in Developing Countries* 3(3): 229–34.
- Karr, Craig D., and Edward L. Jarroll. 2004. "Cyst Wall Synthase: N-Acetylgalactosaminyltransferase Activity Is Induced to Form the Novel N-Acetylgalactosamine Polysaccharide in the Giardia Cyst Wall." *Microbiology* 150(5): 1237–43.
- Keulen, Harry Van et al. 1998. "Cloning of Two Putative Giardia Lamblia Glucosamine 6-Phosphate Isomerase Genes Only One of Which Is Transcriptionally Activated During Encystment." *Journal of Eukaryotic Microbiology* 45(6): 637–42.
- Krieg, N R, and P S Hoffman. 1986. "Microaerophily and Oxygen Toxicity." *Annual Review of Microbiology* 40(1): 107–30.
- Lalle, Marco, and Kurt Hanevik. 2018. "Treatment-Refractory Giardiasis: Challenges and Solutions." *Infection and Drug Resistance* 11: 1921–33.
- Land, K. M., and P. J. Johnson. 1999. "Molecular Basis of Metronidazole Resistance in Pathogenic Bacteria and Protozoa." *Drug Resist Updat* 2(5): 289–94.
- Lauwaet, T. et al. 2011. "Mining the Giardia Genome and Proteome for Conserved and Unique Basal Body Proteins." *Int J Parasitol* 41(10): 1079–92.

- Li, Z. J., and N. F. B. Phillips. 1995. "Pyrophosphate-Dependent Phosphofructokinase from *Giardia Lamblia*: Purification and Characterization." *Protein Expression and Purification* 6(3): 319–28.
- Li, Zhimin et al. 2011. "Rational Design, Synthesis and Evaluation of First Generation Inhibitors of the *Giardia Lamblia* Fructose-1,6-Biphosphate Aldolase." *Journal of Inorganic Biochemistry* 105(4): 509–17.
- Lindmark, Donald G. 1980. "Energy Metabolism of the Anaerobic Protozoon *Giardia Lamblia*." *Molecular and Biochemical Parasitology* 1(1): 1–12.
- Linstead, D., and Ma Cranshaw. 1982. "Arginine Catabolism in the Parasitic Flagellate *Trichomonas-Vaginalis*." *Parasitology* 85(OCT): R19–R19.
- Lopez, A. B., K. Sener, E. L. Jarroll, and H. van Keulen. 2003. "Transcription Regulation Is Demonstrated for Five Key Enzymes in *Giardia Intestinalis* Cyst Wall Polysaccharide Biosynthesis." *Mol Biochem Parasitol* 128(1): 51–57.
- López-Velázquez, Gabriel et al. 2004. "An Unusual Triosephosphate Isomerase from the Early Divergent Eukaryote *Giardia Lamblia*." *Proteins: Structure, Function, and Bioinformatics* 55(4): 824–34.
- Luján, H D, M R Mowatt, L G Byrd, and T E Nash. 1996. "Cholesterol Starvation Induces Differentiation of the Intestinal Parasite *Giardia Lamblia*." *Proceedings of the National Academy of Sciences* 93(15): 7628–33.
- Luján, Hugo D. et al. 1995. "Identification of a Novel *Giardia Lamblia* Cyst Wall Protein with Leucine-Rich Repeats: IMPLICATIONS FOR SECRETORY GRANULE FORMATION AND PROTEIN ASSEMBLY INTO THE CYST WALL (*)." *Journal of Biological Chemistry* 270(49): 29307–13.
- Martínez-Gordillo, Mario Noé et al. 2014. "Intraepithelial *Giardia Intestinalis*: A Case Report and Literature Review." *Medicine* 93(29): e277.
- Méndez, Sara-Teresa et al. 2019. "Structure-Based Identification of a Potential Non-Catalytic Binding Site for Rational Drug Design in the Fructose 1,6-Biphosphate Aldolase from *Giardia Lamblia*." *Scientific Reports* 9(1): 11779.
- Mertens, E. 1993. "ATP versus Pyrophosphate: Glycolysis Revisited in Parasitic Protists." *Parasitology Today* 9(4): 122–26.
- Mertens, Emmanuel. 1990. "Occurrence of Pyrophosphate:Fructose 6-Phosphate 1-Phosphotransferase in *Giardia Lamblia* Trophozoites." *Molecular and Biochemical Parasitology* 40(1): 147–49.
- Mertens, Emmanuel, Emile Van Schaftingen, and Miklós Müller. 1989. "Presence of a Fructose-2,6-Bisphosphate-Insensitive Pyrophosphate: Fructose-6-Phosphate Phosphotransferase in the Anaerobic Protozoa *Trichomonas Foetus*, *Trichomonas Vaginalis* and *Isotricha Prostoma*." *Molecular and Biochemical Parasitology* 37(2): 183–90.
- Mitra, Sanghamitra, Jike Cui, Phillips W Robbins, and John Samuelson. 2010. "A Deeply Divergent Phosphoglucomutase (PGM) of *Giardia Lamblia* Has Both PGM and Phosphomannomutase Activities." *Glycobiology* 20(10): 1233–40.

- Mok, Myth T. S. et al. 2005. "Giardia Intestinalis: Molecular Characterization of UDP-N-Acetylglucosamine Pyrophosphorylase." *Gene* 357(1): 73–82.
- Morf, L. et al. 2010. "The Transcriptional Response to Encystation Stimuli in Giardia Lamblia Is Restricted to a Small Set of Genes." *Eukaryot Cell* 9(10): 1566–76.
- Morrison, H. G. et al. 2007. "Genomic Minimalism in the Early Diverging Intestinal Parasite *Giardia Lamblia*." *Science* 317(5846): 1921–26.
- Mowatt, M. R., E. C. Weinbach, T. C. Howard, and T. E. Nash. 1994. "Complementation of an Escherichia Coli Glycolysis Mutant by Giardia Lamblia Triosephosphate Isomerase." *Experimental Parasitology* 78(1): 85–92.
- Osman, Marwan et al. 2016. "Prevalence and Risk Factors for Intestinal Protozoan Infections with Cryptosporidium, Giardia, Blastocystis and Dientamoeba among Schoolchildren in Tripoli, Lebanon." *Plos Neglected Tropical Diseases* 10(3): e0004496.
- Paget, Timothy A. et al. 1989. "Respiration in the Cysts and Trophozoites of Giardia Muris." *Microbiology* 135(1): 145–54.
- . 1993. "The Effects of Oxygen on Fermentation in Giardia Lamblia." *Molecular and Biochemical Parasitology* 57(1): 65–71.
- Paget, Timothy A., Michael H. Raynor, Donald W.E. Shipp, and David Lloyd. 1990. "Giardia Lamblia Produces Alanine Anaerobically but Not in the Presence of Oxygen." *Molecular and Biochemical Parasitology* 42(1): 63–67.
- Panaro, Maria Antonietta et al. 2007. "Caspase-Dependent Apoptosis of the HCT-8 Epithelial Cell Line Induced by the Parasite Giardia Intestinalis." *FEMS Immunology & Medical Microbiology* 51(2): 302–9.
- Park, Jeong-Hyun, Philip J. Schofield, and Michael R. Edwards. 1997. "Pyruvate Kinase Is Present In Giardia Intestinalis." *Experimental Parasitology* 87(2): 153–56.
- Phillips, Nelson F. B., and Zujin Li. 1995. "Kinetic Mechanism of Pyrophosphate-Dependent Phosphofructokinase from Giardia Lamblia." *Molecular and Biochemical Parasitology* 73(1): 43–51.
- Reeves, Richard E., Dorothy J. South, Harold J. Blytt, and Lionel G. Warren. 1974. "Pyrophosphate:D-Fructose 6-Phosphate 1-Phosphotransferase: A NEW ENZYME WITH THE GLYCOLYTIC FUNCTION OF 6-PHOSPHOFRUCTOKINASE." *Journal of Biological Chemistry* 249(24): 7737–41.
- Rendtorff, Robert C. 1954. "The Experimental Transmission of Human Intestinal Protozoan Parasites: II: Giardia Lamblia Cysts given in Capsules." *American Journal of Epidemiology* 59(2): 209–22.
- Reyes-Vivas, Horacio et al. 2014. "Giardial Triosephosphate Isomerase as Possible Target of the Cytotoxic Effect of Omeprazole in Giardia Lamblia." *Antimicrobial Agents and Chemotherapy* 58(12): 7072–82.

- Rice, Eugene W., and Frank W. Schaefer. 1981. "Improved In Vitro Excystation Procedure for Giardia Lamblia Cysts." *Journal of Clinical Microbiology* 14(6): 709–10.
- Rogawski, Elizabeth T. et al. 2017. "Determinants and Impact of Giardia Infection in the First 2 Years of Life in the MAL-ED Birth Cohort." *Journal of the Pediatric Infectious Diseases Society* 6(2): 153–60.
- Roxstrom-Lindquist, K. et al. 2006. "Giardia Immunity--an Update." *Trends Parasitol* 22(1): 26–31.
- Rozario, Catherine, and Miklós Müller. 1995. "Primary Structure of a Putative Adenylate Kinase Gene of Giardia Lamblia." *Molecular and Biochemical Parasitology* 71(2): 279–83.
- Sánchez, Lidya B. 1998. "Aldehyde Dehydrogenase (CoA-Acetylating) and the Mechanism of Ethanol Formation in the Amitochondriate Protist, Giardia Lamblia." *Archives of Biochemistry and Biophysics* 354(1): 57–64.
- Sánchez, Lidya B., Michael Y. Galperin, and Miklós Müller. 2000. "Acetyl-CoA Synthetase from the Amitochondriate Eukaryote Giardia Lamblia Belongs to the Newly Recognized Superfamily of Acyl-CoA Synthetases (Nucleoside Diphosphate-Forming) *." *Journal of Biological Chemistry* 275(8): 5794–5803.
- Savioli, L., H. Smith, and A. Thompson. 2006. "Giardia and Cryptosporidium Join the 'Neglected Diseases Initiative.'" *Trends Parasitol* 22(5): 203–8.
- Schofield, Philip J., Michael R. Edwards, Jacqueline Matthews, and Justine R. Wilson. 1992. "The Pathway of Arginine Catabolism in Giardia Intestinalis." *Molecular and Biochemical Parasitology* 51(1): 29–36.
- Schofield, P.J., M. Costello, M.R. Edwards, and W.J. O'sullivan. 1990. "The Arginine Dihydrolase Pathway Is Present in Giardia Intestinalis." *International Journal for Parasitology* 20(5): 697–99.
- Scott, Kevin G.-E., Linda C. H. Yu, and André G. Buret. 2004. "Role of CD8+ and CD4+ T Lymphocytes in Jejunal Mucosal Injury during Murine Giardiasis." *Infection and Immunity* 72(6): 3536–42.
- Singer, S. M., and T. E. Nash. 2000. "The Role of Normal Flora in Giardia Lamblia Infections in Mice." *J Infect Dis* 181(4): 1510–12.
- Steimle, P. A., D. G. Lindmark, and E. L. Jarroll. 1997. "Purification and Characterization of Encystment-Induced Glucosamine 6-Phosphate Isomerase in Giardia." *Mol Biochem Parasitol* 84(1): 149–53.
- Sun, C. H. et al. 2002. "A Novel Myb-Related Protein Involved in Transcriptional Activation of Encystation Genes in Giardia Lamblia." *Mol Microbiol* 46(4): 971–84.
- Svensden, Anna Tølbøll, Peter Bytzer, and Anne Line Engsbro. 2019. "Systematic Review with Meta-Analyses: Does the Pathogen Matter in Post-Infectious Irritable Bowel Syndrome?" *Scandinavian Journal of Gastroenterology* 54(5): 546–62.
- Timothy Macechko, P. et al. 1992. "Galactosamine-Synthesizing Enzymes Are Induced When Giardia Encyst." *Molecular and Biochemical Parasitology* 56(2): 301–9.

- Torgerson, Paul R. et al. 2015. "World Health Organization Estimates of the Global and Regional Disease Burden of 11 Foodborne Parasitic Diseases, 2010: A Data Synthesis." *Plos Medicine* 12(12): e1001920.
- Troeger, Hanno et al. 2007. "Effect of Chronic Giardia Lamblia Infection on Epithelial Transport and Barrier Function in Human Duodenum." *Gut* 56(3): 328–35.
- Watkins, R. R., and L. Eckmann. 2014. "Treatment of Giardiasis: Current Status and Future Directions." *Curr Infect Dis Rep* 16(2): 396.

Chapter 2: Development of Defined Medium for *in vitro* Metabolic Assays: Amino Acids, Not Glucose, Have a Significant Effect on ATP Generation and Transcriptional Response to Nutrient Availability

INTRODUCTION

Although *Giardia* was first described in 1681 by the exquisitely curious Antonie van Leeuwenhoek, it was only in 1960 when the first attempt to culture *Giardia in vitro* occurred. Karapetyan reported that he had been able to culture a strain of *Giardia* for seven months, after the trophozoites were isolated from a human patient. This first attempt involved three organisms: *Giardia*, chicken (specifically their fibroblasts), and *Candida guilliermondii*. He was able to improve upon this method by co-culturing *Giardia* with *Saccharomyces cerevisiae*; fibroblasts were no longer necessary. Several problems persisted, though. First, the culture was not axenic, and second, no other researchers were able to culture *Giardia* using Karapetyan's methods (Meyer and Pope 1965).

The first axenic culture was established by Meyer in 1976 and used HSP-1 medium. In 1980, Visvesvara was able to transition Meyer's cell line to TP-S-1 medium, which shortened generation time to 12 hours and increased cell yields (Keister 1983). The main components of TP-S-1 Medium were casein peptone, yeast extract, maltose, and horse serum. In 1981, Gillin & Diamond were able to culture trophozoites in TYI-S-33 medium as well, but only after a reducing agent was added. Twenty reducing agents were tested and only L-cysteine, N-acetyl cysteine, glutathione, and mercaptopropionyl glycine supported growth. L-cysteine had the strongest effect. With the other 3 reducing compounds, the effect on growth was reduced: 7-33% of that observed with L-cysteine. In the absence of reducing agents, trophozoites did not survive (Gillin and Diamond 1981b).

As oxygen concentration increased, supplementation with 0.2% cysteine also delayed the onset of cell death. Although cysteine did have a protective effect when oxygen was present, it was also necessary

for viability under anoxic or hypoxic conditions. Ascorbic acid had no effect on growth, but did provide protection from damage due to oxygen exposure. In the absence of both cysteine and ascorbic acid, the trophozoites no longer attached to the cell culture tube surface (Gillin and Diamond 1981a).

It stands to reason that attempting to mimic the *in vivo* environmental conditions with the *in vitro* growth medium would further improve growth. As the *in vitro* conditions become closer to *in vivo* condition, the *in vitro* metabolic analyses become more biologically relevant. It had long been suspected that bile had a positive interaction with *Giardia*, as trophozoites localized to the small intestine where bile concentrations are highest.

Before *in vitro* culture was possible, bile experiments were conducted in animal models. When bile salts were added to the food of rats, the concentration of bile available was increased by the presence of bile salts, which also stimulated increased bile secretion by the animal. When rats infected with *Giardia muris* were put on a diet supplemented with bile salts, the number of trophozoites in the intestine was significantly increased when compared to control rats (Hegner and Eskridge 1937). The opposite was observed when infected rats were surgically altered to prevent the flow of bile into the small intestine. In all of the surgically altered rats, there was no presence of trophozoites on day one post-infection (Bemrick 1963).

Based on these observations, the next improvement to the *in vitro* medium composition was the addition of bile to the modified TYI-S-33 medium. Before the addition of bile, trophozoites had a mean generation time of 12 hours. After the addition of bile, the mean generation time was reduced to 7.5 hours with a concomitant increase in trophozoite numbers (M. J. G. Farthing, Varon, and Keusch 1983). Bile stimulated parasite uptake of cholesterol and lecithin, which has a positive effect on *Giardia* growth as *Giardia* does not have the capacity to synthesize membrane lipids and is dependent on preformed membrane phospholipids that are available in the small intestine (M. J. Farthing, Keusch, and Carey

1985; Lujan, Mowatt, and Nash 1996). The concentration of bile is important, though, because at high bile concentrations, encystation is induced (Gillin et al. 1987).

In 1983, Keister described the medium formulation that is the foundation of the medium that is used today for trophozoite growth. He called it “modified TYI-S-33” and it included a phosphate buffer, tryptone, glucose, cysteine, ascorbic acid, ferric ammonium citrate, bile, and adult bovine serum (Keister 1983). Modern laboratories may make small modifications to this recipe, primarily small changes in ascorbic acid or ferric ammonium citrate concentration. The DawsonLab makes one of the larger modifications, where half of the adult bovine serum is replaced with fetal bovine serum (Table 1). Fetal bovine serum has a high amount of growth factors and a very low level of antibodies.

Despite all of these improvements, only a handful of *Giardia* isolates can be grown *in vitro*. The workhorse of *Giardia* research is the WBC6 isolate (*Giardia intestinalis* assemblage A) and since it has been maintained *in vitro* for almost 60 years, genetic tools have been able to be developed that alter gene expression or allow for the tagging of proteins of interest. The GS isolate (from *Giardia intestinalis* assemblage B) can also be cultured *in vitro*, but is worked with less and doesn't have the wide range of genetic manipulation tools available that WBC6 does. Overall, this is very limited view of *Giardia intestinalis* biology because there are many isolates within assemblages A and B, and six other assemblages (Adam 2021).

Giardia has a two-phase life cycle, but *in vitro* methods have been focused on the trophozoite form of the parasite. In animals, trophozoites were primarily observed in the duodenum and cysts were primarily harvested from the jejunum. To induce encystation *in vitro*, an encystation medium was designed to mimic the conditions found in the jejunum. This was primarily accomplished by adding higher concentrations of bile salts to the modified TYI-S-33 medium. Exposure to high concentration of primary bile salts caused a 20-fold increase in the number of oval cells that reacted with encystation

antibodies. However, these oval cells were not water-resistant and so could not be considered true cysts (Gillin et al. 1987). By increasing the pH to 7.8 and keeping the bile concentration high, water-resistant cysts were formed (Gillin F D, Reiner D S, and Boucher S E 1988; Kane et al. 1991; Lujan, Mowatt, and Nash 1996). However, although these *in vitro* derived water-resistant cysts are structurally similar to *in vivo* derived cysts and react with encystation-specific antibodies, the infectivity of the *in vitro* cysts is significantly reduced. It is difficult to successfully infect animals with these cysts. The majority of these *in vitro* cysts also will not excyst to release the trophozoite form, although this may partially be explained by the fact that an efficient excystation medium has not been developed (J. Isaac-Renton et al. 1986; JI Isaac-Renton, Shahriari, and Bowie 1992).

Although there has been a lot of progress in the field of *in vitro Giardia* cultivation, it remains obvious that there are a number of improvements that remain to be made. One of the main drawbacks is that modified TYI-S-33 is undefined, which makes it difficult to study the impact of a specific supplement. Further, this makes *in vitro* metabolic experiments difficult, as the composition of TYI (and thus, metabolite concentrations) varies from batch to batch. Thus, the development of a defined medium for *Giardia* growth is the next logical step for progression of *in vitro* culturing techniques.

The undefined components of modified TYI-S-33 medium are the yeast extract, peptone, bovine/ovine bile, and bovine serum (Table 1). These must be replaced with defined components. For the purposes of this research, in which I wanted to specifically study the effect of individual metabolites on *Giardia* growth, a *Giardia* Base Medium (GBM) was first designed so that then metabolites and other supplements could be added to in a modular manner.

GBM was designed to be a metabolite-depleted maintenance medium, in which cells can survive but growth and ATP production would be abolished. To maintain osmotic balance and a stable pH, inorganic salts and MOPS buffer were used. Future experiments would investigate the contribution of

carbohydrates, amino acids, and lipids to *Giardia* growth, so these components were not included in GBM. Since this is a serum-free medium, all vitamins, nucleosides, and trace elements were provided. Cysteine and ascorbic acid were also added as components of GBM as they have been previously found to be essential for *Giardia* growth (see Table 2 for detailed information on GBM composition). Sodium hydroxide was used to bring the pH to 7.0 before use.

Giardia metabolism has been described in detail in Chapter 1. Based on what is known about *Giardia* metabolism, the contribution of carbohydrates, amino acids, and/or lipids to ATP production and transcriptional regulation investigated for this project. Each component was added to GBM individually or in combination (Figure 1, Table 3). Thus, the two endpoints for these experiments were ATP generation and transcriptomic response, measured by the Cell-Titer Glo viability assay and RNA-Seq, respectively.

METHODS

***Giardia* trophozoite culture conditions**

Giardia intestinalis (ATCC 50803) WBC6 was cultured in modified TYI-S-33 (TYI) medium (Keister 1983) supplemented with 6.5% bovine bile, 5% adult bovine serum, and 5% fetal bovine serum (Table 1) in sterile 16-ml screw-cap disposable tubes (BD Falcon) and incubated upright at 37C° without shaking. For metabolism and transcriptomic experiments, trophozoites were also cultured in various medium formulations (see Table 3). 100 mM stocks of each amino acid were made using standard lab reagents, except in the case of L-glutamine, where GlutaMAX (ThermoFisher) was used instead as it is much more stable in culture medium.

Quantification of ATP production

To quantify ATP production, trophozoites were first grown to confluency in 16-ml tubes. Cells were detached and harvested by incubating at 4°C for 15 minutes and pelleting by centrifugation at 900 x g for five minutes. Cells were counted using a Luna-II Automated Cell Counter (Logos Bio) and resuspended to the appropriate concentration in *Giardia* Base Medium (GBM) with or without additives. For ATP assays, cells were plated in white 96 well plates and incubated at 37°C in anoxic boxes (Mitsubishi). Three biological replicates were analyzed and each biological replicate was plated in triplicate. Each plate included a positive control (WB6 grown in TYI) and negative controls (media alone). After anaerobic incubations, ATP levels were determined using the Cell-Titer Glo Luminescent Cell Viability Assay (Promega) on a Victor X3 plate reader using 3 second exposures. Luminescence data was collected until values started to decrease. The highest luminescence value was used for data analysis and, depending on the experiment, the data was analyzed by either unpaired t-test or one-way ANOVA with post-hoc test (Tukey or Dunnett's).

Total RNA extraction and RNA-seq library preparation

For RNA extraction, cells were incubated in 25-ml cell culture flasks at 37°C in anoxic boxes. For RNA seq experiments, trophozoites were seeded at 1.0×10^6 cells/ml in 10 ml GBM with or without additives (Table 3) and incubated in T-25 tissue culture flasks in anoxic boxes at 37°C for six hours. After incubation, the medium was decanted and cells were detached using 1.5 ml TRI reagent (Zymo). RNA extraction was completed using the Direct-zol RNA Miniprep Kit (Zymo). RNA quantity was determined using the Qubit RNA BR Assay Kit (Thermo-Fisher) and RNA size fractions were visualized using 1% bleach, 1% agarose, 1X TAE, 0.5 µl/ml ethidium bromide denaturing gels. Four biological replicates were collected for each condition.

Stranded RNA libraries were prepared using the Zymo-Seq RiboFree Total RNA Library Kit (Zymo), which included a ribosomal RNA depletion step. Each library was quantified using the Qubit HS DNA Assay Kit (Thermo-Fisher) and samples were pooled in equimolar amounts. The library was sequenced using an Illumina iSeq 100 (1 x 75 bp). For GBM, there was not enough of Sample 1 to pool, so only three replicates were sequenced for this condition.

Transcriptome QC and comparative analyses

Comparative transcriptomic analyses were conducted on the Galaxy server, Release v 21.09 (Afgan et al. 2018). One of the four samples from the GBM + 10 mM arginine condition would not upload to Galaxy, so only three replicates were analyzed for this condition.

Raw sequences were trimmed using Trim Galore! (Galaxy Version 0.6.7+galaxy0) (<https://github.com/FelixKrueger/TrimGalore>) and quality was assessed using FastQC (Galaxy Version 0.7.3+galaxy0) (Andrews 2010). Trimmed sequences were mapped to the *Giardia* genome (Version: GiardiaDB-56) using RNA STAR (Galaxy Version 2.7.8a+galaxy0) (Dobin et al. 2013). Aligned reads were counted using htseq-count (Galaxy Version 0.9.1+galaxy1) (Anders, Pyl, and Huber 2015) and converted to TPM using StringTie (Galaxy Version 2.1.7+galaxy1) (Pertea et al. 2015). For information on total number of raw reads, number of trimmed reads, and mapping percentages for each sample, see Table 5.

For comparative transcriptomic analyses of medium conditions, the iDEP.95 web application (integrated Differential Expression and Pathway analysis) (Ge, Son, and Yao 2018) was used for differential gene analysis. Transcriptomic data was analyzed by both DESeq2 (Love, Huber, and Anders 2014) and limma voom (Law et al. 2014) and only genes that were identified by both programs were called as differentially expressed. Genes were considered significant when the false discovery rate (FDR) was <0.05.

Functional transcriptome annotation, metabolic pathway mapping, and partitioning analyses

Cellular functions were inferred for significant differentially expressed *Giardia* genes using analytical tools associated with GiardiaDB (<http://giardiadb.org/giardiadb/>) with subsequent manual inspection and curation of homology, functional domains, and cellular process designations according to prior experimental and bioinformatic evidence.

RESULTS

Composition and rationale for GBM + additions

Giardia Base Medium (GBM) was designed to be composed of defined reagents and lacking metabolites. GBM included a buffering system (MOPS), inorganic salts (CaCl₂, MgO₄S, KCl, NaCl, H₂NaO₄P), vitamin mix, nucleosides, and trace elements (Table 2). Cysteine was also included as it had been previously found to be required for trophozoite viability (Gillin and Diamond 1981a). Confirmation that *Giardia* cells did not lyse or die under these conditions was conducted microscopically, observing the characteristic tear-drop trophozoite shape, attachment to the culture tube wall, and motility.

For proof of concept, peptone was added to GBM. A gradient of peptone concentration was tested. There was a concentration-dependent increase in ATP production as peptone percentage increased. At 2% and 5% peptone, there was no significant difference in ATP production when compared to TYI (Figure S1). This is positive support for the GBM formulation as 2% peptone is also the concentration of peptone in TYI medium (Table 1).

Addition of peptides or amino acids alone to Giardia Base Medium returns ATP production to levels of conventional TYI medium

Metabolic components (see Table 3 and Figure 1) were added back to GBM and the Cell Titer Glo assay was used to monitor ATP generation, which used luminescence as a proxy of ATP concentration. When

known, metabolites were added back to GBM at the same concentration as used in TYI (e.g. 50 mM glucose). As peptone is undefined (and variable between batches), the concentration of 1 mM of each amino acid was chosen after comparing the amino acid concentration in common defined media. Previous research has shown that arginine is rapidly depleted from TYI medium (Edwards et al. 1992), thus, a higher concentration of arginine was used (10 mM) when arginine was the only metabolite available (GR) in order to prevent arginine depletion before experiments were completed. The actual concentration of arginine in TYI is 3 mM, but that information was obtained from collaborators after all experiments had been completed.

When incubated in GBM, *Giardia* generated significantly less ATP than when incubated in the conventional TYI medium (ordinary one-way ANOVA with Dunnett's multiple comparisons test, $p < 0.0001$) (Figure 2A). The addition of lipids alone to GBM showed no significant increase of ATP when compared to GBM and remained significantly less than TYI (ordinary one-way ANOVA with Dunnett's multiple comparisons test, $p > 0.9999$). The addition of 50 mM glucose (the concentration in TYI) also showed no significant increase in ATP production when compared to GBM (ordinary one-way ANOVA with Dunnett's multiple comparisons test, $p = 0.1618$). Only the addition of 2% peptone (the concentration in TYI) brought ATP levels up to same level as seen with TYI (ordinary one-way ANOVA with Dunnett's multiple comparisons tests, $p = 0.7974$).

As peptone is an undefined component of media, amino acids were added to GBM at a concentration of 1 mM of each of the 20 amino acids (Figure 2B). When compared to incubation in TYI, there was a significant increase in ATP when incubated in GAA (ordinary one-way ANOVA with Dunnett's multiple comparisons test, $p < 0.0001$). However, the addition of 50 mM glucose (GAAG) slightly decreased the level of ATP to the point where there was no significant difference between TYI and GAAG (ordinary one-way ANOVA with Dunnett's multiple comparisons test, $p = 0.2086$). The addition of lipids to the

amino acid mix significantly reduced ATP when compared to amino acids alone (ordinary one-way ANOVA with Dunnett's multiple comparisons test, $p=0.0002$).

When amino acids were added to GBM at a concentration of 0.1 mM each (Figure 2C), no significant increase in ATP was observed when compared to GBM (ordinary one-way ANOVA with Dunnett's multiple comparisons test, $p=0.0504$). Only when amino acids were added at a concentration of 1 mM each did ATP levels rise to the levels observed in TYI (ordinary one-way ANOVA with Dunnett's multiple comparisons test, $p<0.0001$).

In Figure 2D, when the concentration of amino acids was low (0.1 mM), the addition of 10 mM glucose did not significantly raise the level of ATP from that seen in GBM (ordinary one-way ANOVA with Dunnett's multiple comparisons test, $p=0.99916$). There was also no significant difference in ATP levels when 10 mM glucose was added to the 1 mM amino acid medium (ordinary one-way ANOVA with Dunnett's multiple comparisons test, $p=0.9322$).

The addition of lipids consistently reduced the level of ATP production, although they had no effect on ATP production when they were the only metabolic component present (Welch's t-test, $p=0.9349$). When added in the presence of glucose, ATP levels were significantly reduced when compared to glucose alone (Welch's t-test, $p=0.0374$), (Figure 2E). The same was seen when lipids were added to the 1 mM amino acid composition, but to a greater extent (Welch's t-test, $p<0.0001$).

Cells cultured in GDMM produced significantly more ATP when compared to cells cultured in TYI (Welch's t-test, $p<0.0001$) (Figure 2F).

Nanoluc is a small luciferase tag used to monitor protein expression. I created two C-terminal Nanoluc (NLuc) fusions of key metabolic enzymes: arginine deiminase (ADI) protein and the pyruvate:orthophosphate dikinase (POD) protein. These strains were incubated under different nutrient

conditions *in vitro*. Nanoluc expression (the proxy for protein level) was measured using the Nano-Glo Reporter Assay System (Promega).

Both ADI and POD protein expression was responsive to changes in nutrient availability, but ADI showed a much more robust response when incubated in any other medium besides TYI (Supplemental Figure S3A). Under other nutrient conditions (where amino acids, glucose, and lipids are either not present or provided in defined amounts), ADI_NLuc was increased in comparison to TYI, indicating that the ADI protein is significantly upregulated when nutrients are scarce, perhaps in an attempt to increase the trophozoite's scavenging ability. POD_NLuc showed a slight increase under all conditions when compared to TYI (Supplemental Figure S3B), but the response was not as great as that seen with ADI, indicating that arginine metabolism is the primary pathway adjusted when nutrient levels are changed (perhaps because of its ability to quickly generate ATP).

Medium formations that include amino acid supplements have more similar transcriptomes

Using principal component analysis, the transcriptomes from eight different culture conditions clustered into 4 distinct groups. Group 1 contains GBM, GG, and GL, which correlates with the Cell Titer Glo data as adding 50 mM glucose or a lipid mix back to the GBM did not significantly increase ATP levels. Group 2 contains GAA, GAAG, GAAL, and GDMM. These metabolic compositions are all similar to each other and each one provides the full complement of 20 amino acids for *Giardia* metabolism. GDMM combines the components of GAA, GAAG, and GAAL into one formulation and is the only form of defined medium (from this experiment) that provides glucose, amino acids, and lipids. TYI clusters by itself and forms Group 3. It is somewhat close to the Group 2 cluster, but has a significantly different transcriptional response. Group 4 (GR) behaves distinctly different from all other group.

Four primary groupings of transcriptomes are associated with either supplementation of amino acids, arginine, or glucose

Four distinct transcriptional profiles can be seen in the heat map and correlate with the clustering seen in the PCA plot. Group 1 (GBM, GG, and GL) appeared to have a completely opposite transcriptional response from that seen in Group 2 (GAA, GAAG, GAAL, and GDMM), indicating that there is a specific metabolic response to the presence of amino acids. When arginine is the only metabolite available (Group 3 - GR), there is a third transcriptional profile, which differs significantly from any of the other conditions, including the ones where all 20 amino acids were present. The TYI group (Group 4) is distinctly different from the other three groups, even though the media from Group 2 is the most similar to the composition of TYI medium. However, based on similarity analysis, Group 2 and Group 4 are more similar to each other than either of them are to Group 1 or Group 3. Biological replicates tended to have the most similar transcriptional profiles.

Each group has a set of unique genes that are always differentially expressed when compared to the other three groups

In Group 1 (low metabolic potential), there were 43 genes that were always upregulated and 31 genes that were always downregulated when compared to Groups 2-4. 22 of the 43 upregulated genes were annotated as hypothetical proteins and an additional 2 genes were unspecified products (Table 6, Supplemental Table S1). Among the genes that had some annotations were those involved in membrane transport (GL50803_95904: Amino acid transporter system N2, putative; GL50803_17315: Multidrug resistant ABC transporter ATP-binding and permease protein), mitotic regulation (GL50803_4912: Kinase, NEK; GL50803_22451: Kinase, NEK; GL50803_17075: Spindle pole protein, putative), transcription factor (GL50803_15000: TFIIH P44), amino acid metabolism (GL50803_15090: L-serine dehydratase), and lipid metabolism (GL50803_16286: Lecithin-cholesterol acyl transferase, putative) (Supplemental Table S1).

Of the downregulated genes, 19 of the 31 were hypotheticals. Genes involved in protein degradation (GL50803_21331: 26S protease regulatory subunit 7) and encystation (GL50803_15276: Glucosamine-6-phosphate isomerase, putative; GL50803_40376: High cysteine non-variant cyst protein) were annotated downregulated genes (Supplemental Table S1).

In comparison to the other three groups, Group 2 (defined amino acid mix) had few unique genes that were differentially expressed: 7 upregulated genes and 4 downregulated genes (Table 6). The upregulated genes consisted of hypotheticals (four of the seven), protein folding (GL50803_9413: Protein disulfide isomerase PDI2), and cysteine-rich membrane proteins (GL50803_113836: High cysteine membrane protein EGF-like; GL50803_87628: VSP). The downregulated genes were relatively uninformative hypothetical or Protein 21.1 genes (Supplemental Table S2).

Group 3 (arginine supplementation) has an obviously unique transcriptional profile that can be seen on the heat map (Figure 4), specifically the block of magenta genes in the middle of the chart, so unsurprisingly there was a large number of unique genes that were differentially expressed when only arginine is present for metabolism. There are 85 genes that are consistently upregulated under this condition (Table 6). More than half (52 genes) are annotated as hypothetical proteins and additionally there are 7 kinases (Supplemental Table S3).

The annotated genes include genes involved in pyruvate metabolism (GL50803_16667: Acyl-CoA synthetase; GL50803_10329: Ferredoxin Fd3), lipid metabolism (GL50803_16906: Phosphatidate cytidyltransferase), membrane transport (GL50803_8227: ATP-binding cassette protein 5; GL50803_15106: Importin beta-3 subunit), transcription (GL50803_24133: 5'-3' exoribonuclease 2; GL50803_17187: DNA-directed RNA polymerase subunit B; GL50803_16143: Transcription regulatory protein SNF2), vesicles (GL50803_102108: Clathrin heavy chain; GL50803_89622: Mu adaptin;

GL50803_16520: Sec24-like), and stress response (GL50803_17432: Heat shock protein 70; GL50803_7349: Ubiquitin) (Supplemental Table S3).

There were 35 genes that consistently downregulated in Group 3 (Table 6), but 24 of those genes were annotated as hypothetical, 5 were unspecified product, and most of the remaining genes were uninformatively annotated (Supplemental Table S3).

Group 4 (TYI) also had an obvious block of upregulated genes on the heatmap (Figure 4). There were 65 genes that were upregulated compared to the other three groups (Table 6), but the majority are hypothetical proteins or unspecified products and it was difficult to see any particular gene activity from the few annotated genes (Supplemental Table S4).

Lastly, there were 33 genes that were downregulated in Group 4 (Table 6), 18 of those being hypothetical proteins. Genes involved in transcription (GL50803_101594: CCAAT-box-binding transcription factor; GL50803_29436: DNA-directed RNA polymerase subunit B) and lipid metabolism (GL50803_7259: CDP-diacylglycerol-glycerol-3-phosphate 3-phosphatidyltransferase; GL50803_4197: Phosphatidylinositol transfer protein alpha isoform) were among those being downregulated (Supplemental Table S4).

Transcriptional differences are seen between TYI and GDMM

When compared to TYI, 71 genes were upregulated at least 2-fold in GDMM and 96 genes were downregulated at least 2-fold, but there was also a subset of these genes that showed larger fold changes. At 5-fold, 27 genes remained on the upregulation list and 17 genes were downregulated, and at 10-fold, 10 genes remained upregulated and 3 genes were downregulated (Figure 5).

Out of the genes that were upregulated at least 5-fold, 13 were hypothetical. Other genes that were upregulated included genes involved in membrane transport and signaling (GL50803_7259: CDP-

diacylglycerol-glycerol-3-phosphate 3-phosphatidyltransferase; GL50803_15008: High cysteine membrane group protein 1; GL50803_4197: Phosphatidylinositol transfer protein alpha isoform; GL50803_32658: Plasma membrane calcium-transporting ATPase 2), kinases (GL50803_16235: Kinase, CAMK CAMKL; GL50803_4191: Kinase, CMGC CDK), transcription (GL50803_101594: CCAAT-box-binding transcription factor; GL50803_6616: RNA helicase, putative), and protein folding (GL50803_9413: Protein disulfide isomerase PDI2; GL50803_11992: TCP-1 chaperonin subunit epsilon).

Out of the genes that were downregulated at least 5-fold, the majority were hypothetical or unspecified products. Four remaining genes had at least a partial annotation, but even with this information, it was difficult to identify what cellular processes are being affected (GL50803_3099: Cathepsin L-like protease; GL50803_115054: Protein 21.1; GL50803_11930: Retinoic acid induced 17-like protein; GL50803_17109: Vacuolar protein sorting 11).

DISCUSSION

ATP generation is stimulated by the presence of amino acids, but not glucose

Previous metabolic research primarily focused on either purified enzyme kinetics or whole cell response to the supplementation of undefined medium. This current research recapitulates much of what has been observed, using a simple experimental set-up where the effect of each metabolite could be observed without the confounding variables that undefined medium brings. The potential energy yield of ATP from the arginine dihydrolyase pathway (ADI) had been calculated to be 7-8-fold greater than that from glycolysis (Schofield et al. 1992). When arginine is the only metabolite available, more than two times the amount of ATP is produced than with TYI (Supplemental Figure S2A). This may partially be due to the fact that there is a different concentration of arginine in GR (10 mM) when compared to TYI

(3 mM). Significantly more ATP is also produced when arginine is the only amino acid present compared to conditions where all 20 amino acids are present (Supplemental Figure S2A).

These experiments were only run for six hours, so conclusions can only be made about metabolism occurring during the early period of colonization, but this data does suggest that arginine provides the most energetic gain during the first few hours. Further research should be conducted to further elucidate the role of arginine during early growth by comparing conditions where arginine concentration is the same (TYI should be compared to 3 mM arginine). It would also be interesting to take arginine out of the complete amino acid mix and determine the contribution of the other 19 amino acids alone without the influence of arginine.

It has been well established that metabolite flux through glycolysis is slower than flux through the ADI pathway (Schofield et al. 1992), however our current data shows that glucose makes even less of a contribution to energy production than originally predicted. The presence of glucose did not stimulate ATP production, either when glucose is the only metabolite present (Figure 2A) or when glucose is added to the complete amino acid mix (Figure 2D). Amino acid metabolism appears to be the primary player during initial colonization, but more experiments should be conducted that increase incubation time, as it has been shown that arginine is completely depleted from TYI within 48 hours (Edwards et al. 1992), so glycolysis may play a larger role as *Giardia* replicates and arginine becomes less available.

Unique transcription profiles correspond with nutrient choice and availability

An RNA-Seq experiment can only be as informative as the genome that it is being mapped back to. The first *Giardia* genome was published in 2007 (Morrison et al. 2007) and was recently updated using PacBio long-read sequencing, which resulted in a near-complete genome with improved annotations that was used for this analysis (Xu, Jex, and Svärd 2020).

Giardia uses an anaerobic metabolism and lacks some of the canonical eukaryotic organelles, including mitochondria and the Golgi apparatus, and was originally considered to be one earliest-branching eukaryotic organism (Sogin et al. 1989). The availability of genome sequencing has led to a revision of that view as *Giardia* was found to have genes for many of the missing organelles. The alternative view is that *Giardia* more likely has a reduced genome and originally had those organelles and gradually lost them as it transitioned into a parasitic lifestyle (Morrison et al. 2007). However, *Giardia* still diverged quite early and has little genetic similarity to other eukaryotes, thus, 43% of its predicted genes are annotated as “hypothetical proteins” and have no homology to any other organism and there is a lack of functional information for many of the protein coding genes (Ansell et al. 2019; Morrison et al. 2007; Xu, Jex, and Svärd 2020).

Despite these limitation, RNA-Seq experiments can still be informative and useful. More than half the genome is annotated (although sometimes this is limited to protein domain information) and these experiments also help classify hypothetical genes into groups that are responsive to specific stimuli.

When trophozoites are cultured in low-nutrient media (Group 1 – GBM, GG, GL), 43 genes were upregulated and 31 genes were downregulated. Two genes involved in membrane transport were upregulated in low-nutrient conditions, suggesting that *Giardia* may be increasing its scavenging capabilities. The fact that L-serine dehydratase was upregulated under these conditions was quite interesting. L-serine dehydratase converts serine into pyruvate and *Giardia* can metabolize pyruvate in three different ways, with one of those pathways also generating a molecule of ATP. Pyruvate is usually generated as the end product of glycolysis, but this could potentially be a way that *Giardia* can shift its metabolism to prolong its survival under stressful conditions.

Lastly, there were two genes associated with encystation were downregulated in low-nutrient conditions. Encystation may be thought of as a way for a cell to survive a stressful environment, but it is

a complex process that requires the production of high quantities of cyst-specific proteins and carbohydrates. It has been hypothesized that the arginine dihydrolase (ADH) pathway is the main source of ATP production during encystation and perhaps in conditions where the ADH pathway is not functioning and ATP yield has been significantly reduced, encystation may not be able to occur.

There was a small cluster of genes associated with amino acid metabolism (Group 2 – GAA, GAAG, GAAL, GDMM). Seven genes were upregulated and 4 were downregulated. The majority of these genes are hypothetical proteins. This could be an interesting group of hypotheticals for further study as amino acid availability was correlated with ATP production, but it remains unclear as to what pathways are associated with this production.

The greatest number of differentially expressed genes between all four groups occurred when arginine was the only metabolite available (Group 3 – GR). 85 genes are consistently upregulated and 35 genes were downregulated. Arginine had already been shown to have the greatest effect on ATP production (Supplemental Figure S2) so this was not unexpected.

There seems to be a lot of activity when arginine is the only metabolite available and genes are upregulated that are involved in transcription, membrane transport, vesicle transport, stress response, lipid metabolism, and pyruvate metabolism. However, this activity may be mostly a response to stress. The trophozoites should be able to quickly generate ATP through the arginine dihydrolase (ADH) pathway, but since they are depleted of other metabolites, these trophozoites may be ATP-rich, but unable to replicate, encyst, or build any new cellular structures. These trophozoites appear to be under stress when compared to the other three conditions, with heat shock protein 70, ubiquitin, and ferredoxin are all upregulated in Group 3.

There was also a specific gene response when trophozoites were grown in the undefined TYI medium. There were 65 upregulated genes and 33 downregulated genes in Group 4. However, the majority of the upregulated genes are hypothetical genes and the majority of those are noted as being deprecated, so there may be a less of a real response than what has been seen here.

Transcriptional regulation in response to nutrient availability

The structure of the *Giardia* genome creates a lot of questions about how the parasite controls transcription. The genome is extremely compact (Xu, Jex, and Svärd 2020) and promoter analysis indicated that only 50 bp or less upstream from the transcription start site was necessary to drive expression. These promoter regions were not similar to each other or to known eukaryotic promoter motifs, although there was AT-bias in the upstream region for many genes (Elmendorf et al. 2001).

The *Giardia* genome was analyzed to identify homologues to RNA polymerase (RNAP) subunits and transcription factors. *Giardia* contained homologues to 21 of the 28 polypeptides that compose eukaryotic RNAPI, RNAPII, and RNAPIII. Those 21 homologues comprise the catalytic core of each of the three eukaryotic RNAPs, but there may be *Giardia*-specific non-catalytic subunits that interact with the common eukaryotic subunits in order to form the complete RNA polymerase molecule (Best et al. 2004).

A search for transcription factors (TFs) in the *Giardia* genome was also conducted, using conserved DNA binding domains (DBDs). Transcription factors usually account for 2-8% of the genome. *Giardia* has about 5000 genes, so 100-200 TFs would be expected. Only 36 TFs were identified in the genome based on these DBD motifs (Aurrecochea et al. 2017). However, about 500 genes do possess more general DNA/protein interaction domains (e.g. basic leucine-zipper domains). The most well-studied *Giardia* TFs are those that regulate expression of cyst wall components. *Giardia* has five encystation-specific TFs: Myb2, PAX1, PAX2, ARID1, and WRKY homologues (Chuang et al. 2012; Pan et al. 2009; Sun et al. 2002;

Wang, Su, and Sun 2007). Encystation is an important decision in *Giardia's* life cycle so it makes sense that this process would have multiple regulation points. However, there are no known TFs that regulate gene expression during the other stages of *Giardia's* lifecycle or in response to environmental conditions, such as nutrient availability or oxidative stress.

The present work has identified transcription factors that are up or down regulated in response to nutrient availability. When nutrients are scarce (Group 1 – GBM, GG, GL), the transcription factor TFIIH P44 (GL50803_15000) is upregulated, along with several genes involved in transcription (GL50803_6616: RNA helicase, putative; GL50803_3408: U2 small nuclear ribonucleoprotein A, putative). Although there is a small set of genes that are uniquely up or downregulated during amino acid metabolism (Group 2 – GAA, GAAG, GAAL, GDMM), there are no TFs in this group.

The largest unique response to nutrient availability occurs when arginine is the only metabolic present (Group 3). There is one annotated TF (GL50803_16143: Transcription regulatory protein SNF2) that is upregulated under this condition. There were also two genes involved in transcription that were upregulated (GL50803_17187: DNA-directed RNA polymerase subunit B; GL50803_24133: 5'-3' exoribonuclease 2) and one involved in nuclear transport (GL50803_15106: Importin beta-3 subunit). The majority of genes in this list are annotated as hypothetical proteins, so there may be other kinds of regulation occurring that have not been identified yet.

When cultured in TYI, there were actually two downregulated genes that were involved with transcription: GL50803_101594 (CCAAT-box-binding transcription factor), GL50803_29436 (DNA-directed RNA polymerase subunit B). As was seen with Group 3, the majority of the genes differentially expressed in Group 4 (TYI) are also annotated as hypothetical proteins and may be sources of a *Giardia*-specific transcriptional response. Regardless, these are the first TFs candidates that react to nutrient availability and deserve further study.

Successful development of a defined metabolic medium but further work needs to be done to develop a defined growth medium

Giardia defined metabolic medium (GDMM) was designed to be a nutrient rich source of carbohydrates, amino acids, and lipids. This mirrors the nutrient-rich TYI, which also provides a source of carbohydrates, amino acids, and lipids. Despite those similarities, trophozoites react quite differently in each of these conditions. Trophozoites generate significantly more ATP when grown in GDMM for six hours than in TYI.

There was also a significantly different transcriptional response (Figure 5). In particular, genes involved in membrane transport, membrane signaling, and transcription were upregulated in GDMM compared to TYI (Table S5). This was not unexpected, as TYI is much more complex medium than GDMM. The addition of serum (with its combination of growth factors and growth inhibitors), bile, and a peptone mix creates an entirely different environment than what seen in GDMM.

This partially explains why GDMM was named defined “metabolic” medium, as it is not a true complete medium. Trophozoites actively metabolize in GDMM, but they do not seem to be able to replicate. The cells also begin to die after about 10 hours of incubation in GBMM, which is why all of the experiments were performed after 6 hours of incubation, collecting data about early metabolism. Further modification will have to be done to develop a defined metabolic medium that cells can survive in long-term, in order to be able to study what is occurring late in metabolism (when nutrients are beginning to be depleted and waste is starting to build up). The ultimate goal would be to develop a *Giardia* defined complete medium, where trophozoites are able to replicate. The complete medium could then be further modified in order to design defined versions of encystation and excystation media.

The next step in this process would be to add bile back to the defined medium. The bile used in TYI is undefined, harvested from animals, but purified individual bile salts could be substituted. A previous

study tested pure sodium taurocholate (TC), glycocholate (GC), and taurodeoxycholate (TDC) in the place of native bile. Each of these bile salts did support growth, but not to the same level as native bile (M. J. Farthing, Keusch, and Carey 1985). However, it is a promising place to start.

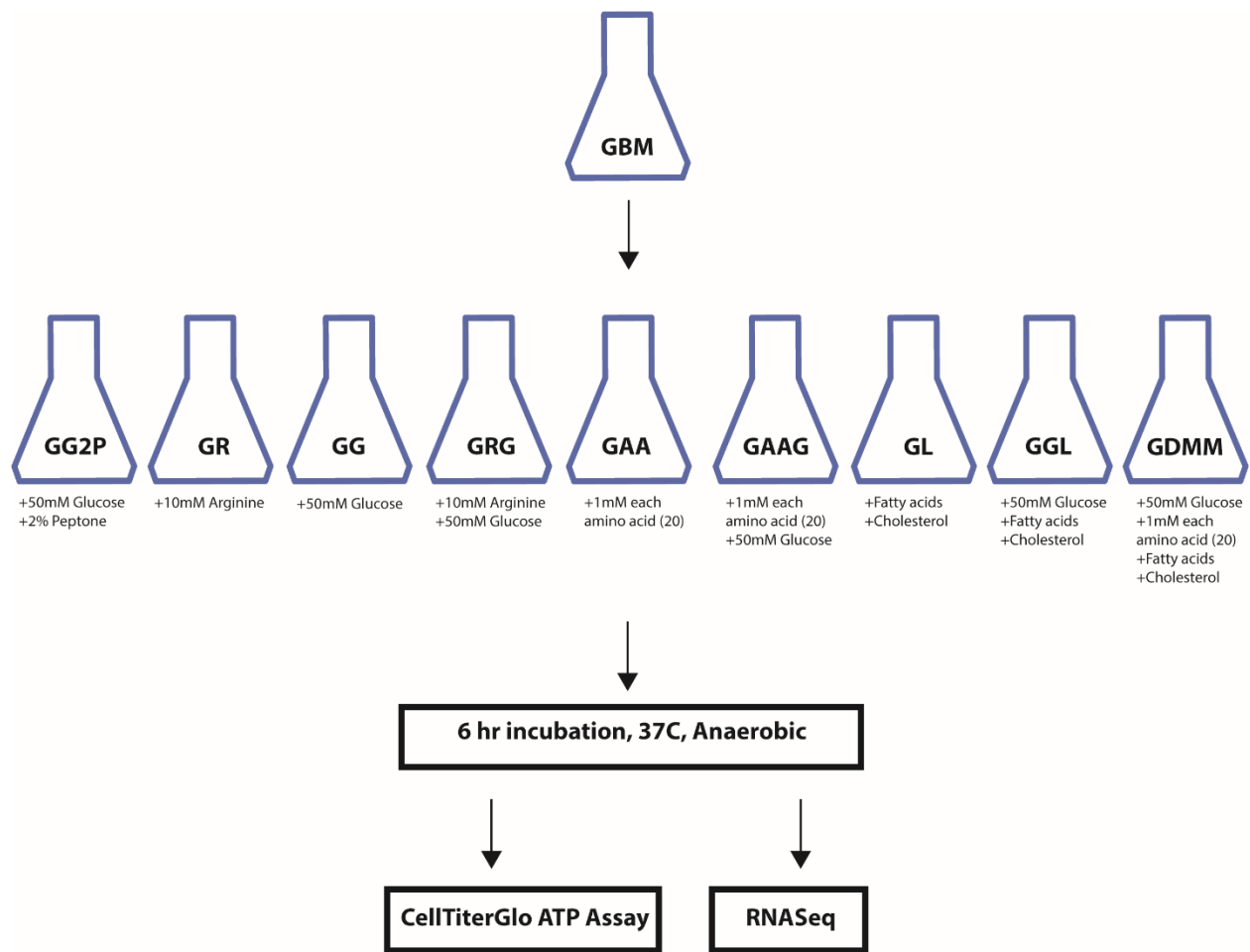


Figure 1. Schematic of experimental set-up. Amino acids, glucose, and lipids were added to GBM, both as individual components and in combination, resulting in nine culture media formulations. *Giardia* trophozoites were incubated in the defined medium for six hours under anoxic conditions. Following incubation, ATP levels were measured using the Cell Titer Glo assay or RNA was extracted for RNASeq.

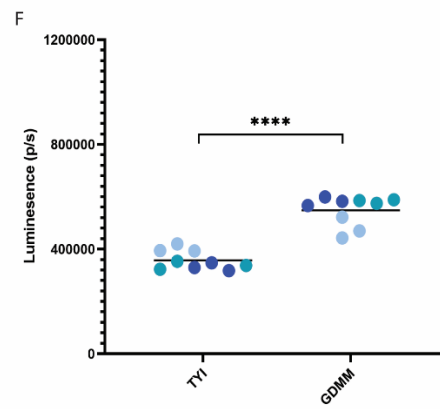
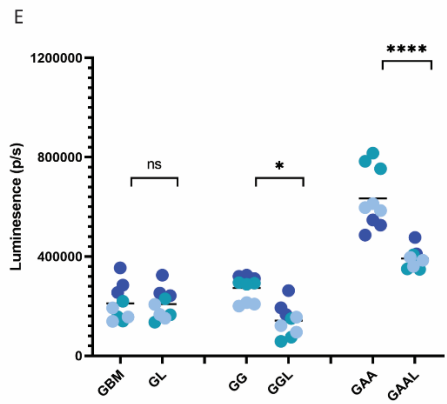
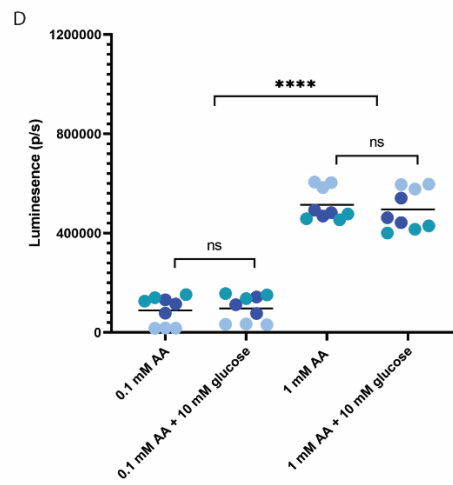
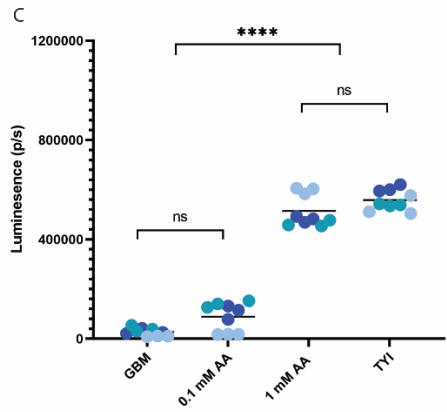
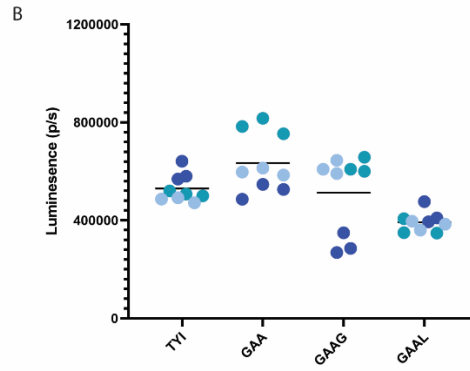
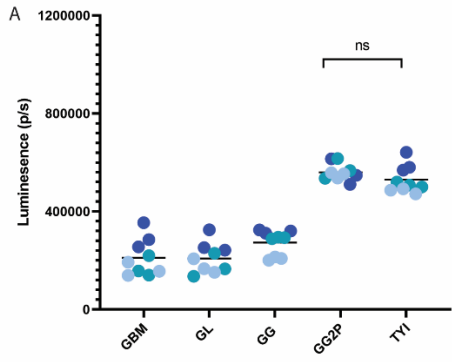


Figure 2. Sole additions of 2% peptone or amino acids in the absence of glucose to the GBM returns ATP production up to the levels observed in conventional TYI medium. **A.** No significant difference in ATP production is seen between TYI and GG2P (GBM + 50 mM glucose + 2% peptone). **B.** No significant difference in ATP production is seen between TYI and GAA (*Giardia* Base Medium + 1 mM of each of the 20 amino acids). **C.** In order to produce ATP at the same level as TYI, amino acids need to be added to GBM at a concentration of at least 1 mM. **D.** Addition of 50 mM glucose has no effect on ATP production, which is independent of amino acid concentration. **E.** The addition of lipids usually reduces ATP production. **F.** Cells cultured in GDMM produced significantly more ATP than cells cultured in TYI. Asterisk(s) indicate significance ($p < 0.05$) calculated by a one-way ANOVA (panels **A-D**) or an unpaired t-test (panel **E-F**).

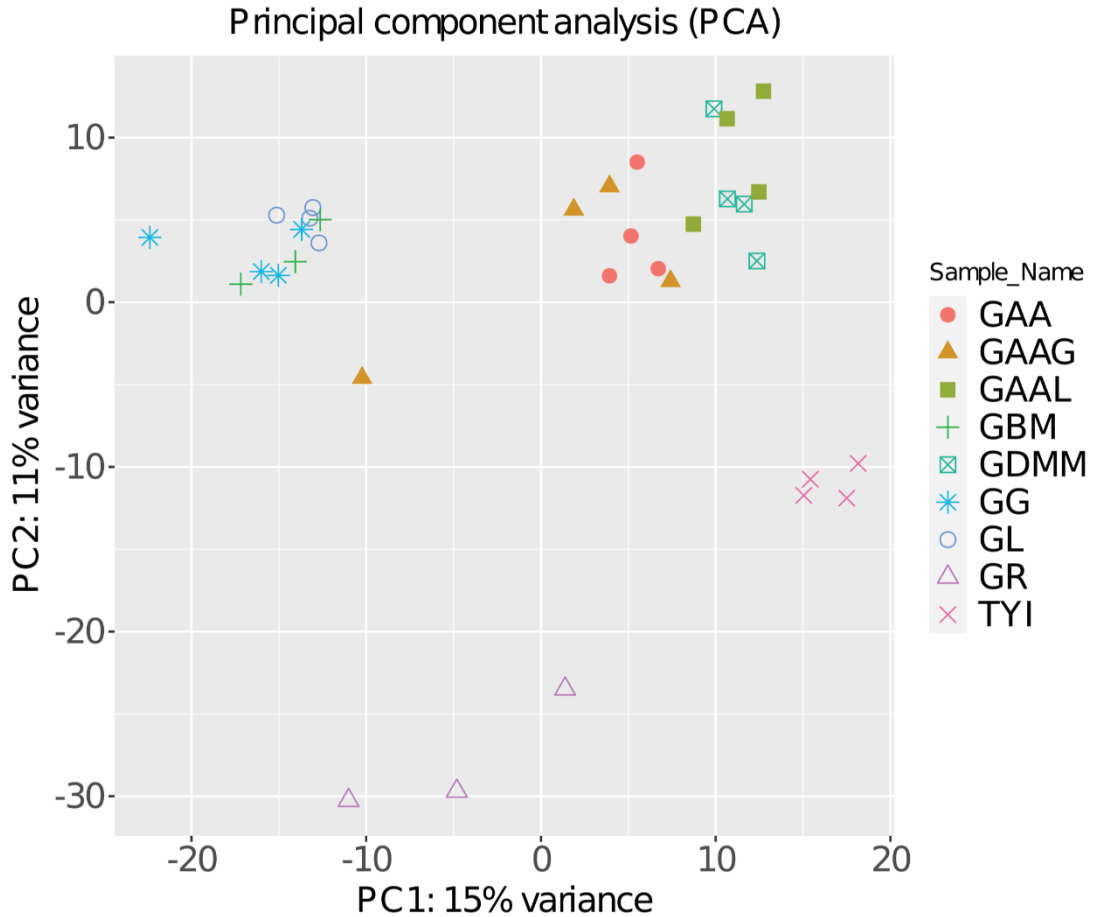


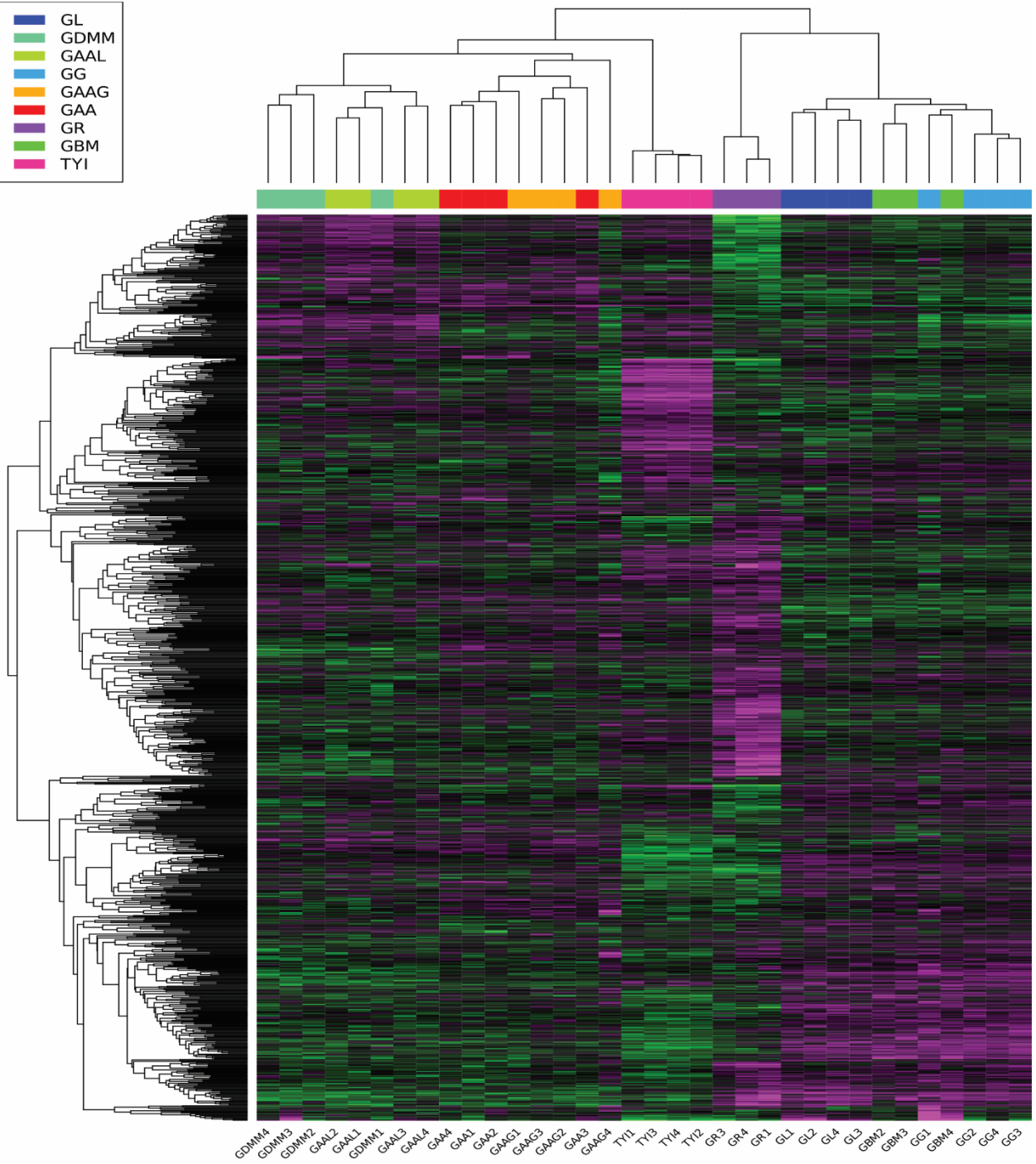
Figure 3. Media formations that include amino acid supplements have more similar transcriptomes.

Principal component analysis of transcriptomes from eight different *in vitro* culture conditions.

Biological replicates clustered together. The eight conditions clustered into four distinct groups: Group 1

(GBM, GG, and GL), Group 2 (GAA, GAAG, GAAL, and GDMM), Group 3 (TYI), and Group 4 (GR).

- GL
- GDMM
- GAAL
- GG
- GAAG
- GAA
- GR
- GBM
- TYI



CDM4
 CDM3
 CDM2
 GAAL2
 GAAL1
 CDM1
 GAAL3
 GAAL4
 GAA
 GAAL
 GAAL2
 GAAL1
 GAAL3
 GAAL2
 GAAL4
 TYI1
 TYI3
 TYI4
 TYI2
 GR3
 GR4
 GR1
 GL1
 GL2
 GL4
 GL3
 GBM2
 GBM3
 GG1
 GBM4
 GG2
 GG4
 GG3

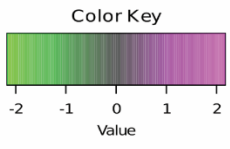


Figure 4. Four primary groupings of transcriptomes are associated with either supplementation of amino acids, arginine, or glucose. Heatmap of RNA-Seq expression z-scores computed for differentially expressed genes (FDR <0.05, fold change 2+) corresponding to the four biological replications for each culture condition or supplementation. Color represents the normalized expression level (calculated by subtracting the overall average gene abundance from the raw expression for each gene and dividing that result by the standard deviation of all of the measured counts across all samples) for each *Giardia* gene (magenta is higher than average, green is lower).

A

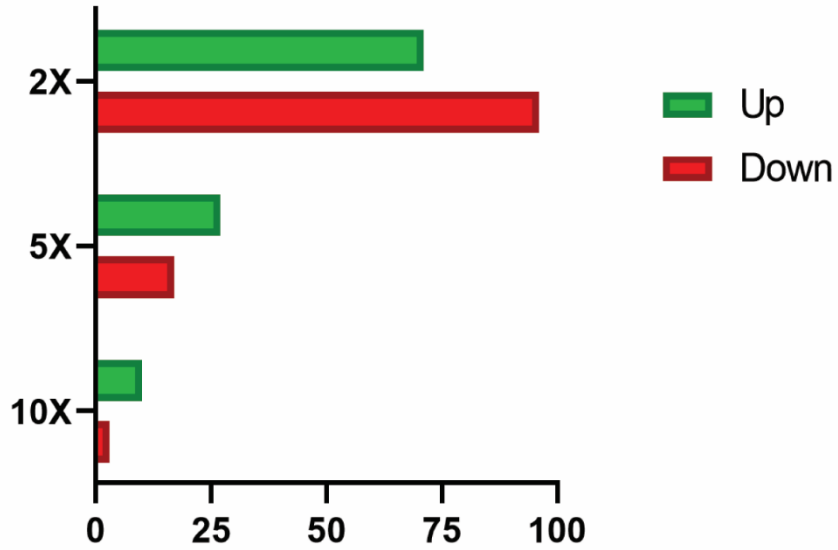


Figure 5. There were a significant number of genes that were differentially expressed when GDMM and TYI were compared. The number of up and down regulated genes (FDR < 0.005) for three fold change values are plotted. Green indicates genes that were upregulated in GDMM compared to TYI and red indicates genes that were downregulated in GDMM.

Table 1. Composition of TYI Medium (Dawson Lab Formulation)

Component	Molarity	Purpose
Potassium phosphate monobasic	4.41 mM	Buffer, phosphate source
Potassium phosphate dibasic trihydrate	5.70 mM	Buffer, phosphate source
Glucose	55.51 mM	Carbohydrate source
Sodium chloride	34.22 mM	Essential ions, osmotic balance
Yeast extract	n/a (or 1% w/v)	Amino acids, peptides, water soluble vitamins, carbohydrates, trace elements
Peptone from milk solids	n/a (or 2% w/v)	Amino acids, peptides, proteins
Cysteine-HCl	12.69 mM	Reducing agent
Ascorbic acid	0.57 mM	Antioxidant
Ferric ammonium citrate	26.11 μ M	Iron source
Bovine/ovine bile	n/a (or 0.05% w/v)	<i>Giardia</i> specific, mimics small intestine environment
Anti-Anti (Penicillin, Streptomycin)	n/a (or 1% v/v)	Anti-bacterial, anti-fungal
Bovine serum (50% adult, 50% fetal)	n/a (or 10% v/v)	Albumin, lipids, growth factors and nutrients, carriers and transfer proteins

Table 2. Composition of *Giardia* Base Medium (GBM).

Component	Final Concentration
Calcium dichloride (CaCl ₂)	1.80 mM
Magnesium sulfate (MgO ₄ S)	811.83 μM
Potassium chloride (KCl)	5.37 mM
Sodium chloride (NaCl)	109.51 mM
Dihydrogen monosodium phosphate (H ₂ NaO ₄ P)	908.84 μM
MOPS	20 mM
Sodium acetate	5 mM
EDTA	1 mM
Cysteine-HCl	12.69 mM
Ascorbic acid	0.57 mM
40X Diamond Vitamin Tween 80 Solution (Millipore-Sigma, Cat No: 58980C)	1X
100X EmbryoMax Nucleosides (Millipore-Sigma, Cat No: ES-008)	1X
1000X MP Biomedicals Trace Element Solution 1 (Fisher Scientific, Cat No: ICN676549)	1X

Table 3. Sugar, amino acid, and lipid additives to GBM Medium for comparative *in vitro* ATP and transcriptome analyses.

	Arginine GR	Glucose GG	Arginine + Glucose GRG	Glucose + Peptone GG2P	20 Amino Acids GAA	20 Amino Acids + Glucose GAAG	Lipids GL	Glucose + Lipids GGL
<i>Giardia</i> Base Medium	•	•	•	•	•	•	•	•
10 mM Arginine	•		•					
50 mM Glucose		•	•	•		•		•
2% Peptone from milk solids (Millipore-Sigma, Cat No: 212750)				•				
Complete amino acid mix (1mM each)					•	•		
Fatty Acid Supplement (Millipore-Sigma, Cat No: F7050)							•	•
SyntheChol NS0 Supplement (Millipore-Sigma, Cat No: S5442)							•	•

Table 4. Composition of *Giardia* Defined Metabolic Medium (GDMM).

Component	Final Concentration
<i>Giardia</i> Base Medium	1X
Glucose	50 mM
Complete amino acid mix	1 mM each
Fatty Acid Supplement (Millipore-Sigma, Cat No: F7050)	0.5 ml/L
500X SyntheChol NS0 Supplement (Millipore-Sigma, Cat No: S5442)	1X

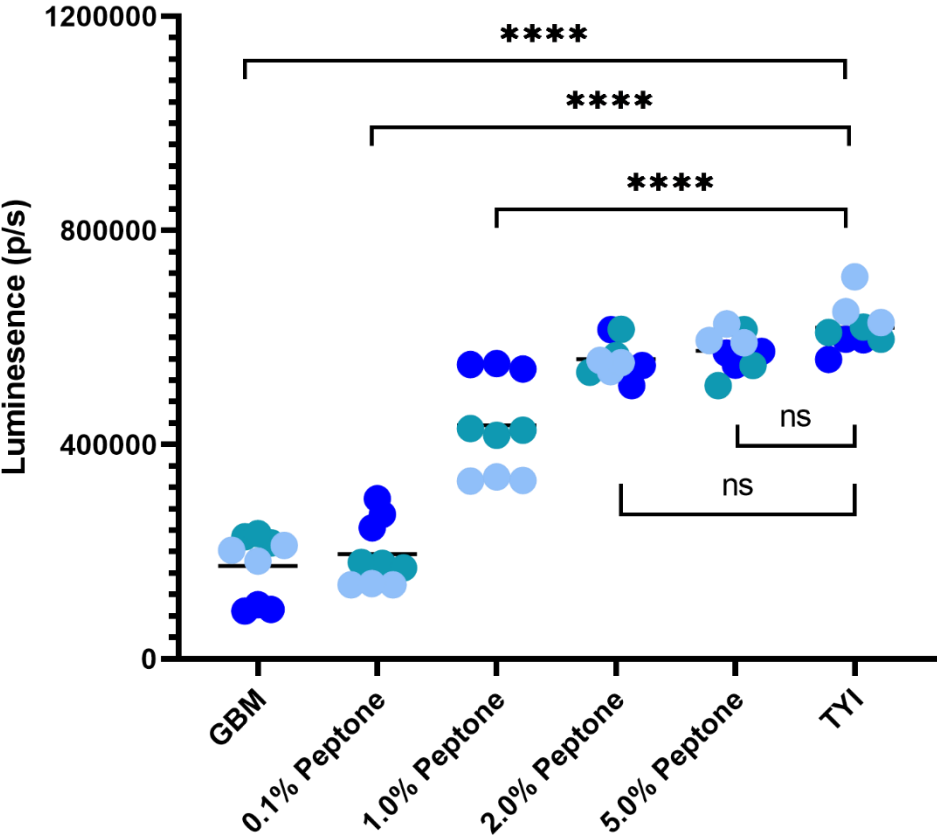
Table 5. Sequencing and mapping statistics.

	# of raw reads	# of trimmed reads	% mapped
TYI1	197091	196630	98.94
TYI2	249716	247993	98.24
TYI3	190491	189919	98.72
TYI4	227525	225415	98.51
GBM2	199927	194048	96.29
GBM3	186565	179479	95.86
GBM4	283779	237030	81.2
GG1	461505	337480	59.88
GG2	220551	218404	97.69
GG3	204206	202547	97.77
GG4	258700	250786	95.55
GL1	185853	165373	87.38
GL2	144170	130314	88.47
GL3	182062	171802	93.05
GL4	170240	159672	92.54
GR1	194509	194048	96.29
GR3	180038	179479	95.86
GR4	162951	160637	97.57
GAA1	193668	192437	77.48
GAA2	224204	218658	73.08
GAA3	258135	245044	91.09
GAA4	217527	214172	76.23
GAAG1	260514	254946	73.04
GAAG2	183834	179632	92.55
GAAG3	186261	182258	93.45
GAAG4	161536	158590	93.33
GAAL1	168446	162566	95.2
GAAL2	148305	144878	96.17
GAAL3	166773	159606	93.97
GAAL4	154181	150323	95.75
GDMM1	182158	178816	97.16
GDMM2	133189	131302	97.65
GDMM3	213672	192876	88.06
GDMM4	142548	128832	94.73

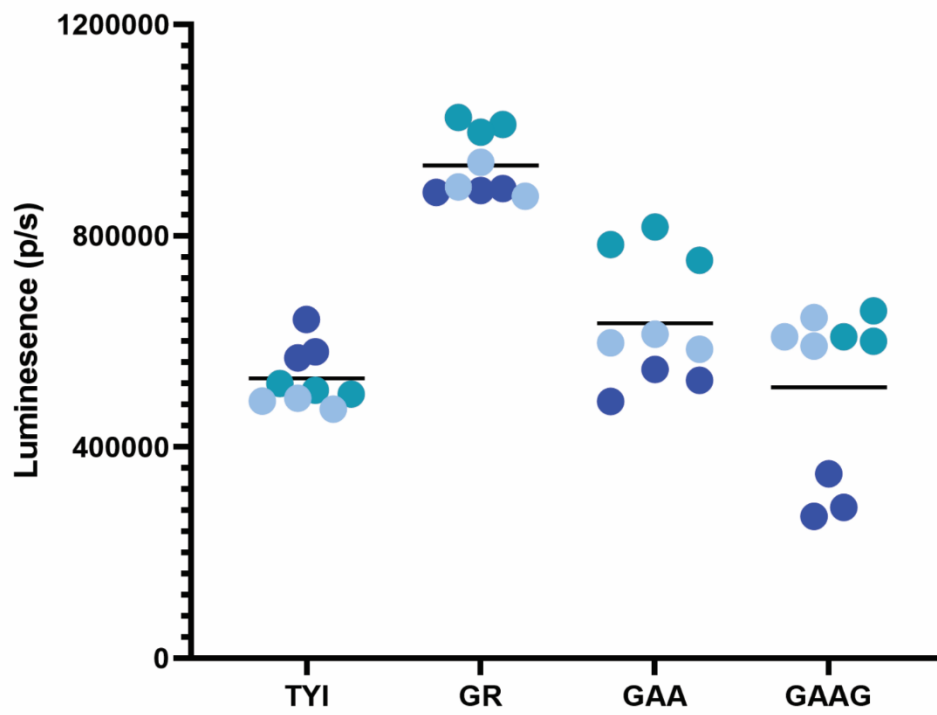
Table 6. Number of unique differentially expressed genes from each group.

	Up-regulated	Down-regulated
Group 1 (GBM, GG, GL)	43	31
Group 2 (GAA, GAAG, GAAL, GDMM)	7	4
Group 3 (GR)	85	35
Group 4 (TYI)	65	33

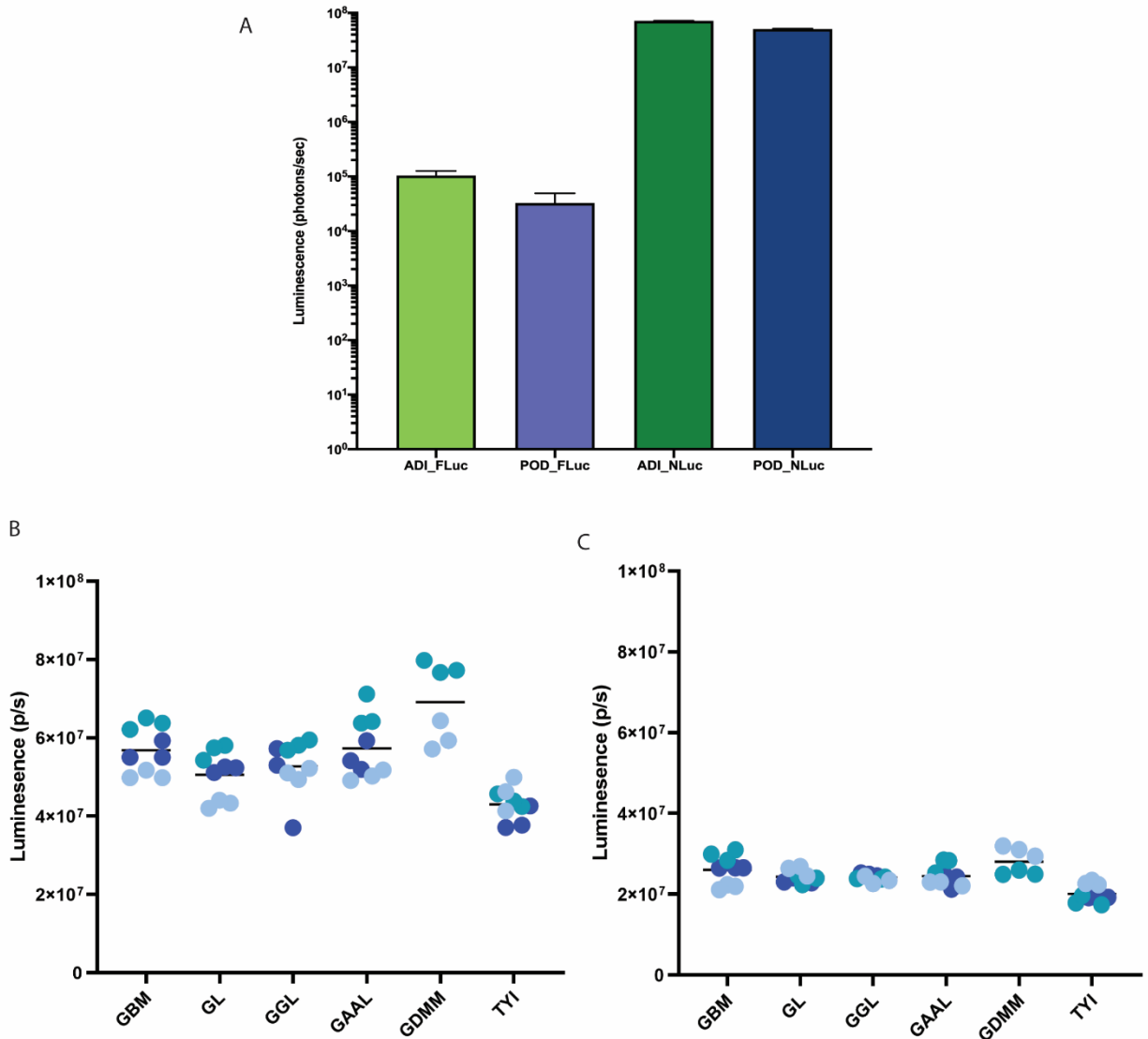
SUPPLEMENTAL MATERIAL



Supplemental Figure S1. Adding peptone to GBM increases ATP production. When there is at least 2% peptone present, ATP levels are not significantly different from TYI. TYI medium contains 2% peptone. Asterisk(s) indicate significance ($p < 0.05$) calculated by a one-way ANOVA.



Supplemental Figure S2. ATP levels were highest in GR and almost twice as high as seen in TYI, measured using Cell Titer Glo.



Supplemental Figure S3. C-terminal Nanoluc fusions were created to measure protein level *in vitro*. **A.** Nanoluc is a modified luciferase that is much brighter than firefly luciferase. **B.** ADI_NLuc protein levels were very responsive to changes in nutrient availability when compared to ADI_NLuc protein levels when grown in TYI medium. **C.** POD_NLuc protein levels were not as responsive to changes in nutrient availability as ADI_NLuc protein levels.

Supplemental Table S1. Differentially expressed genes that are specific to Group 1 (GBM, GG, GL).

Group 1 (GBM, GG, GL)

Upregulated

Gene ID	Product Description	Deprecated?	Protein Length	Pfam ID	Pfam Description
GL50803_102110	hypothetical protein	No	810	N/A	N/A
GL50803_102477	hypothetical protein	Yes	85	N/A	N/A
GL50803_10758	hypothetical protein	No	443	N/A	N/A
GL50803_112846	Kinesin-3	No	1095	PF00225	Kinesin motor domain
GL50803_11380	hypothetical protein	No	493	N/A	N/A
GL50803_114230	hypothetical protein	No	605	N/A	N/A
GL50803_11446	hypothetical protein	No	673	N/A	N/A
GL50803_13947	hypothetical protein	No	704	N/A	N/A
GL50803_14208	hypothetical protein	No	832	PF00752;PF00867	XPG N-terminal;XPG-I domain
GL50803_15000	TFIIH P44	No	406	PF04056	Ssl1-like
GL50803_15090	L-serine dehydratase	No	516	PF03313;PF03315	Serine dehydratase-like, alpha subunit;Serine dehydratase beta chain
GL50803_15404	hypothetical protein	No	1056	PF02278;PF08124	Polysaccharide lyase family 8, central domain;Polysaccharide lyase 8, N-terminal alpha-helical
GL50803_15416	hypothetical protein	No	1054	N/A	N/A
GL50803_15988	hypothetical protein	No	1215	N/A	N/A
GL50803_16184	hypothetical protein	No	624	N/A	N/A
GL50803_16222	hypothetical protein	No	1703	N/A	N/A
GL50803_16286	Lecithin-cholesterol acyl transferase, putative	No	1058	PF02450	Lecithin:cholesterol/phospholipid:diacylglycerol acyltransferase
GL50803_16444	Protein 21.1	No	759	PF12796	Ankyrin repeat-containing domain
GL50803_16672	Protein 21.1	No	960	PF12796	Ankyrin repeat-containing domain
GL50803_16793	hypothetical protein	No	1263	N/A	N/A
GL50803_17075	Spindle pole protein, putative	No	780	N/A	N/A
GL50803_17315	Multidrug resistance ABC transporter ATP-binding and permease protein	No	933	PF00005	ABC transporter-like
GL50803_17406	Phosphoinositide-3-kinase, class 3	No	1638	PF00454;PF00792	Phosphatidylinositol 3-/4-kinase, catalytic domain;Phosphatidylinositol 3-kinase, C2 domain
GL50803_17593	hypothetical protein	No	845	N/A	N/A
GL50803_221691	Histone methyltransferase HMT2	No	677	PF00856	SET domain
GL50803_22451	Kinase, NEK	No	1017	PF00069	Protein kinase domain
GL50803_29181	hypothetical protein	No	376	N/A	N/A
GL50803_31597	unspecified product	Yes	200	N/A	N/A

GL50803_3169	Cathepsin L precursor	No	564	PF00112	Peptidase C1A, papain C-terminal
GL50803_3408	U2 small nuclear ribonucleoprotein A, putative	No	385	PF14580	N/A
GL50803_3647	hypothetical protein	No	701	N/A	N/A
GL50803_4912	Kinase, NEK	No	296	PF00069	Protein kinase domain
GL50803_5248	hypothetical protein	No	229	PF00249;PF13921	SANT/Myb domain
GL50803_6616	RNA helicase, putative	No	792	PF00270;PF00271	DEAD/DEAH box helicase domain;Helicase, C-terminal
GL50803_7710	Protein 21.1	No	727	PF12796	Ankyrin repeat-containing domain
GL50803_7723	hypothetical protein	No	702	PF00787	Phox homologous domain
GL50803_8738	hypothetical protein	No	661	PF14779	Bardet-Biedl syndrome 1, N-terminal
GL50803_87472	hypothetical protein	No	1515	N/A	N/A
GL50803_8803	Protein 21.1	No	942	PF12796	Ankyrin repeat-containing domain
GL50803_92673	CHL1-like protein	No	808	PF06733;PF13307	DEAD2;ATP-dependent helicase, C-terminal
GL50803_9367	hypothetical protein	No	813	N/A	N/A
GL50803_95904	Amino acid transporter system N2, putative	No	559	PF01490	Amino acid transporter, transmembrane domain
GL50803_9605	hypothetical protein	No	637	N/A	N/A

Downregulated

Gene ID	Product Description	Deprecated?	Protein Length	Pfam ID	Pfam Description
GL50803_104234	hypothetical protein	No	643	N/A	N/A
GL50803_10783	Thiosulfate sulfurtransferase	No	395	PF00581	Rhodanese-like domain
GL50803_11034	hypothetical protein	No	223	N/A	N/A
GL50803_114671	Protein 21.1	No	631	PF00023;PF12796	Ankyrin repeat;Ankyrin repeat-containing domain
GL50803_13993	hypothetical protein	Yes	75	N/A	N/A
GL50803_14390	hypothetical protein	No	1529	N/A	N/A
GL50803_15276	Glucosamine-6-phosphate isomerase, putative	No	568	PF02585	N-acetylglucosaminyl phosphatidylinositol deacetylase-related
GL50803_15292	hypothetical protein	No	335	PF04193	PQ-loop repeat
GL50803_15338	Kinase, NEK-frag	No	313	PF00069	Protein kinase domain
GL50803_15573	hypothetical protein	No	744	N/A	N/A
GL50803_15897	hypothetical protein	No	631	PF00258;PF00667	Flavodoxin/nitric oxide synthase;Sulfite reductase [NADPH] flavoprotein alpha-component-like, FAD-binding
GL50803_16424	hypothetical protein	No	252	N/A	N/A
GL50803_16948	Nucleolar protein NOP2	No	502	PF01189;PF17125	SAM-dependent methyltransferase RsmB/NOP2-type;Ribosomal RNA small subunit methyltransferase F, N-terminal
GL50803_19276	hypothetical protein	Yes	111	N/A	N/A
GL50803_20849	hypothetical protein	Yes	124	N/A	N/A
GL50803_21331	26S protease regulatory subunit 7	No	401	PF00004;PF17862	ATPase, AAA-type, core;AAA ATPase, AAA+ lid domain

GL50803_2777	hypothetical protein	No	140	N/A	N/A
GL50803_31383	hypothetical protein	Yes	204	N/A	N/A
GL50803_32234	hypothetical protein	Yes	95	N/A	N/A
GL50803_33592	hypothetical protein	No	805	N/A	N/A
GL50803_33956	hypothetical protein	Yes	78	N/A	N/A
GL50803_37353	Ser/Thr protein kinase	No	828	PF12796	Ankyrin repeat-containing domain
GL50803_3867	hypothetical protein	No	533	N/A	N/A
GL50803_38948	hypothetical protein	Yes	66	N/A	N/A
GL50803_40376	High cysteine non-variant cyst protein	No	1609	PF03302	Giardia variant-specific surface protein
GL50803_4246	PRIP-interacting protein PIPMT	No	300	PF09445	RNA cap guanine-N2 methyltransferase
GL50803_5661	RNA binding protein	No	236	PF01778;PF04874	Ribosomal L28e/Mak16;Mak16 protein
GL50803_94542	hypothetical protein	No	1471	N/A	N/A
GL50803_95449	hypothetical protein	Yes	119	N/A	N/A
GL50803_97130	Kinase, NEK	No	697	PF00069;PF12796	Protein kinase domain;Ankyrin repeat-containing domain
GL50803_9894	Protein phosphatase 2A regulatory subunit, putative	No	892	PF13499;PF17958	EF-hand domain;PP2A regulatory subunit B'', EF-hand domain

Supplemental Table S2. Differentially expressed genes that are specific to Group 2 (GAA, GAAG, GAAL, GDCM).

Group 2 (GAA, GAAG, GAAL, GDCM)

Upregulated

Gene ID	Product Description	Deprecated?	Protein Length	PFam ID	PFam Description
GL50803_113836	High cysteine membrane protein EGF-like	No	1691	N/A	N/A
GL50803_16543	hypothetical protein	No	577	N/A	N/A
GL50803_27479	hypothetical protein	Yes	43	N/A	N/A
GL50803_31469	hypothetical protein	Yes	89	N/A	N/A
GL50803_38475	hypothetical protein	Yes	55	N/A	N/A
GL50803_87628	VSP	No	616	PF03302	Giardia variant-specific surface protein
GL50803_9413	Protein disulfide isomerase PDI2	No	449	PF00085;PF13848	Thioredoxin domain

Downregulated

Gene ID	Product Description	Deprecated?	Protein Length	PFam ID	PFam Description
GL50803_115054	Protein 21.1	No	947	PF12796;PF13920	Ankyrin repeat-containing domain
GL50803_32741	TAR RNA loop binding protein, putative	No	1127	PF00588	tRNA/rRNA methyltransferase, SpoU type
GL50803_41467	Protein 21.1, putative	No	1130	PF12796;PF13920	Ankyrin repeat-containing domain
GL50803_9807	hypothetical protein	No	1403	PF13923	N/A

Supplemental Table S3. Differentially expressed genes that are specific to Group 3 (GR).

Group 3 (GR)

Upregulated

Gene ID	Product Description	Deprecated?	Protein Length	PFam ID	PFam Description
GL50803_101194	hypothetical protein	No	1416	PF07885	Potassium channel domain
GL50803_101699	Protein 21.1	No	1062	PF12796	Ankyrin repeat-containing domain
GL50803_102108	Clathrin heavy chain	No	1871	PF00637;PF13838	Clathrin, heavy chain/VPS, 7-fold repeat
GL50803_102322	hypothetical protein	No	901	PF13641	N/A
GL50803_103125	hypothetical protein	No	1728	N/A	N/A
GL50803_10329	Ferredoxin Fd3	No	64	PF13187	4Fe-4S ferredoxin-type, iron-sulphur binding domain
GL50803_10361	P60 katanin	No	648	PF00004	ATPase, AAA-type, core
GL50803_10573	Protein 21.1	No	369	PF12796	Ankyrin repeat-containing domain
GL50803_10764	hypothetical protein	No	838	N/A	N/A
GL50803_10766	hypothetical protein	No	461	N/A	N/A
GL50803_10875	hypothetical protein	No	928	N/A	N/A
GL50803_10880	hypothetical protein	No	532	N/A	N/A
GL50803_112121	hypothetical protein	No	3902	N/A	N/A
GL50803_11290	Kinase, CMGC CDK	No	554	PF00069	Protein kinase domain
GL50803_11488	hypothetical protein	No	519	N/A	N/A
GL50803_11497	hypothetical protein	No	939	N/A	N/A
GL50803_11716	hypothetical protein	No	742	PF01974	tRNA intron endonuclease, catalytic domain-like
GL50803_11960	hypothetical protein	No	509	N/A	N/A
GL50803_13225	Zinc finger domain protein	No	264	N/A	N/A
GL50803_13323	hypothetical protein	No	839	N/A	N/A
GL50803_13393	Protein 21.1	No	678	PF12796	Ankyrin repeat-containing domain
GL50803_13771	hypothetical protein	No	1330	N/A	N/A
GL50803_14326	hypothetical protein	No	224	N/A	N/A
GL50803_14565	hypothetical protein	No	217	N/A	N/A
GL50803_14949	hypothetical protein	No	789	N/A	N/A
GL50803_15106	Importin beta-3 subunit	No	1151	N/A	N/A

GL50803_15218	WD-40 repeat protein	No	787	PF00400	WD40 repeat
GL50803_16021	hypothetical protein	No	935	N/A	N/A
GL50803_16143	Transcription regulatory protein SNF2	No	2079	PF00176;PF00271;PF00439	SNF2-related, N-terminal domain;Helicase, C-terminal;Bromodomain
GL50803_16240	hypothetical protein	No	384	N/A	N/A
GL50803_16332	Coiled-coil protein	No	1737	N/A	N/A
GL50803_16464	hypothetical protein	No	857	PF12678	Zinc finger, RING-H2-type
GL50803_16520	Sec24-like	No	1177	PF04810;PF04811;PF08033	Zinc finger, Sec23/Sec24-type;Sec23/Sec24, trunk domain;Sec23/Sec24 beta-sandwich
GL50803_16577	hypothetical protein	No	637	N/A	N/A
GL50803_16667	Acyl-CoA synthetase	No	905	PF13380;PF13549;PF13607	CoA-binding;Succinyl-CoA synthetase-like, flavodoxin domain
GL50803_16668	hypothetical protein	No	694	N/A	N/A
GL50803_16677	hypothetical protein	No	485	N/A	N/A
GL50803_16751	hypothetical protein	No	566	N/A	N/A
GL50803_16906	Phosphatidate cytidyltransferase	No	376	PF01148	N/A
GL50803_16930	hypothetical protein	No	1371	N/A	N/A
GL50803_17110	hypothetical protein	No	981	PF08506	Exportin-2, central domain
GL50803_17174	hypothetical protein	No	1903	PF00501	AMP-dependent synthetase/ligase
GL50803_17187	DNA-directed RNA polymerase subunit B	No	1238	PF00562;PF04560;PF04561;PF04563;PF04565;PF04566;PF04567	DNA-directed RNA polymerase, subunit 2, hybrid-binding domain;RNA polymerase Rpb2, domain 7;RNA polymerase Rpb2, domain 2;RNA polymerase, beta subunit, protrusion;RNA polymerase Rpb2, domain 3;RNA polymerase Rpb2, domain 4;RNA polymerase Rpb2, domain 5
GL50803_17199	Sun/nucleolar protein family protein	No	742	PF01189	SAM-dependent methyltransferase RsmB/NOP2-type
GL50803_17231	Kinase, NEK	No	1006	PF00069;PF12796	Protein kinase domain;Ankyrin repeat-containing domain
GL50803_17332	hypothetical protein	No	1656	N/A	N/A
GL50803_17432	Heat shock protein 70	No	1243	PF00012	Heat shock protein 70 family
GL50803_22268	hypothetical protein	No	1285	N/A	N/A
GL50803_22806	hypothetical protein	No	334	PF13870	Domain of unknown function DUF4201
GL50803_23330	hypothetical protein	No	257	PF00612	IQ motif, EF-hand binding site

GL50803_24133	5'-3' exoribonuclease 2	No	902	PF03159;PF17846	Putative 5-3 exonuclease;Xrn1, helical domain
GL50803_24734	hypothetical protein	No	1853	N/A	N/A
GL50803_3421	hypothetical protein	No	376	N/A	N/A
GL50803_34701	hypothetical protein	No	1985	N/A	N/A
GL50803_35630	hypothetical protein	Yes	33	N/A	N/A
GL50803_35639	hypothetical protein	Yes	100	N/A	N/A
GL50803_38907	hypothetical protein	Yes	66	N/A	N/A
GL50803_4917	hypothetical protein	Yes	88	N/A	N/A
GL50803_5274	hypothetical protein	No	677	N/A	N/A
GL50803_5468	Protein 21.1	No	942	PF00023;PF12796	Ankyrin repeat;Ankyrin repeat-containing domain
GL50803_5809	hypothetical protein	No	823	N/A	N/A
GL50803_6082	hypothetical protein	No	2658	PF12796	Ankyrin repeat-containing domain
GL50803_6262	Kinesin-3	No	1073	PF00225	Kinesin motor domain
GL50803_6614	hypothetical protein	Yes	174	N/A	N/A
GL50803_7103	Kinase, NEK	No	500	PF00069;PF12796	Protein kinase domain;Ankyrin repeat-containing domain
GL50803_7349	Ubiquitin	No	587	PF13898	Deubiquitinating enzyme MINDY-3/4, conserved domain
GL50803_7390	hypothetical protein	No	462	PF01207	tRNA-dihydrouridine synthase
GL50803_8227	ATP-binding cassette protein 5	No	1065	PF00005;PF12698	ABC transporter-like
GL50803_8508	Basal body protein	No	605	N/A	N/A
GL50803_8586	hypothetical protein	No	869	N/A	N/A
GL50803_8587	Kinase, AGC NDR	No	482	PF00069	Protein kinase domain
GL50803_86815	hypothetical protein	No	1216	N/A	N/A
GL50803_86945	hypothetical protein	No	2009	N/A	N/A
GL50803_8704	hypothetical protein	No	345	N/A	N/A
GL50803_87202	Protein F54C1.5	No	688	PF13414;PF14559	N/A
GL50803_8850	Protein 21.1	No	751	PF12796	Ankyrin repeat-containing domain
GL50803_89535	hypothetical protein	No	910	N/A	N/A
GL50803_89622	Mu adaptin	No	448	PF00928	Mu homology domain
GL50803_90343	Kinase, Wnk	No	568	PF00069	Protein kinase domain
GL50803_91334	Kinase, NEK-frag	No	1003	PF00069;PF12796	Protein kinase domain;Ankyrin repeat-containing domain
GL50803_9183	hypothetical protein	No	1904	N/A	N/A
GL50803_92741	Kinase, CMGC CLK	No	444	PF00069	Protein kinase domain
GL50803_94646	hypothetical protein	No	2011	N/A	N/A
GL50803_95880	hypothetical protein	No	403	N/A	N/A
GL50803_9697	hypothetical protein	No	1382	N/A	N/A

Group 3 (GR)

Downregulated

Gene ID	Product Description	Deprecated?	Protein Length	PFam ID	PFam Description
GL50803_100327	unspecified product	Yes	68	N/A	N/A
GL50803_11304	hypothetical protein	Yes	131	N/A	N/A
GL50803_113416	High cysteine membrane protein TMK-like	No	2516	PF03302	Giardia variant-specific surface protein
GL50803_15053	hypothetical protein	No	96	N/A	N/A
GL50803_16537	Protein 21.1	No	549	PF12796	Ankyrin repeat-containing domain
GL50803_17203	SacB	No	363	PF11380	Stealth protein CR2, conserved region 2
GL50803_19220	hypothetical protein	Yes	129	N/A	N/A
GL50803_19508	hypothetical protein	No	135	N/A	N/A
GL50803_20056	hypothetical protein	Yes	117	N/A	N/A
GL50803_20134	hypothetical protein	Yes	117	N/A	N/A
GL50803_20276	hypothetical protein	No	150	N/A	N/A
GL50803_20816	hypothetical protein	Yes	102	N/A	N/A
GL50803_20836	hypothetical protein	Yes	282	N/A	N/A
GL50803_20864	hypothetical protein	Yes	132	N/A	N/A
GL50803_25406	hypothetical protein	Yes	43	N/A	N/A
GL50803_27191	unspecified product	Yes	73	N/A	N/A
GL50803_29061	hypothetical protein	Yes	58	N/A	N/A
GL50803_29319	unspecified product	Yes	231	N/A	N/A
GL50803_31271	hypothetical protein	Yes	90	N/A	N/A
GL50803_31374	hypothetical protein	Yes	51	N/A	N/A
GL50803_31783	hypothetical protein	Yes	244	N/A	N/A
GL50803_31873	hypothetical protein	Yes	106	N/A	N/A
GL50803_32002	hypothetical protein	Yes	105	N/A	N/A
GL50803_35735	hypothetical protein	Yes	47	N/A	N/A
GL50803_37811	Hypothetical protein	No	127	N/A	N/A
GL50803_38104	Phospholipid-transporting ATPase IIB, putative	No	1322	PF00122;PF13246;PF16209;PF16212	P-type ATPase, N-terminal;P-type ATPase, C-terminal
GL50803_38460	Hypothetical protein	Yes	54	N/A	N/A
GL50803_38748	unspecified product	Yes	59	N/A	N/A
GL50803_39483	Ribosomal protein S29A	No	137	PF00253	Ribosomal protein S14
GL50803_39496	hypothetical protein	Yes	69	N/A	N/A
GL50803_6666	hypothetical protein	No	318	N/A	N/A
GL50803_8051	hypothetical protein	No	219	N/A	N/A
GL50803_8254	hypothetical protein with antisense transcription	No	92	N/A	N/A
GL50803_8513	ATP-binding protein	No	267	PF03029	GPN-loop GTPase
GL50803_94863	unspecified product	Yes	73	N/A	N/A

Supplemental Table S4. Differentially expressed genes that are specific to Group 4 (TYI).

Group 4 (TYI)

Upregulated

Gene ID	Product Description	Deprecated?	Protein Length	PFam ID	PFam Description
GL50803_100635	hypothetical protein	Yes	82	N/A	N/A
GL50803_105913	hypothetical protein	Yes	131	N/A	N/A
GL50803_106137	hypothetical protein	Yes	83	N/A	N/A
GL50803_112080	hypothetical protein	No	496	N/A	N/A
GL50803_114625	Protein convertase subtilisin/kexin type 5 precursor	No	578	N/A	N/A
GL50803_12148	Kinase, NEK	No	785	PF00069	Protein kinase domain
GL50803_12231	hypothetical protein	No	940	N/A	N/A
GL50803_14262	hypothetical protein	Yes	325	N/A	N/A
GL50803_14408	hypothetical protein	No	400	N/A	N/A
GL50803_15232	Protein 21.1	No	847	PF00023;PF12796	Ankyrin repeat;Ankyrin repeat-containing domain
GL50803_15412	Protein 21.1	No	665	PF12796;PF13920	Ankyrin repeat-containing domain
GL50803_15907	hypothetical protein	Yes	212	N/A	N/A
GL50803_16722	Xaa-Pro dipeptidase	No	450	PF00557	Peptidase M24
GL50803_17584	hypothetical protein	No	312	N/A	N/A
GL50803_18771	unspecified product	Yes	109	N/A	N/A
GL50803_19023	hypothetical protein	Yes	173	N/A	N/A
GL50803_19502	hypothetical protein	Yes	199	N/A	N/A
GL50803_20427	unspecified product	Yes	105	N/A	N/A
GL50803_20613	hypothetical protein	Yes	254	N/A	N/A
GL50803_20794	hypothetical protein	Yes	141	N/A	N/A
GL50803_23064	DNA polymerase epsilon, catalytic subunit	No	2590	PF00136;PF03104	DNA-directed DNA polymerase, family B, multifunctional domain;DNA-directed DNA polymerase, family B, exonuclease domain
GL50803_2382	hypothetical protein	No	962	N/A	N/A
GL50803_27393	unspecified product	Yes	35	N/A	N/A
GL50803_29106	hypothetical protein	Yes	127	N/A	N/A
GL50803_29582	hypothetical protein	No	177	N/A	N/A
GL50803_3099	Cathepsin L-like protease	No	429	PF00112	Peptidase C1A, papain C-terminal
GL50803_31203	hypothetical protein	Yes	66	N/A	N/A
GL50803_31243	hypothetical protein	Yes	52	N/A	N/A
GL50803_31624	hypothetical protein	No	104	N/A	N/A
GL50803_31661	hypothetical protein	Yes	124	N/A	N/A
GL50803_32000	hypothetical protein	Yes	161	N/A	N/A
GL50803_32069	hypothetical protein	Yes	205	N/A	N/A
GL50803_32099	hypothetical protein	Yes	99	N/A	N/A
GL50803_32146	hypothetical protein	Yes	90	N/A	N/A

GL50803_32206	hypothetical protein	Yes	243	N/A	N/A
GL50803_32238	hypothetical protein	Yes	90	N/A	N/A
GL50803_32309	hypothetical protein	Yes	193	N/A	N/A
GL50803_32310	hypothetical protein	Yes	86	N/A	N/A
GL50803_32319	hypothetical protein	Yes	38	N/A	N/A
GL50803_32359	hypothetical protein	Yes	144	N/A	N/A
GL50803_32391	hypothetical protein	Yes	156	N/A	N/A
GL50803_32434	hypothetical protein	Yes	121	N/A	N/A
GL50803_34726	hypothetical protein	Yes	107	N/A	N/A
GL50803_34775	hypothetical protein	Yes	81	N/A	N/A
GL50803_34836	unspecified product	Yes	76	N/A	N/A
GL50803_35157	hypothetical protein	Yes	185	N/A	N/A
GL50803_36523	unspecified product	Yes	48	N/A	N/A
GL50803_37071	Hypothetical protein	Yes	88	N/A	N/A
GL50803_37588	hypothetical protein	Yes	73	N/A	N/A
GL50803_37589	unspecified product	Yes	33	N/A	N/A
GL50803_37953	hypothetical protein	Yes	197	N/A	N/A
GL50803_38134	Thermosome beta subunit	Yes	83	N/A	N/A
GL50803_38378	hypothetical protein	No	51	N/A	N/A
GL50803_38553	hypothetical protein	Yes	52	N/A	N/A
GL50803_39014	hypothetical protein	Yes	155	N/A	N/A
GL50803_39094	hypothetical protein	Yes	113	N/A	N/A
GL50803_40005	Protein 21.1	No	625	PF12796	Ankyrin repeat-containing domain
GL50803_6243	hypothetical protein	Yes	196	N/A	N/A
GL50803_86888	hypothetical protein	Yes	109	N/A	N/A
GL50803_88178	hypothetical protein	Yes	74	N/A	N/A
GL50803_91951	hypothetical protein	Yes	73	N/A	N/A
GL50803_93499	unspecified product	Yes	132	N/A	N/A
GL50803_93501	hypothetical protein	Yes	66	N/A	N/A
GL50803_93503	hypothetical protein	Yes	92	N/A	N/A
GL50803_93721	Cyclin fold protein 1, putative	No	250	PF00134	Cyclin, N-terminal
GL50803_95023	hypothetical protein	No	988	N/A	N/A
GL50803_99709	hypothetical protein	Yes	63	N/A	N/A

Downregulated

Gene ID	Product Description	Deprecated?	Protein Length	PFam ID	PFam Description
GL50803_101594	CCAAT-box-binding transcription factor	No	1059	PF03914	CCAAT-binding factor
GL50803_114209	hypothetical protein	No	3123	PF06920	Dedicator of cytokinesis, C-terminal
GL50803_114751	hypothetical protein	No	1847	N/A	N/A

GL50803_11763	hypothetical protein	No	305	PF04263	Thiamin pyrophosphokinase, catalytic domain
GL50803_11992	TCP-1 chaperonin subunit epsilon	No	553	PF00118	Chaperonin Cpn60/TCP-1 family
GL50803_12867	hypothetical protein	No	530	N/A	N/A
GL50803_137749	hypothetical protein	No	1577	N/A	N/A
GL50803_13996	Alpha-15 giardin	No	303	N/A	N/A
GL50803_14135	Nucleoside diphosphate kinase	No	387	PF00334	Nucleoside diphosphate kinase-like domain
GL50803_14901	hypothetical protein	No	969	N/A	N/A
GL50803_16037	hypothetical protein	No	1568	N/A	N/A
GL50803_16599	hypothetical protein	No	2190	PF00211	Adenylyl cyclase class-3/4/guanylyl cyclase
GL50803_16734	hypothetical protein	No	2653	PF14538	Raptor, N-terminal CASPase-like domain
GL50803_16804	Dynein heavy chain	No	2297	PF08385;PF08393;PF12774	Dynein heavy chain, domain-1;Dynein heavy chain, domain-2;Dynein heavy chain, hydrolytic ATP-binding dynein motor region
GL50803_17164	Sec24-like	No	971	PF04810;PF04811;PF04815;PF08033	Zinc finger, Sec23/Sec24-type;Sec23/Sec24, trunk domain;Sec23/Sec24, helical domain;Sec23/Sec24 beta-sandwich
GL50803_23833	Vacuolar protein sorting 35	No	765	PF03635	Vacuolar protein sorting-associated protein 35
GL50803_27616	hypothetical protein	Yes	48	N/A	N/A
GL50803_29436	DNA-directed RNA polymerase subunit B	No	1235	PF00562;PF04560;PF04563;PF04565;PF06883	DNA-directed RNA polymerase, subunit 2, hybrid-binding domain;RNA polymerase Rpb2, domain 7;RNA polymerase, beta subunit, protrusion;RNA polymerase Rpb2, domain 3;DNA-directed RNA polymerase I subunit RPA2, domain 4
GL50803_30795	hypothetical protein	Yes	63	N/A	N/A
GL50803_31998	hypothetical protein	No	841	N/A	N/A
GL50803_3449	Kinase, NEK	No	860	PF00023;PF00069;PF12796	Ankyrin repeat;Protein kinase domain;Ankyrin repeat-containing domain
GL50803_35985	High cysteine protein	Yes	115	N/A	N/A
GL50803_3599	hypothetical protein	No	391	PF12796	Ankyrin repeat-containing domain
GL50803_4151	hypothetical protein	No	685	N/A	N/A
GL50803_4191	Kinase, CMGC CDK	No	545	PF00069	Protein kinase domain
GL50803_4197	Phosphatidylinositol transfer protein alpha isoform	No	345	PF02121	Phosphatidylinositol transfer protein
GL50803_4657	hypothetical protein	No	1595	N/A	N/A
GL50803_7259	CDP-diacylglycerol-glycerol-3-phosphate 3-phosphatidyltransferase	No	297	PF01066	CDP-alcohol phosphatidyltransferase
GL50803_7590	hypothetical protein	No	257	N/A	N/A
GL50803_7896	26S proteasome non-ATPase regulatory subunit 7	No	286	PF01398	JAB1/MPN/MOV34 metalloenzyme domain
GL50803_7909	Amino acid transporter family	No	557	PF01490	Amino acid transporter, transmembrane domain
GL50803_90024	hypothetical protein	No	5730	N/A	N/A
GL50803_92602	hypothetical protein	No	3088	N/A	N/A

REFERENCES

- Adam, Rodney D. 2021. "Giardia Duodenalis: Biology and Pathogenesis." *Clinical Microbiology Reviews* 34(4): e00024-19.
- Afgan, Enis et al. 2018. "The Galaxy Platform for Accessible, Reproducible and Collaborative Biomedical Analyses: 2018 Update." *Nucleic Acids Research* 46(W1): W537–44.
- Anders, Simon, Paul Theodor Pyl, and Wolfgang Huber. 2015. "HTSeq—a Python Framework to Work with High-Throughput Sequencing Data." *Bioinformatics* 31(2): 166–69.
- Andrews, S. 2010. "FastQC A Quality Control Tool for High Throughput Sequence Data [Online]."
- Ansell, Brendan R E et al. 2019. "Annotation of the Giardia Proteome through Structure-Based Homology and Machine Learning." *GigaScience* 8(1): giy150.
- Aurrecoechea, Cristina et al. 2017. "EuPathDB: The Eukaryotic Pathogen Genomics Database Resource." *Nucleic Acids Research* 45(D1): D581–91.
- Bemrick, Wj. 1963. "Effect of Bile Flow on Giardia Duodenalis Race Simoni in Intestine of a Laboratory Strain of Rattus Norvegicus." *Journal of Parasitology* 49(6): 956-.
- Best, A. A. et al. 2004. "Evolution of Eukaryotic Transcription: Insights from the Genome of Giardia Lamblia." *Genome Res* 14(8): 1537–47.
- Chuang, Shen-Fung et al. 2012. "Functional Redundancy of Two Pax-like Proteins in Transcriptional Activation of Cyst Wall Protein Genes in Giardia Lamblia." *PLoS One* 7(2): e30614.
- Dobin, Alexander et al. 2013. "STAR: Ultrafast Universal RNA-Seq Aligner." *Bioinformatics* 29(1): 15–21.
- Edwards, Michael R., Philip J. Schofield, William J. O'Sullivan, and M. Costello. 1992. "Arginine Metabolism during Culture of Giardia Intestinalis." *Molecular and Biochemical Parasitology* 53(1): 97–103.
- Elmendorf, H. G. et al. 2001. "Initiator and Upstream Elements in the Alpha2-Tubulin Promoter of Giardia Lamblia." *Mol Biochem Parasitol* 113(1): 157–69.
- Farthing, M. J., G. T. Keusch, and M. C. Carey. 1985. "Effects of Bile and Bile Salts on Growth and Membrane Lipid Uptake by Giardia Lamblia. Possible Implications for Pathogenesis of Intestinal Disease." *The Journal of Clinical Investigation* 76(5): 1727–32.
- Farthing, M.J.G., S.R. Varon, and G.R. Keusch. 1983. "Mammalian Bile Promotes Growth of Giardia Lamblia in Axenic Culture." *Transactions of The Royal Society of Tropical Medicine and Hygiene* 77(4): 467–69.
- Ge, Steven Xijin, Eun Wo Son, and Runan Yao. 2018. "IDEP: An Integrated Web Application for Differential Expression and Pathway Analysis of RNA-Seq Data." *BMC Bioinformatics* 19(1): 534.

- Gillin F D, Reiner D S, and Boucher S E. 1988. "Small-Intestinal Factors Promote Encystation of Giardia Lamblia in Vitro." *Infection and Immunity* 56(3): 705–7.
- Gillin, Frances D. et al. 1987. "Encystation and Expression of Cyst Antigens by Giardia Lamblia in Vitro." *Science* 235(4792): 1040–43.
- Gillin, Frances D., and Louis S. Diamond. 1981a. "Entamoeba Histolytica and Giardia Lamblia: Effects of Cysteine and Oxygen Tension on Trophozoite Attachment to Glass and Survival in Culture Media." *Experimental Parasitology* 52(1): 9–17.
- . 1981b. "Entamoeba Histolytica and Giardia Lamblia: Growth Responses to Reducing Agents." *Experimental Parasitology* 51(3): 382–91.
- Hegner, R., and L. Eskridge. 1937. "The Influence of Bile Salts on Giardia Infections in Rats." *American Journal of Hygiene* 26(1): 186–92.
- Isaac-Renton, J., E.M. Proctor, R. Prameya, and Q. Wong. 1986. "A Method of Excystation and Culture of Giardia Lamblia." *Transactions of The Royal Society of Tropical Medicine and Hygiene* 80(6): 989–90.
- Isaac-Renton, JI, H. Shahriari, and Wr Bowie. 1992. "Comparison of an Invitro Method and an Invivo Method of Giardia Excystation." *Applied and Environmental Microbiology* 58(5): 1530–33.
- Kane, Anne V., Honorine D. Ward, Gerald T. Keusch, and Miercio E. A. Pereira. 1991. "In Vitro Encystation of Giardia Lamblia: Large-Scale Production of In Vitro Cysts and Strain and Clone Differences in Encystation Efficiency." *The Journal of Parasitology* 77(6): 974–81.
- Keister, D. B. 1983. "Axenic Culture of Giardia Lamblia in TYI-S-33 Medium Supplemented with Bile." *Transactions of the Royal Society of Tropical Medicine and Hygiene* 77(4): 487–88.
- Law, Charity W., Yunshun Chen, Wei Shi, and Gordon K. Smyth. 2014. "Voom: Precision Weights Unlock Linear Model Analysis Tools for RNA-Seq Read Counts." *Genome Biology* 15(2): R29.
- Love, Michael I., Wolfgang Huber, and Simon Anders. 2014. "Moderated Estimation of Fold Change and Dispersion for RNA-Seq Data with DESeq2." *Genome Biology* 15(12): 550.
- Lujan, Hugo D., Michael R. Mowatt, and Theodore E. Nash. 1996. "Lipid Requirements and Lipid Uptake by Giardia Lamblia Trophozoites in Culture." *Journal of Eukaryotic Microbiology* 43(3): 237–42.
- Meyer, Ernest A., and Betty L. Pope. 1965. "Culture in Vitro of Giardia Trophozoites from the Rabbit and Chinchilla." *Nature* 207(5004): 1417–18.
- Morrison, H. G. et al. 2007. "Genomic Minimalism in the Early Diverging Intestinal Parasite *Giardia Lamblia*." *Science* 317(5846): 1921–26.
- Pan, Yu-Jiao, Chao-Cheng Cho, Yu-Yun Kao, and Chin-Hung Sun. 2009. "A Novel WRKY-like Protein Involved in Transcriptional Activation of Cyst Wall Protein Genes in Giardia Lamblia." *Journal of Biological Chemistry* 284(27): 17975–88.

Pertea, Mihaela et al. 2015. "StringTie Enables Improved Reconstruction of a Transcriptome from RNA-Seq Reads." *Nature Biotechnology* 33(3): 290–95.

Schofield, Philip J., Michael R. Edwards, Jacqueline Matthews, and Justine R. Wilson. 1992. "The Pathway of Arginine Catabolism in *Giardia Intestinalis*." *Molecular and Biochemical Parasitology* 51(1): 29–36.

Sogin, Mitchell L. et al. 1989. "Phylogenetic Meaning of the Kingdom Concept: An Unusual Ribosomal RNA from *Giardia Lamblia*." *Science* 243(4887): 75–77.

Sun, C. H. et al. 2002. "A Novel Myb-Related Protein Involved in Transcriptional Activation of Encystation Genes in *Giardia Lamblia*." *Mol Microbiol* 46(4): 971–84.

Wang, Chih-Hung, Li-Hsin Su, and Chin-Hung Sun. 2007. "A Novel ARID/Bright-like Protein Involved in Transcriptional Activation of Cyst Wall Protein 1 Gene in *Giardia Lamblia*." *Journal of Biological Chemistry* 282(12): 8905–14.

Xu, Feifei, Aaron Jex, and Staffan G. Svärd. 2020. "A Chromosome-Scale Reference Genome for *Giardia Intestinalis* WB." *Scientific Data* 7(1): 38.

Chapter 3: Knockout of the Arginine Deiminase (ADI) Gene Causes Significant Reduction in ATP Generation Through the ADH Pathway and Down Regulates Genes Associated With Amino Acid Metabolism

INTRODUCTION

The presence of the arginine dihydrolase (ADH) pathway in *Giardia lamblia* was identified in 1990 (P.J. Schofield et al. 1990). This came as somewhat of a surprise, as the ADH pathway is primarily a prokaryotic pathway and the only other eukaryote in which the ADH pathway had been found was *Trichomonas vaginalis*, which is also an anaerobic protozoan parasite (Linstead and Cranshaw 1983). The ADH pathway is composed of three enzymes: arginine deiminase (ADI, GL50803_112103), ornithine carbamoyltransferase (OCT, GL50803_10311), and carbamate kinase (CK, GL50803_16453).

The ability to consume arginine gives *Giardia* an advantage when arginine is present. First, arginine can be consumed as a source of energy. Through the ADH pathway, one molecule of ATP is produced from one molecule of arginine. The potential arginine flux is also greater than the potential glucose flux. *In vitro*, at equimolar concentrations, the potential flux through arginine is about 15-fold greater than the potential flux through glucose and the potential energy yield from arginine is approximately 7-8 fold higher than that from glucose (Philip J. Schofield et al. 1992). The energy that is produced through the ADH pathway is also thought to compensate for the reduction of ATP production from glycolysis that occurs during encystation (Morf et al. 2010; Touz et al. 2008).

Both ADI and OCT are found in the cytosol of the trophozoite and they are also secreted into the environment (Ringqvist et al. 2008; Stadelmann et al. 2013). Thus, ADI (and OCT to a lesser extent) is also considered a virulence factor as it can compete with the host and microbiome and deplete local arginine concentrations (Allain et al. 2017; Banik et al. 2013). Arginine is required for host-generated nitric oxide (NO), which has an antimicrobial and antiparasitic defense response (Eckmann et al. 1999;

Gogoi et al. 2016; Li, Zhou, and Singer 2006). Thus, the ability of *Giardia* to consume arginine reduces the amount of arginine available for the host to utilize to produce NO, which can significantly reduce the effectiveness of this innate immune response to the presence of *Giardia* (Eckmann et al. 1999; Gogoi et al. 2016) (For more detailed information about the ADH pathway, see Chapter 1).

The presence of the ADH pathway in *Giardia* opens up many questions. Why has *Giardia* maintained this prokaryotic pathway? How does *Giardia* sense environmental arginine and glucose and how does it adjust its metabolism in response? Research into these questions has been limited as genetic manipulation has been difficult in the parasite. This is due to a number of reasons which include the fact there are two diploid nuclei present in the WBC6 trophozoite (Bernander, Palm, and Svard 2001), making the WBC6 trophozoites tetraploid (the trophozoite form of the life cycle is the form that has been used for genetic manipulation). Both nuclei are transcriptionally active (Kabnick and Peattie 1990) and genetically equivalent (Morrison et al. 2007). There had also been few antibiotics that had been identified as effective selectable markers in *Giardia* (Gourguechon and Cande 2011).

Using puromycin as the main selectable marker, bacterial plasmids can be transfected into *Giardia* and stably maintained (Singer, Yee, and Nash 1998). The plasmid can also be integrated into the genome, if it is linearized and has flanking homology regions (Singer, Yee, and Nash 1998), by homologous recombination machinery (García-Lepe et al. 2022). Morpholino oligonucleotides have been used to repress translation in *Giardia* (House et al. 2011; Paredes et al. 2011; Woessner and Dawson 2012), but morpholinos are expensive, lack complete penetrance, and are transient (washing out in less than 48 hours), making them not useful to study infection dynamics *in vivo* (Barash 2017). Although *Giardia* does have the conserved components of the RNA interference (RNAi) machinery, RNAi has not been shown to effectively silence genes in *Giardia* (Krtkova and Paredes 2017).

The recent application of the CRISPR/Cas9 system to gene editing has revolutionized genetic engineering in eukaryotes (Gilbert et al. 2013; Larson et al. 2013; Qi et al. 2013). CRISPR uses the bacterial Cas9 protein, which is an RNA-guided endonuclease originally used as a defense strategy in prokaryotes. The Cas9 protein can be directed to any site in the genome when co-expressed with a guide RNA (gRNA). Cas9 will then cleave the DNA at that specific location. Genome mutations can be created by the action of non-homologous end joining during DNA double-stranded break repair. Foreign DNA, including protein tags or antibiotic selectable markers, can also be inserted at that break position (Doudna and Charpentier 2014; Hsu, Lander, and Zhang 2014). The CRISPR interference system (CRISPRi) can be used to create stable, inducible, or reversible gene knockdown in eukaryotes (Gilbert et al. 2013). In CRISPRi, the Cas9 protein is slightly modified to prevent endonuclease activity, which creates a catalytically dead Cas9 (dCas9) protein, which can still be directed to a specific site in the genome using a gRNA, but will not cause double-stranded breaks at that site. Instead, the dCas9 sits at the targeted site in the genome and causes steric interference, blocking transcription (Gilbert et al. 2013).

The DawsonLab has recently modified the CRISPR/Cas9 system to work in *Giardia* and published on the first CRISPRi-mediated transcriptional repression of both exogenous and endogenous genes in *Giardia* (McInally SG et al. 2019). A *Giardia*-specific nuclear localization signal was needed in order to target dCas9 to both nuclei before repression could be induced. Knockdown phenotypes were observed when one gRNA was expressed or when two gRNAs were expressed concurrently (McInally SG et al. 2019). With the identification of three more selectable markers for *Giardia*, complete knockout of genes (i.e., all four copies are disrupted) was now possible and this paper provides data on the first complete metabolic mutant that has been developed in *Giardia*, with the arginine deaminase (ADI) gene being completely knocked out. When ADI is knocked out, ATP generation was significantly reduced when arginine was the only metabolite present, but no change in ATP generation was seen when the knockout strain (ADI4XKO) was incubated with glucose alone. Transcriptomic data found that genes involved in

amino acid metabolism were downregulated in the knockout strain when compared to the wild type strain. Two potential transcription factors were also identified that were upregulated in wild type compared to the knockout strain.

METHODS

***Giardia* trophozoite culture conditions**

All *Giardia* strains were cultured in modified TYI-S-33 medium supplemented with 5% adult bovine serum and 5% fetal bovine serum (Keister 1983) in sterile 16-ml screw-cap disposable tubes (BD Falcon) and incubated upright at 37°C without shaking.

Design of guide RNAs for CRISPR and CRISPRi genetic modification

For CRISPRi, guide RNAs (gRNAs) were designed that target within the first 150 bps of arginine deiminase (ADI, GL50803_112103), ornithine carbamoyltransferase (OCT, GL50803_10311), and carbamate kinase (CK, GL50803_16453). For CRISPR-mediated ADI knockout, gRNAs were designed that target the middle of the ADI gene (the ADI gene is 1743 bp, so the gRNA was directed toward bp 870). gRNAs (20 nucleotides) were designed with the CRISPR “Design and Analyze Guides” tool from Benchling (<https://benchling.com/crispr>) using a NGG PAM sequence and the *Giardia lamblia* ATCC 50803 genome (GenBank Assembly: GCA_000002435.1). gRNAs were designed to target the non-template strand (Supplemental Table 1) with 4-base overhangs complementary to the vector sequence overhangs.

Construction of CRISPRi strains of the three genes in the arginine dihydrolase (ADH) pathway

gRNA oligonucleotides were annealed and cloned into BbsI-digested dCas9g1pac (GenBank accession number: MH037009). Vectors were transfected into WBC6 trophozoites by electroporation (20 µg DNA) as previously described (Hagen et al. 2011). Strains were maintained with antibiotic selection (50 µg/ml puromycin).

Construction of 4X knock-out of arginine deiminase (ADI) using CRISPR machinery

gRNAs oligonucleotides were annealed and cloned into BbsI-digested Cas9U6g1pac (Supplemental Figure S1). Linear repair templates were designed with a left homology arm (750 bp upstream of the CRISPR cut site), an antibiotic resistance cassette, and a right homology arm (750 bp downstream of the CRISPR cut site). Two forms of repair template were designed: one with a blasticidin (bsd) resistance cassette and one with a hygromycin B (hyg) resistance cassette. Linear repair templates were synthesized by Twist Bioscience.

The CRISPR plasmid (Cas9U6gipac_112103g870) was electroporated into WBC6 trophozoites (20 µg DNA) as previously described (Hagen et al. 2011). The Cas9_112103g870 strain was maintained with antibiotic selection (50 µg/ml puromycin). The bsd linear repair template (20 ng) was then electroporated into the Cas9_112103g870 strain. Selection was maintained for the Cas9 plasmid with 50 µg/ml puromycin and selection for integration of the repair template started at 75 µg/ml blasticidin, which was increased to 150 µg/ml blasticidin as the electroporated cells recovered. Blasticidin repair template integration was confirmed by PCR.

Next, the hyg linear repair template (20 ng) was electroporated into the Cas9_112103g870 strain that had the bsd repair template integrated at least once in the *Giardia* genome. Selection was maintained for the Cas9 plasmid with 50 µg/ml puromycin and selection for integration of the repair template started at 600 µg/ml hygromycin B, which was increased to 1200 µg/ml hygromycin B as the electroporated cells recovered. Hygromycin B repair template integration was confirmed by PCR.

Once a strain was confirmed to have both the bsd resistance cassette and hyg resistance cassette integrated into the genome, that strain was diluted to obtain clonal populations of this strain. First, the cells were diluted to 2 cells/ml, then 250 µl (0.5 cell) was added to each well of a 96 well tissue culture plate. The cells were incubated for one week in an anoxic box without antibiotics. Theoretically, if there

was growth in a well, that population had arisen from a single cell and was now clonal. The contents of positive wells (those with growth) were transferred first to 6 ml TYI medium, and then up to 12 ml TYI medium. Clones were screened for complete knockout of the ADI gene by PCR (Supplemental Figure 2A) using primers that bound to the 5'- and 3'-ends of the ADI gene. If an antibiotic cassette had been inserted into the ADI gene, the PCR product would be increased by a known amount. One of the clones was selected for downstream analysis.

Quantification of ATP production

ATP levels were quantified as described in Chapter 2 using the Cell Titer Glo assay (Promega). ATP was quantified after two-hour and six-hour incubation in TYI medium, *Giardia* Base Medium (GBM) supplemented with 3 mM arginine (GR), and GBM supplemented with 50 mM glucose (GG) (see Chapter 2, Table 2 for GBM composition).

Total RNA extraction, RNA-seq library preparation, and comparative analyses

All RNA-seq preparation and analyses was performed as described in Chapter 2. Total RNA from biological replicates was collected for wild type (WT) WBC6, and ADI4XKO strains. Stranded RNA libraries were prepared using the Zymo-Seq RiboFree Total RNA Library Kit (Zymo) and samples were pooled in equimolar amounts. The library was sequenced using an Illumina iSeq 100 (1 x 75 bp). For information on total number of raw reads, number of trimmed reads, and mapping percentages for each sample, see Table 1.

RESULTS

ADH knockdown strains produce less ATP than wild type when glucose is present, but arginine alone had limited effect

When arginine is the only metabolite available, only the knockdown of ADI showed significantly less ATP production when compared to wild type trophozoites (ordinary one-way ANOVA with Dunnett's multiple comparisons test: ADI_kd96R: at two hours: $p=0.0091$; at six hours: $p=0.0017$) (Figure 1). The knockdown of OCT and CK had no effect on ATP production when compared to wild type (Figure 1).

When glucose is the only metabolite available, almost every knockdown strain generated less ATP than wild type trophozoites after two- and/or six-hour incubations (Figure 2). Both of the ADI knockdown strains had significantly reduced ATP production after both two- and six-hour incubation (At two hours: ADI_kd96R $p=0.0006$; ADI_kd130R $p=0.0013$. At six hours: both ADI_kd96R and ADI_130R $p<0.0001$) (Figure 2). After two hours, one of the OCT knockdown strains showed significantly reduced ATP production (OCT_kd54R $p=0.0147$), while after six hours, a different OCT knockdown strain showed significantly reduced ATP production (OCT_kd81R $p=0.0200$). CK only exhibited significant reduction in ATP production after 6 hours of incubation (both CK_kd62R and CK_kd132R $p<0.0001$).

There was an intermediate response when the trophozoites were incubated in TYI medium (Figure 3), which provides both arginine and glucose, along with other undefined metabolites. After two hours of incubation, one of the ADI knockdown strains and all of the OCT knockdown strains showed significantly reduced ATP production (ADI_kd96R $p=0.0107$; OCT_kd24R, OCT_kd54R, and OCT_kd81R $p<0.0001$). After six hours of incubation, only one of the CK knockdown strains had a significant reduction in ATP production (CK_kd62R $p=0.0071$).

The ADI_96R knockdown strain was the only strain that consistently produced significantly less ATP in all conditions and at all time points (Figures 1-3). The knockdown of CK showed the smallest effect on ATP production across all three conditions (Figures 1-3), with significant reduction of ATP observed only after 6 hours of incubation in GBM + 50 mM glucose medium and in TYI medium (Figure 2, Figure 3).

Knockout of ADI affects arginine metabolism but has no effect on glucose metabolism

The ADI knockout strain generated about 80% less ATP than wild type when incubated in GR medium after both two and six hours of incubation. The ADI knockout strain also generated less ATP when incubated in TYI medium (40% less at 2 hours, 25% less at 6 hours). Consistent with the hypothesis that there is no direct metabolic interaction between the ADH pathway and glycolysis, the ADI knockout strain generated the same amount of ATP as the wild type when glucose is the only metabolite present (Figure 4).

Arginine deiminase (ADI) is significantly downregulated in the ADI4XKO compared to wild type

ADI4XKO and wild type WBC6 trophozoites had distinctly different transcriptional profiles after a six hour incubation in TYI medium (Figure 5). There were 49 genes that were upregulated in wild type when compared to the ADI4XKO strain and 58 genes that were downregulated (Figure 6). Arginine deiminase is one of the genes that is significantly upregulated in wild type when compared to the knockout strain (Supplementary Table S2). ADI transcripts were not completely abolished.

Of the 49 upregulated genes, 13 were annotated as hypothetical proteins and five were annotated as unspecified products. However, all of the unspecified product ORFs were also deprecated and four of the five were less than 100 amino acids long. There was a large cluster of variant surface protein genes that were upregulated (n=14). Two of the genes that were upregulated in wild type are potential transcription factor candidates (GL50803_17540: ARID1 AT-rich interaction domain protein; GL50803_101594: CCAAT-box-binding transcription factor) (Table S2).

Two of the upregulated genes are involved in DNA organization and replication (GL 50803_135231: Histone H3; GL50803_16127: Replication factor C, subunit 5); translation (GL50803_17547: Ribosomal protein L4; GL50803_3570: Ribosomal protein S28); and cell cycle regulation (GL50803_2661: Cyclin-dependent kinases regulatory subunit; GL50803_9870: Kinase, NEK). Two genes were upregulated that were associated with redox reactions (GL50803_15009: Flavohemoprotein lateral transfer candidate;

GL50803_16076: Peroxiredoxin 1). In addition to ADI, two other genes potentially associated with amino acid metabolism were also upregulated (GL50803_4059: 5-methylthioadenosine nucleosidase; GL50803_16519: AstB/chuR-related protein) (Table S2).

Among the genes that were downregulated in wild type when compared to the ADI4XKO strain included 14 hypothetical proteins. There was also a large cluster of variant surface protein genes that were downregulated (n=18), which were annotated as either VSPs, high cysteine proteins, or CXC-rich proteins. Two copies of the elongation factor 1-alpha translation factor were downregulated (GL50803_112304; GL50803_112312) (Table S2).

Three NEK kinases were downregulated (GL50803_103944; GL50803_137733; GL50803_98050). As to metabolism, glyceraldehyde 3-phosphate dehydrogenase (GL50803_6687), the sixth enzyme in the glycolytic pathway, and both copies of the pyruvate-flavodoxin oxidoreductase (PFOR) genes (GL50803_114609; GL50803_17063) were downregulated. A small cluster of genes associated with the cytoskeleton (GL50803_103676: Alpha-tubulin; GL50803_112079: Alpha-tubulin; GL50803_37985: Dynein heavy chain) were also downregulated (Table S2).

DISCUSSION

Knockout of the ADI gene has a significant effect on ATP production and transcription

The results from the CRISPRi knockdown were somewhat surprising. Unfortunately, there was no opportunity to quantify the level of knockdown of each ADH gene by qPCR and the ADI4XKO strain was in process of being developed so focus was transferred to the complete knockout strain. Thus, all of the CRISPRi knockdown data should be analyzed with the knowledge that the percent knockdown of each strain has not been quantified.

The flux through the ADH pathway is very fast, so it was possible that just knocking down the expression of these genes would not have a significant effect on arginine metabolism, which is what was observed. The OCT gene has the lowest activity (170 ± 22 nmoles min^{-1} mg protein^{-1}) (Edwards et al. 1992), so it was hypothesized that knockdown of that gene in the ADH pathway would have the greatest effect on flux through the pathway and concomitant ATP production when arginine is the only metabolite available. However, the data showed that the knockdown of OCT had no significant effect on ATP production when incubated in GR medium for 2 and for 6 hours (Figure 1).

The ADH knockdown strains were also incubated in GG medium (where glucose is the only metabolite for energy available). The ADH pathway has been shown to have no interaction with glycolysis, so growing the knockdown strain with glucose only was hypothesized to be more like a negative control and that there would be no significant effect on ATP production under these conditions as the only ATP generating pathway that was available was glycolysis. However, the knockdown strains of all three genes in the ADH pathway had a significant effect on ATP production, generally causing a reduction in ATP production as compared to WT strains (Figure 2).

Some of the knockdown strains also reduced ATP generation when incubated in TYI medium. However, since the knockdowns had no effect when arginine was the only metabolite available, it is hypothesized that the knockdowns are also affecting glycolysis in this condition (Figure 3). It is unclear what exactly is happening here, but the CRISPRi plasmid may be causing some off-target effects. There may also be some interaction and regulation occurring between the ATP generating pathways as the trophozoites respond and adapt to nutrient availability. If the ADH CRISPRi knockdowns experiments are continued, qPCR should first be done to determine percent knockdown. It would also be informative to run a RNA-Seq experiment with the knockdowns (especially the ADI_kd96R, which most often reduced ATP generation) to check for any off-target effects as well how the other enzymes in the ADH pathway respond to the knockdown of one of the required enzymes. However, with the development of the first

complete metabolic knockout in *Giardia* (ADI4XKO strain), the remainder of this chapter will focus on the effects of the complete knockout of the ADI gene.

The ADI4XKO strain behaved as predicted when grown under different nutrient conditions. When arginine was the only metabolite available, ATP generation was reduced 80% when compared to wild type trophozoites. When glucose was the only metabolite available, there was no significant difference in ATP generation between the ADI4XKO strain and wild type (Figure 4), supporting that hypothesis that the depletion of ADI does not affect glycolysis, as would be expected.

The ADI4XKO strain also had reduced ATP generation compared to wild type when grown in TYI medium, but not to as great an extent as observed with arginine alone (Figure 4). In TYI, the ADI4XKO strain still produced more ATP than when wild type was incubated in glucose alone, indicating that the ATP generation seen with TYI is not being produced solely from glycolysis. There is evidence *Giardia* has genes for metabolism of lipids and amino acids other than arginine, but these have not been well studied.

Transcriptomics also supports that the ADI4XKO strain had disrupted ADI transcripts. When compared to wild type, ADI was significantly downregulated in the ADI4XKO strain (Table S2). Transcript generation was not completely abolished, but further analysis needs to be done with those transcripts that are mapping back to the ADI gene. Based on our knockout strategy, the first 870 base pairs of the ADI gene are not disrupted, so these could be partial transcripts or antisense transcripts.

When comparing wild type to the ADI4XKO strain, two other potential amino metabolic genes are also upregulated in wild type (Supplemental Table S2). The end products of the ADH pathway feed into amino acid metabolism and protein biosynthesis, so if the first enzyme in the ADH pathway has been knocked out, downstream genes that interact with its products may also be expected to be

transcriptionally down regulated. Two potential transcription factors were also upregulated in wild type (Supplemental Table S2) and may suggest transcriptional regulation of amino acid metabolism.

Glyceraldehyde 3-phosphate dehydrogenase (GAPDH), the sixth enzyme of glycolysis, was downregulated in wild type when compared to the ADI4XKO (Supplemental Table S2). This suggests that when arginine cannot be metabolized, *Giardia* may be upregulating genes in other metabolic pathways to compensate. As seen with the ATP data, when incubated in TYI medium, after two hours, ATP generation in the ADI4XKO strain was reduced 40% compared to wild type, but after six hours, ATP generation was only 25% less than wild type (Figure 4). This indicates that *Giardia* may be upregulating gene expression for genes in the glycolysis pathway when arginine metabolism is blocked and that can be seen as the ATP reduction of the ADI4XKO strain was lessened over time, perhaps as more glycolytic enzymes are being produced.

Transcriptomics also indicated that a large subset of the genes that were both upregulated or downregulated were genes involved in surface antigen presentation (Supplemental Table S2). This was not seen in the RNA-Seq data from Chapter 2, where transcriptional response was recorded in response to nutrient availability. The *Giardia* genome contains several families of cysteine-rich membrane proteins, which include the Variant-specific Surface Proteins (VSPs) (Rodríguez-Walker et al. 2022). These genes are primarily known to be involved in antigenic variation, but it is unclear why they are being differentially expressed in this condition, where wild type was compared to the ADI4XKO strain incubated in TYI.

This project highlights the first complete metabolic mutant that has been created in *Giardia*. This opens a new era of *Giardia* research, where the impact of individual genes can be evaluated. The next step is to evaluate how knocking out the ADI gene affects encystation. It has been generally assumed that the ADH pathway compensates for the glycolytic shunt that occurs during encystation, but that has not been

conclusively shown (Touz et al. 2008). It will be interesting to see how the ADI knockout affects cyst formation *in vitro*. I would hypothesize that there would be less cysts produced by the ADI4XKO strain because the ADH pathway can no longer be an ATP-generating pathway that compensates for the glycolytic shift that occurs during encystation. This experiment would also provide the first direct evidence that the ADH pathway is actually compensating for the reduction of ATP produced from glucose.

The ADH pathway is also thought to play an important role during infection. Since arginine catabolism rapidly can produce ATP, it is thought that the ADH pathway plays a large role in generating ATP during the initial phase of colonization and growth (Edwards et al. 1992). Since glycolysis generates 7-8 fold less ATP than ADH in the same time period (Philip J. Schofield et al. 1992), the slower generation of ATP when the ADH pathway is blocked may prohibit successful invasion and attachment to the gastrointestinal epithelium.

In the host, the growth and replication of the ADI4XKO trophozoites may be stunted, even if attachment is not impeded. ADI is a potential virulence factor, as ADI is secreted and may compete with the host cells for arginine – an essential substrate for the host nitrite oxide (NO) response required as a host defense. Host neuronal nitric oxide synthase, for example, is necessary for eliminating parasites in mice (Li, Zhou, and Singer 2006). *In vitro* experiments where *Giardia* trophozoites are co-cultured with human epithelial cells demonstrate that the presence of *Giardia* increased the consumption of arginine in the co-culture and also inhibited epithelial NO production (Eckmann et al. 2000). The ADI4XKO would not be able to cause a significant depletion of host arginine, thus, the host NO response may be more robust and result in the death of a high number of trophozoites

Lastly, the ADI knockout may play an important role in transmission, if it reduces cyst load. Thus, both phases of the *Giardia* life cycle may be affected *in vivo*, at different stages of a course of infection. All of

this work would determine if the ADI gene is a good drug target candidate, which is useful as current drug treatments are limited and *Giardia* does show some resistance to these drugs (Saghaug, Klotz, and Kallio 2021).

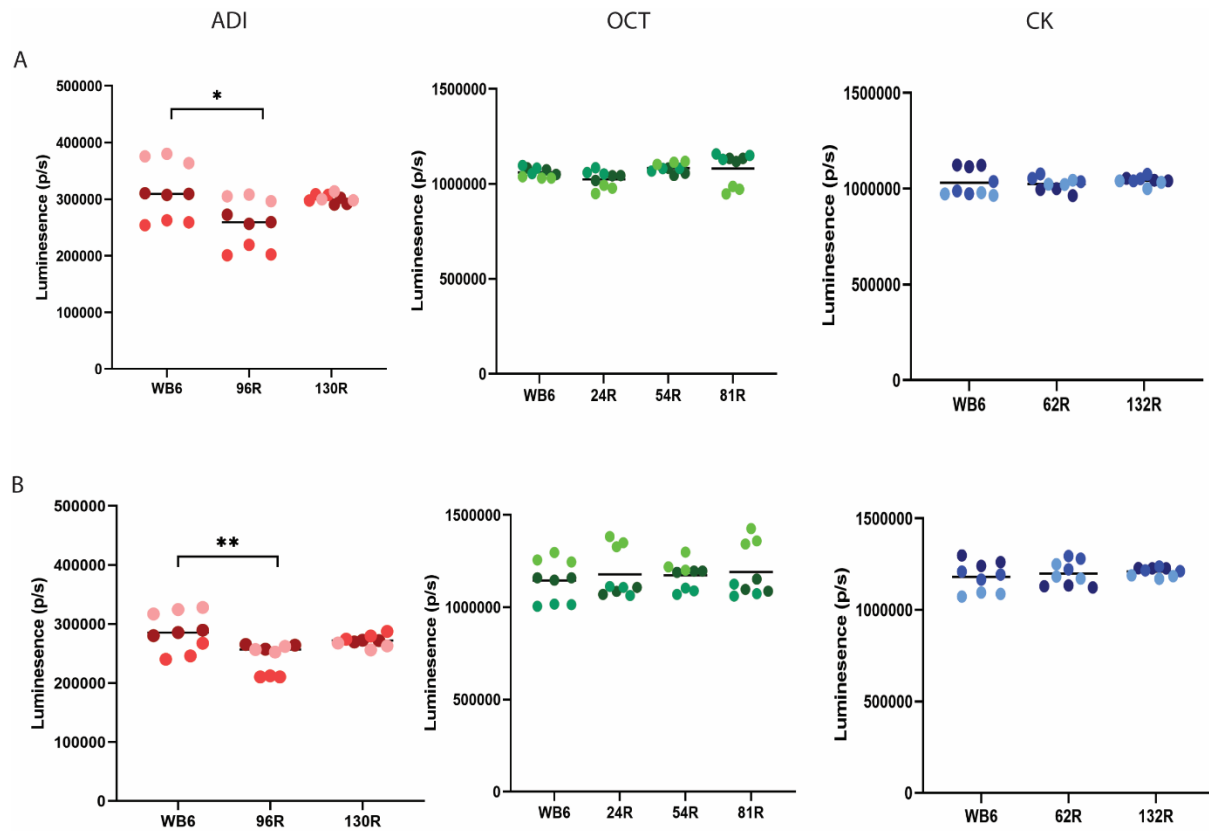


Figure 1. When arginine is the only metabolite available, knockdown of ADH genes had little effect on ATP production. ATP production of ADH knockdown strains was analyzed in GBM + 3 mM arginine, after two-hour (A) and six-hour (B) incubations (ADI knockdown strains: red; OCT knockdown strains: green; CK knockdown: blue strains). Only the knockdown of ADI at position 96 had any effect on ATP production. Asterisk(s) indicate significance ($p < 0.05$) calculated by a one-way ANOVA.

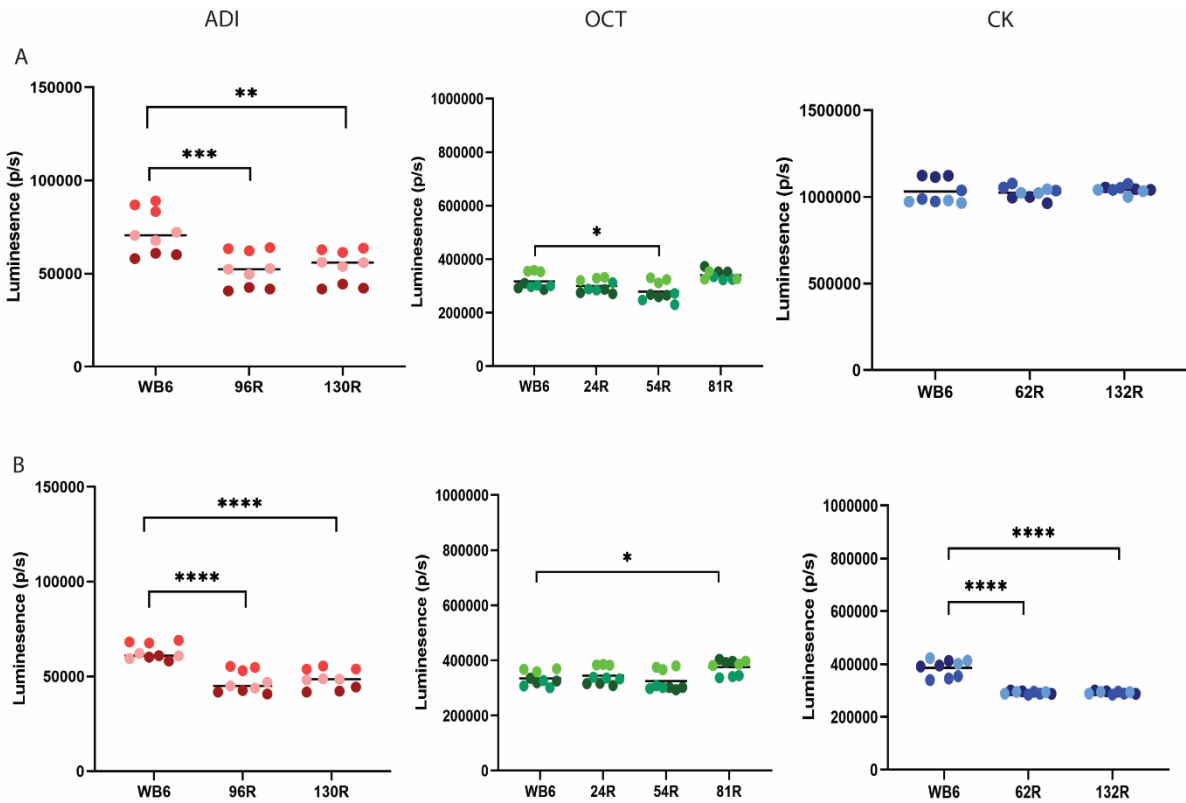


Figure 2. When glucose is the only metabolite available, ADH knockdown strains generated significantly less ATP than WT WBC. ATP production of ADH knockdown strains was analyzed in GBM + 50 mM glucose, after two-hour (A) and six-hour (B) incubations (ADI knockdown strains: red; OCT knockdown strains: green; CK knockdown strains: blue). Asterisk(s) indicate significance ($p < 0.05$) calculated by a one-way ANOVA.

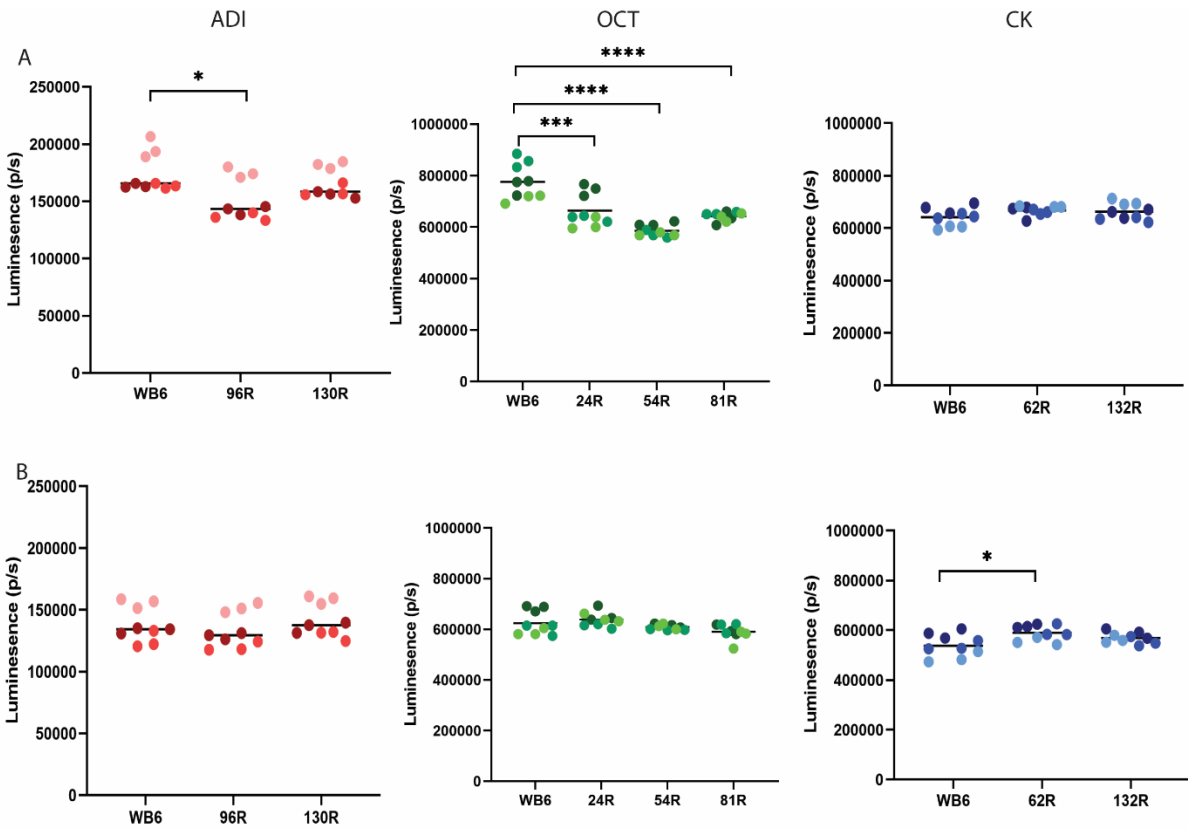
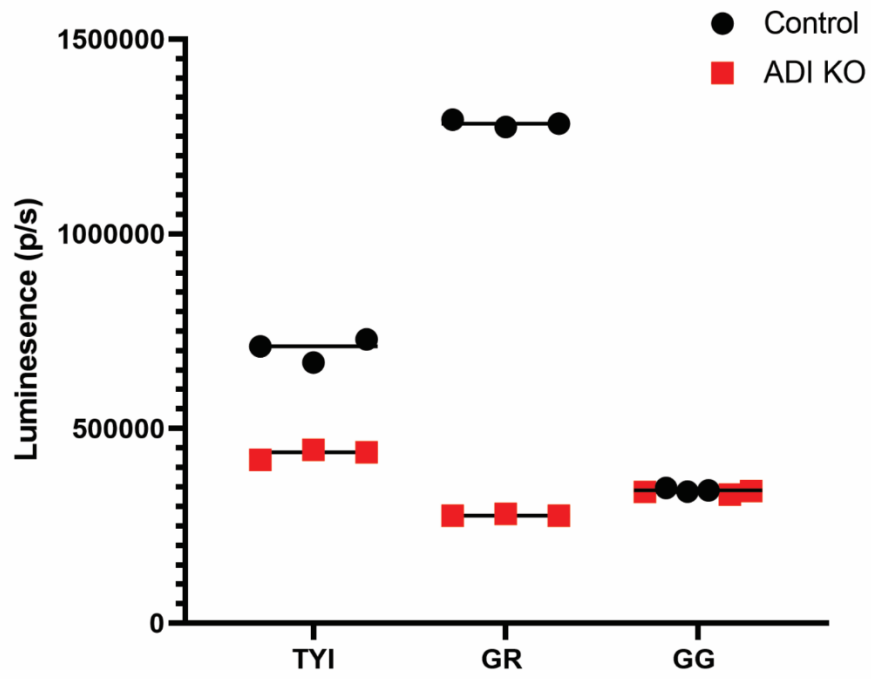


Figure 3. When incubated in TYI medium (which contains 3 mM arginine and 50 mM glucose), ATP generation in the OCT knockdown strains are significantly lowered after two hours of incubation. ATP production of ADH knockdown strains was analyzed in TYI medium, after two-hour (A) and six-hour (B) incubations (ADI knockdown strains: red; OCT knockdown strains: green; CK knockdown strains: blue). Asterisk(s) indicate significance ($p < 0.05$) calculated by a one-way ANOVA.

A



B

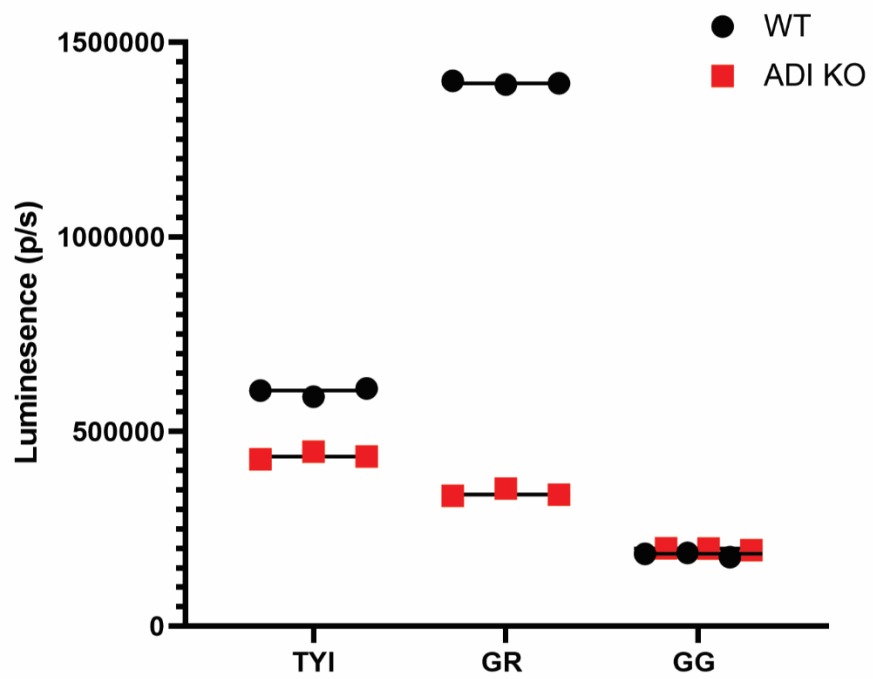


Figure 4. When ADI was knocked out, there was a significant reduction in ATP production when arginine was the only metabolite present (GR) and a moderate reduction of ATP production in TYI medium (A: two-hour incubation; B: six-hour incubation). However, the knockout of ADI has no effect on ATP production when glucose is the only metabolite present (GG).

TYI
ADI4XKO

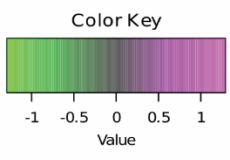
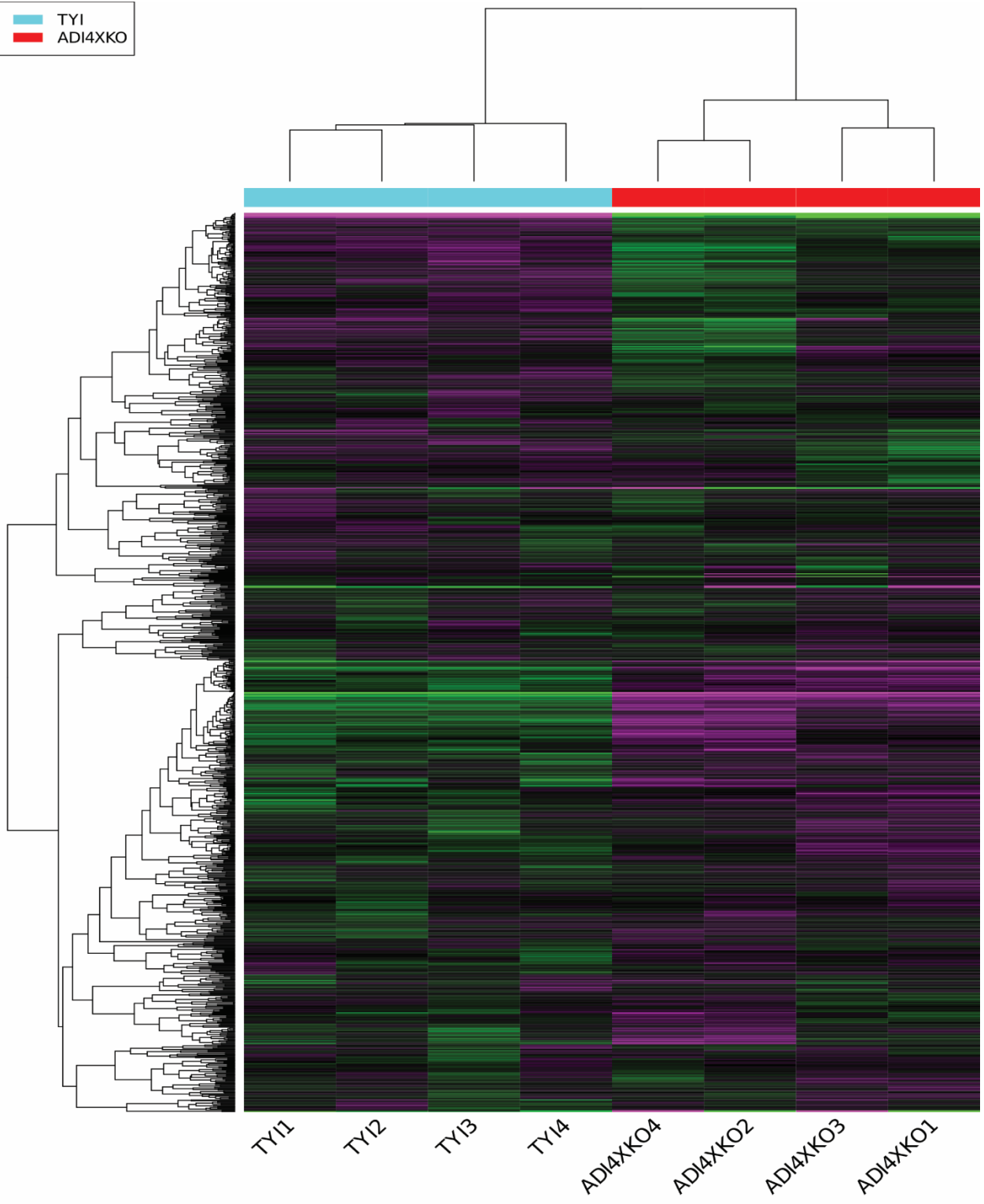


Figure 5. The ADI4XKO had a distinctly different transcriptional profile when compared to wild type after incubation in TYI medium for six hours. Heatmap of RNA-Seq expression z-scores computed for differentially expressed genes (FDR <0.05, fold change 2+). Color represents the normalized expression level (calculated by subtracting the overall average gene abundance from the raw expression for each gene and dividing that result by the standard deviation of all of the measured counts across all samples) for each *Giardia* gene (magenta is higher than average, green is lower).

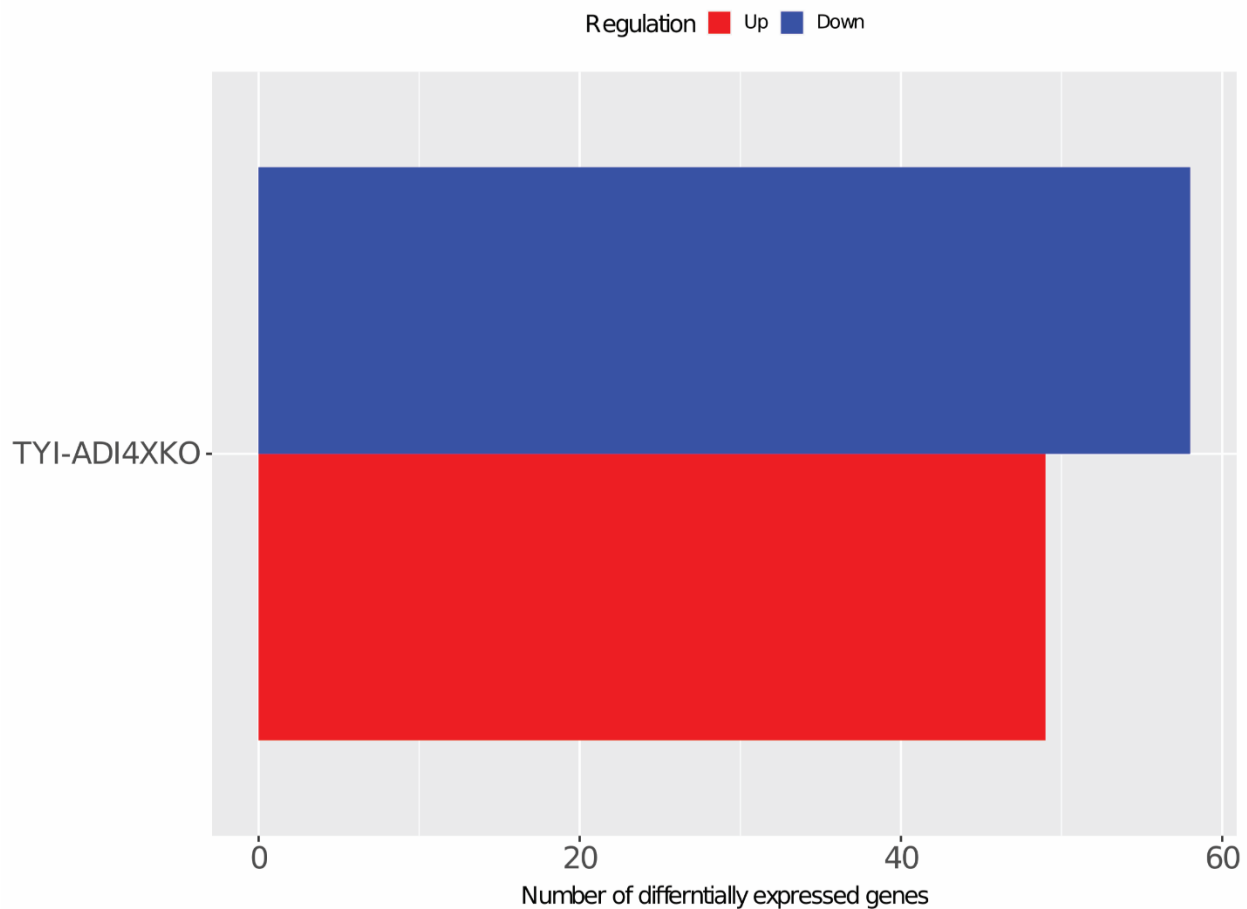
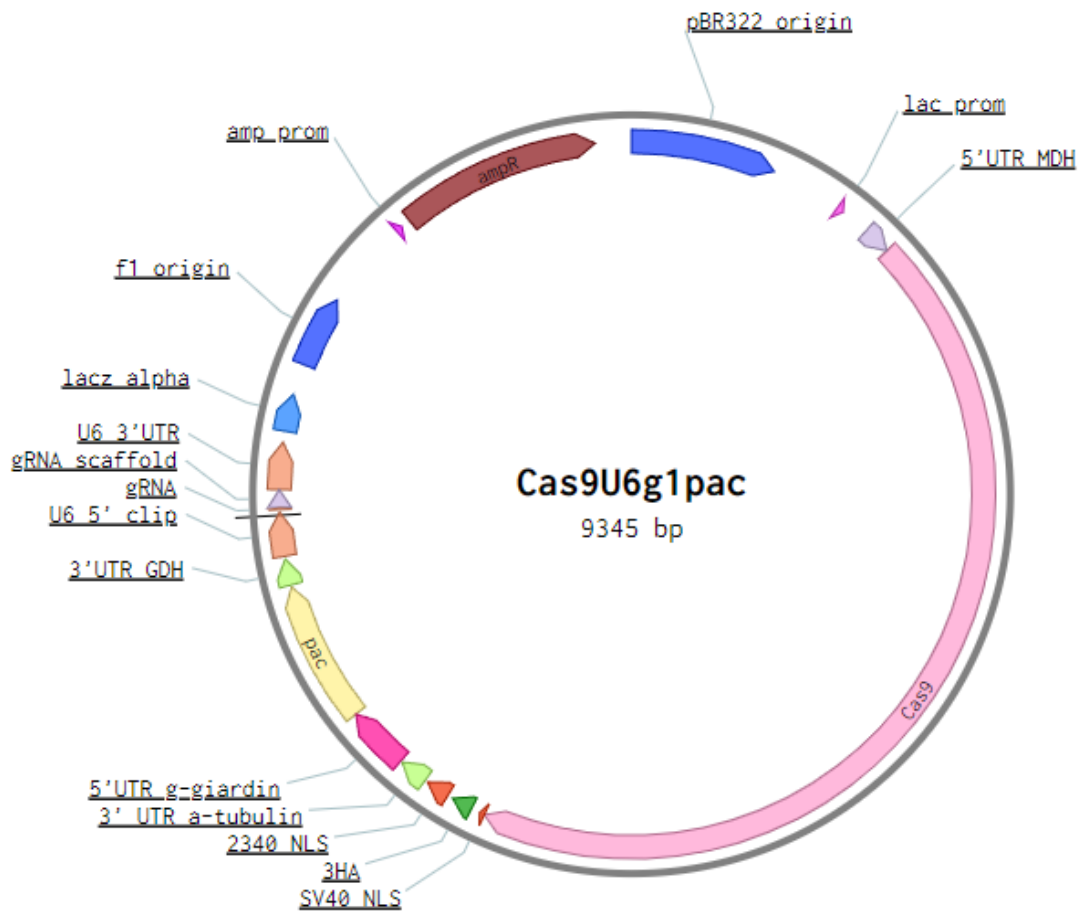


Figure 6. There was a significant number of genes that were differentially expressed when wild type was compared to ADI4XKO. 49 genes were upregulated in wild type compared to the knockout (red bar) and 58 genes were downregulated (blue bar).

Table 1. Sequencing and mapping statistics.

	# of raw reads	# of trimmed reads	% mapped
TYI1	197091	196630	98.94
TYI2	249716	247993	98.24
TYI3	190491	189919	98.72
TYI4	227525	225415	98.51
ADI4XKO1	570992	563440	87.41
ADI4XKO2	660237	646662	85.87
ADI4XKO3	595108	588085	86.63
ADI4XKO4	634560	626562	80.56

SUPPLEMENTAL MATERIAL



Supplemental Figure S1. Plasmid map of Cas9U6g1pac with full length Cas9 protein with a *Giardia*-specific NLS (2340 NLS), puromycin resistance cassette (pac), and gRNA scaffold.



Supplemental Figure S2. Confirmation of antibiotic cassette insertion into all four copies of the ADI gene. The ADI gene was amplified by PCR. The wild type ADI gene is 1.65 kb, WT ADI with the bsd insert is 2.5 kb, and WT ADI with the hyg insert is 3.1 kb. All nine clones showed bands at both 2.5 kb and 3.1 kb, indicating that at least one copy of each antibiotic cassette had been inserted into one copy of the ADI gene. The wild type band (1.65 kb) was seen only in the wild type strain and not in any of the clones, indicating that all four copies of the ADI gene in the clones had been disrupted by the insertion of an antibiotic cassette.

Supplemental Table S1: Sequence of oligonucleotides used for CRISPR/CRISPRi cloning.

Target/Position	Strand	Direction	Primer Sequence (5'-3')
For CRISPRi:			
112103_gRNA_96	-1	F	caaaTCAAGAACGACGTTCCCTGA
		R	aaacTCAGGGAACGTCGTTCTTGA
112103_gRNA_130	-1	F	caaaTCCTCAAGCAAGTCCCCTC
		R	aaacGAGGGGAACCTTGCTTGAGGA
10311_gRNA_24	-1	F	caaaCAGAGATAGTGAGCAAGTGG
		R	aaacCCAATTGCTCACTATCTCTG
10311_gRNA_54	-1	F	caaaTAAGGTACGCAAGCTCCTTG
		R	aaacCAAGGAGCTTGCGTACCTTA
10311_gRNA_81	-1	F	caaaTCTTCTTCATGTCGAGCGCA
		R	aaacTGCCTCGACATGAAGAAGA
16453_gRNA_62	-1	F	caaaGTCATAGTCCCCCTTCTCT
		R	aaacAGGAGAAGGGGGACTATGAC
16453_gRNA_132	-1	F	caaaCAACCTTATAGCCAGCCTTA
		R	aaacTAAGGCTGGCTATAAGGTTG
For CRISPR:			
112103_gRNA_870	-1	F	cggcCGAGCACCCTAGCTTGTCTG
		R	aaacCGACAAGCTAGTGGTGCTCG

Supplemental Table S2. Differentially expressed genes that are upregulated or downregulated in wild type when compared to the ADI4XKO strain.

Upregulated in wild type WBC6

GeneID	Product Description	Deprecat ed?	Prote in Length	PFam ID	PFam Description
GL50803_94478	ABC-type transport system ATP-binding chain, putative	No	1979	PF00005	ABC transporter-like
GL50803_103676	Alpha-tubulin	No	454	PF00091;PF03953	Tubulin/FtsZ, GTPase domain;Tubulin/FtsZ, 2-layer sandwich domain
GL50803_112079	Alpha-tubulin	No	454	PF00091;PF03953	Tubulin/FtsZ, GTPase domain;Tubulin/FtsZ, 2-layer sandwich domain
GL50803_137716	Axoneme-associated protein GASP-180	No	1585	PF12796	Ankyrin repeat-containing domain
GL50803_15564	Cathepsin B precursor	No	332	PF00112	Peptidase C1A, papain C-terminal
GL50803_17476	CXC-rich protein	No	2169	PF03302	Giardia variant-specific surface protein
GL50803_114915	Cysteine protease	No	637	PF00112	Peptidase C1A, papain C-terminal
GL50803_37985	Dynein heavy chain	No	1072	PF03028;PF12781;PF18198;PF18199	Dynein heavy chain region D6 P-loop domain;Dynein heavy chain, ATP-binding dynein motor region;Dynein heavy chain AAA lid domain;Dynein heavy chain, C-terminal domain
GL50803_112304	Elongation factor 1-alpha	No	442	PF00009;PF03143;PF03144	Transcription factor, GTP-binding domain;Translation elongation factor EFTu/EF1A, C-terminal;Translation elongation factor EFTu-like, domain 2
GL50803_112312	Elongation factor 1-alpha	No	442	PF00009;PF03143;PF03144	Transcription factor, GTP-binding domain;Translation elongation factor EFTu/EF1A, C-terminal;Translation elongation factor EFTu-like, domain 2
GL50803_6687	Glyceraldehyde 3-phosphate dehydrogenase	No	336	PF00044;PF02800	Glyceraldehyde 3-phosphate dehydrogenase, NAD(P) binding domain;Glyceraldehyde 3-phosphate dehydrogenase, catalytic domain
GL50803_113836	High cysteine membrane protein EGF-like	No	1691	N/A	N/A
GL50803_91707	High cysteine membrane protein Group 1	No	689	N/A	N/A
GL50803_113987	High cysteine membrane protein Group 3	No	833	PF03302	Giardia variant-specific surface protein
GL50803_114891	High cysteine membrane protein Group 3	No	832	PF03302	Giardia variant-specific surface protein
GL50803_113319	High cysteine membrane protein TMK-like	No	2529	PF03302	Giardia variant-specific surface protein
GL50803_101589	High cysteine protein	No	393	PF03302	Giardia variant-specific surface protein

GL50803_14 324	High cysteine protein	No	239	N/A	N/A
GL50803_11 1911	hypothetical protein	No	442	N/A	N/A
GL50803_11 2017	hypothetical protein	No	524	N/A	N/A
GL50803_11 3454	hypothetical protein	Yes	54	N/A	N/A
GL50803_11 3673	hypothetical protein	No	1649	N/A	N/A
GL50803_11 4044	hypothetical protein	No	524	N/A	N/A
GL50803_11 4210	hypothetical protein	No	1088	N/A	N/A
GL50803_11 4469	hypothetical protein	No	331	N/A	N/A
GL50803_11 4497	hypothetical protein	No	1062	N/A	N/A
GL50803_12 770	hypothetical protein	No	235	PF01852	START domain
GL50803_13 272	hypothetical protein	No	367	PF01156	Inosine/uridine-preferring nucleoside hydrolase domain
GL50803_13 7678	hypothetical protein	No	236	N/A	N/A
GL50803_13 7682	hypothetical protein	No	269	N/A	N/A
GL50803_13 7690	hypothetical protein	No	263	PF00271	Helicase, C-terminal
GL50803_15 053	hypothetical protein	No	96	N/A	N/A
GL50803_17 273	hypothetical protein	No	363	PF16062	Protein of unknown function DUF4804
GL50803_17 350	hypothetical protein	No	270	N/A	N/A
GL50803_17 351	hypothetical protein	No	477	N/A	N/A
GL50803_31 366	hypothetical protein	No	142	N/A	N/A
GL50803_37 518	hypothetical protein	Yes	40	N/A	N/A
GL50803_64 92	hypothetical protein	No	619	PF03009	Glycerophosphodiester phosphodiesterase domain
GL50803_98 760	hypothetical protein	No	56	N/A	N/A
GL50803_10 3944	Kinase, NEK	No	865	PF00069;PF12796	Protein kinase domain;Ankyrin repeat-containing domain
GL50803_13 7733	Kinase, NEK	No	297	PF00069	Protein kinase domain
GL50803_98 050	Kinase, NEK	No	172	PF07714	Serine-threonine/tyrosine- protein kinase, catalytic domain

GL50803_10 3058	Methyltransferase, putative	No	416	PF01728	Ribosomal RNA methyltransferase FtsJ domain
GL50803_11 4609	Pyruvate-flavodoxin oxidoreductase	No	1253	PF01558;PF01855;PF12838;PF17147	Pyruvate/ketoisovalerate oxidoreductase, catalytic domain;Pyruvate flavodoxin/ferredoxin oxidoreductase, N- terminal;4Fe-4S ferredoxin- type, iron-sulphur binding domain;Pyruvate:ferredoxin oxidoreductase, core domain II
GL50803_17 063	Pyruvate-flavodoxin oxidoreductase	No	1199	PF01558;PF01855;PF02775;PF10371;PF1 2838;PF17147	Pyruvate/ketoisovalerate oxidoreductase, catalytic domain;Pyruvate flavodoxin/ferredoxin oxidoreductase, N- terminal;Thiamine pyrophosphate enzyme, C- terminal TPP-binding;Pyruvate- flavodoxin oxidoreductase, EKR domain;4Fe-4S ferredoxin-type, iron-sulphur binding domain;Pyruvate:ferredoxin oxidoreductase, core domain II
GL50803_11 1935	Reverse transcriptase/endon uclease, putative	No	163	N/A	N/A
GL50803_86 87	Tenascin precursor	No	504	N/A	N/A
GL50803_14 247	TM efflux prot	No	594	PF07690	Major facilitator superfamily
GL50803_11 1933	VSP	No	741	PF03302	Giardia variant-specific surface protein

Downregulated in wild type WBC6

Gene ID	Product Description	Deprecat ed?	Prote in Lengt h	PFam ID	PFam Description
GL50803_944 78	ABC-type transport system ATP-binding chain, putative	No	1979	PF00005	ABC transporter-like
GL50803_103 676	Alpha-tubulin	No	454	PF00091;PF03953	Tubulin/FtsZ, GTPase domain;Tubulin/FtsZ, 2- layer sandwich domain
GL50803_112 079	Alpha-tubulin	No	454	PF00091;PF03953	Tubulin/FtsZ, GTPase domain;Tubulin/FtsZ, 2- layer sandwich domain
GL50803_137 716	Axoneme-associated protein GASP-180	No	1585	PF12796	Ankyrin repeat-containing domain
GL50803_155 64	Cathepsin B precursor	No	332	PF00112	Peptidase C1A, papain C- terminal
GL50803_174 76	CXC-rich protein	No	2169	PF03302	Giardia variant-specific surface protein
GL50803_114 915	Cysteine protease	No	637	PF00112	Peptidase C1A, papain C- terminal
GL50803_379 85	Dynein heavy chain	No	1072	PF03028;PF12781;PF18198;PF18199	Dynein heavy chain region D6 P-loop domain;Dynein heavy chain, ATP-binding dynein motor region;Dynein heavy chain AAA lid

					domain;Dynein heavy chain, C-terminal domain
GL50803_112 304	Elongation factor 1-alpha	No	442	PF00009;PF03143;PF03144	Transcription factor, GTP-binding domain;Translation elongation factor EFTu/EF1A, C-terminal;Translation elongation factor EFTu-like, domain 2
GL50803_112 312	Elongation factor 1-alpha	No	442	PF00009;PF03143;PF03144	Transcription factor, GTP-binding domain;Translation elongation factor EFTu/EF1A, C-terminal;Translation elongation factor EFTu-like, domain 2
GL50803_668 7	Glyceraldehyde 3-phosphate dehydrogenase	No	336	PF00044;PF02800	Glyceraldehyde 3-phosphate dehydrogenase, NAD(P) binding domain;Glyceraldehyde 3-phosphate dehydrogenase, catalytic domain
GL50803_113 836	High cysteine membrane protein EGF-like	No	1691	N/A	N/A
GL50803_917 07	High cysteine membrane protein Group 1	No	689	N/A	N/A
GL50803_113 987	High cysteine membrane protein Group 3	No	833	PF03302	Giardia variant-specific surface protein
GL50803_114 891	High cysteine membrane protein Group 3	No	832	PF03302	Giardia variant-specific surface protein
GL50803_113 319	High cysteine membrane protein TMK-like	No	2529	PF03302	Giardia variant-specific surface protein
GL50803_101 589	High cysteine protein	No	393	PF03302	Giardia variant-specific surface protein
GL50803_143 24	High cysteine protein	No	239	N/A	N/A
GL50803_111 911	hypothetical protein	No	442	N/A	N/A
GL50803_112 017	hypothetical protein	No	524	N/A	N/A
GL50803_113 454	hypothetical protein	Yes	54	N/A	N/A
GL50803_113 673	hypothetical protein	No	1649	N/A	N/A
GL50803_114 044	hypothetical protein	No	524	N/A	N/A
GL50803_114 210	hypothetical protein	No	1088	N/A	N/A
GL50803_114 469	hypothetical protein	No	331	N/A	N/A
GL50803_114 497	hypothetical protein	No	1062	N/A	N/A
GL50803_127 70	hypothetical protein	No	235	PF01852	START domain

GL50803_132 72	hypothetical protein	No	367	PF01156	Inosine/uridine-preferring nucleoside hydrolase domain
GL50803_137 678	hypothetical protein	No	236	N/A	N/A
GL50803_137 682	hypothetical protein	No	269	N/A	N/A
GL50803_137 690	hypothetical protein	No	263	PF00271	Helicase, C-terminal
GL50803_150 53	hypothetical protein	No	96	N/A	N/A
GL50803_172 73	hypothetical protein	No	363	PF16062	Protein of unknown function DUF4804
GL50803_173 50	hypothetical protein	No	270	N/A	N/A
GL50803_173 51	hypothetical protein	No	477	N/A	N/A
GL50803_313 66	hypothetical protein	No	142	N/A	N/A
GL50803_375 18	hypothetical protein	Yes	40	N/A	N/A
GL50803_649 2	hypothetical protein	No	619	PF03009	Glycerophosphodiester phosphodiesterase domain
GL50803_987 60	hypothetical protein	No	56	N/A	N/A
GL50803_103 944	Kinase, NEK	No	865	PF00069;PF12796	Protein kinase domain;Ankyrin repeat-containing domain
GL50803_137 733	Kinase, NEK	No	297	PF00069	Protein kinase domain
GL50803_980 50	Kinase, NEK	No	172	PF07714	Serine-threonine/tyrosine-protein kinase, catalytic domain
GL50803_103 058	Methyltransferase, putative	No	416	PF01728	Ribosomal RNA methyltransferase FtsJ domain
GL50803_114 609	Pyruvate-flavodoxin oxidoreductase	No	1253	PF01558;PF01855;PF12838;PF17147	Pyruvate/ketoisovalerate oxidoreductase, catalytic domain;Pyruvate flavodoxin/ferredoxin oxidoreductase, N-terminal;4Fe-4S ferredoxin-type, iron-sulphur binding domain;Pyruvate:ferredoxin oxidoreductase, core domain II
GL50803_170 63	Pyruvate-flavodoxin oxidoreductase	No	1199	PF01558;PF01855;PF02775;PF10371;PF12838;PF17147	Pyruvate/ketoisovalerate oxidoreductase, catalytic domain;Pyruvate flavodoxin/ferredoxin oxidoreductase, N-terminal;Thiamine pyrophosphate enzyme, C-terminal TPP-binding;Pyruvate-flavodoxin oxidoreductase, EKR domain;4Fe-4S ferredoxin-type, iron-sulphur binding domain;Pyruvate:ferredoxin oxidoreductase, core domain II
GL50803_111 935	Reverse transcriptase/endonuclease, putative	No	163	N/A	N/A

GL50803_8687	Tenascin precursor	No	504	N/A	N/A
GL50803_14247	TM efflux prot	No	594	PF07690	Major facilitator superfamily
GL50803_111933	VSP	No	741	PF03302	Giardia variant-specific surface protein
GL50803_111936	VSP	No	741	PF03302	Giardia variant-specific surface protein
GL50803_115047	VSP	No	587	PF03302	Giardia variant-specific surface protein
GL50803_137612	VSP	No	865	PF03302	Giardia variant-specific surface protein
GL50803_137681	VSP	No	370	PF03302	Giardia variant-specific surface protein
GL50803_137729	VSP	No	403	PF03302	Giardia variant-specific surface protein
GL50803_137752	VSP	No	1035	PF03302	Giardia variant-specific surface protein
GL50803_34357	VSP	No	887	PF03302	Giardia variant-specific surface protein
GL50803_37093	VSP	No	638	PF03302	Giardia variant-specific surface protein
GL50803_101074	VSP with INR	No	739	PF03302	Giardia variant-specific surface protein

REFERENCES

- Allain, Thibault et al. 2017. "Interactions of Giardia Sp. with the Intestinal Barrier: Epithelium, Mucus, and Microbiota." *Tissue Barriers* 5(1): e1274354.
- Banik, S. et al. 2013. "Giardia Duodenalis Arginine Deiminase Modulates the Phenotype and Cytokine Secretion of Human Dendritic Cells by Depletion of Arginine and Formation of Ammonia." *Infect Immun* 81(7): 2309–17.
- Barash, N. R. 2017. "Giardia Colonizes and Encysts in High Density Foci in the Murine Small Intestine." *mSphere* 2(3): e00343-16.
- Bernander, R., J. E. Palm, and S. G. Svard. 2001. "Genome Ploidy in Different Stages of the Giardia Lamblia Life Cycle." *Cell Microbiol* 3(1): 55–62.
- Doudna, J. A., and E. Charpentier. 2014. "Genome Editing. The New Frontier of Genome Engineering with CRISPR-Cas9." *Science* 346(6213): 1258096.
- Eckmann, L. et al. 2000. "Nitric Oxide Production by Human Intestinal Epithelial Cells and Competition for Arginine as Potential Determinants of Host Defense against the Lumen-Dwelling Pathogen Giardia Lamblia." *J Immunol* 164(3): 1478–87.
- Eckmann, L., R. Laurent, F. D. Gillin, and M. F. Kagnoff. 1999. "Giardia Lamblia Inhibits NO Production by Intestinal Epithelial Cells through Limiting Arginine Access." *FASEB Journal* 13(5 PART 2): A734.
- Edwards, Michael R., Philip J. Schofield, William J. O'Sullivan, and M. Costello. 1992. "Arginine Metabolism during Culture of Giardia Intestinalis." *Molecular and Biochemical Parasitology* 53(1): 97–103.
- García-Lepe, Ulises Omar et al. 2022. "Giardia Duodenalis Carries out Canonical Homologous Recombination and Single-Strand Annealing." *Research in Microbiology* 173(8): 103984.
- Gilbert, L. A. et al. 2013. "CRISPR-Mediated Modular RNA-Guided Regulation of Transcription in Eukaryotes." *Cell* 154(2): 442–51.
- Gogoi, Mayuri, Akshay Datey, Keith T Wilson, and Dipshikha Chakravorty. 2016. "Dual Role of Arginine Metabolism in Establishing Pathogenesis." *Current Opinion in Microbiology* 29: 43–48.
- Gourguechon, S., and W. Z. Cande. 2011. "Rapid Tagging and Integration of Genes in Giardia Intestinalis." *Eukaryot Cell* 10(1): 142–45.
- Hagen, K. D. et al. 2011. "Novel Structural Components of the Ventral Disc and Lateral Crest in Giardia Intestinalis." *PLoS Negl Trop Dis* 5(12): e1442.
- House, S. A., D. J. Richter, J. K. Pham, and S. C. Dawson. 2011. "Giardia Flagellar Motility Is Not Directly Required to Maintain Attachment to Surfaces." *PLoS Pathog* 7(8): e1002167.
- Hsu, Patrick D., Eric S. Lander, and Feng Zhang. 2014. "Development and Applications of CRISPR-Cas9 for Genome Engineering." *Cell* 157(6): 1262–78.

- Kabnick, Ks, and Da Peattie. 1990. "Insitu Analyses Reveal That the 2 Nuclei of Giardia-LambliA Are Equivalent." *Journal of Cell Science* 95: 353–60.
- Keister, D. B. 1983. "Axenic Culture of Giardia LambliA in TYI-S-33 Medium Supplemented with Bile." *Transactions of the Royal Society of Tropical Medicine and Hygiene* 77(4): 487–88.
- Krtkova, J., and A. R. Paredez. 2017. "Use of Translation Blocking Morpholinos for Gene Knockdown in Giardia LambliA." *Methods Mol Biol* 1565: 123–40.
- Larson, Matthew H. et al. 2013. "CRISPR Interference (CRISPRi) for Sequence-Specific Control of Gene Expression." *Nature Protocols* 8(11): 2180–96.
- Li, E., P. Zhou, and S. M. Singer. 2006. "Neuronal Nitric Oxide Synthase Is Necessary for Elimination of Giardia LambliA Infections in Mice." *J Immunol* 176(1): 516–21.
- Linstead, David, and Margaret A. Cranshaw. 1983. "The Pathway of Arginine Catabolism in the Parasitic Flagellate Trichomonas Vaginalis." *Molecular and Biochemical Parasitology* 8(3): 241–52.
- McInally SG et al. 2019. "Robust and Stable Transcriptional Repression in Giardia Using CRISPRi." *Molecular Biology of the Cell* 30(1): 119–30.
- Morf, L. et al. 2010. "The Transcriptional Response to Encystation Stimuli in Giardia LambliA Is Restricted to a Small Set of Genes." *Eukaryot Cell* 9(10): 1566–76.
- Morrison, H. G. et al. 2007. "Genomic Minimalism in the Early Diverging Intestinal Parasite Giardia LambliA." *Science* 317(5846): 1921–26.
- Paredez, A. R. et al. 2011. "An Actin Cytoskeleton with Evolutionarily Conserved Functions in the Absence of Canonical Actin-Binding Proteins." *Proc Natl Acad Sci U S A* 108(15): 6151–56.
- Qi, L. S. et al. 2013. "Repurposing CRISPR as an RNA-Guided Platform for Sequence-Specific Control of Gene Expression." *Cell* 152(5): 1173–83.
- Ringqvist, Emma et al. 2008. "Release of Metabolic Enzymes by Giardia in Response to Interaction with Intestinal Epithelial Cells." *Molecular and biochemical parasitology* 159: 85–91.
- Rodríguez-Walker, Macarena et al. 2022. "Comprehensive Characterization of Cysteine-Rich Protein-Coding Genes of Giardia LambliA and Their Role during Antigenic Variation." *Genomics* 114(5): 110462.
- Saghaug, C. S., C. Klotz, and J. P. Kallio. 2021. "Genetic Variation in Metronidazole Metabolism and Oxidative Stress Pathways in Clinical Giardia LambliA Assemblage A and B Isolates (Vol 12, Pg 1221, 2019)." *Infection and Drug Resistance* 14: 3727–3727.
- Schofield, Philip J., Michael R. Edwards, Jacqueline Matthews, and Justine R. Wilson. 1992. "The Pathway of Arginine Catabolism in Giardia Intestinalis." *Molecular and Biochemical Parasitology* 51(1): 29–36.

- Schofield, P.J., M. Costello, M.R. Edwards, and W.J. O'sullivan. 1990. "The Arginine Dihydrolase Pathway Is Present in *Giardia Intestinalis*." *International Journal for Parasitology* 20(5): 697–99.
- Singer, S. M., J. Yee, and T. E. Nash. 1998. "Episomal and Integrated Maintenance of Foreign DNA in *Giardia Lamblia*." *Mol Biochem Parasitol* 92(1): 59–69.
- Stadelmann, Britta et al. 2013. "The Role of Arginine and Arginine-Metabolizing Enzymes during *Giardia* - Host Cell Interactions in Vitro." *Bmc Microbiology* 13: 256.
- Touz, M. C. et al. 2008. "Arginine Deiminase Has Multiple Regulatory Roles in the Biology of *Giardia Lamblia*." *J Cell Sci* 121(Pt 17): 2930–38.
- Woessner, D. J., and S. C. Dawson. 2012. "The *Giardia* Median Body Protein Is a Ventral Disc Protein That Is Critical for Maintaining a Domed Disc Conformation during Attachment." *Eukaryot Cell* 11(3): 292–301.